ICAAS

UNIVERSITY OF FLORIDA
SPACE SCIENCES RESEARCH BLDG.
GAINESVILLE, FLORIDA 32611
AREA CODE 904 PHONE 392-2027

Final Report

INFLUENCE OF CLOUDS ON UV-B PENETRATION TO THE EARTH'S SURFACE

Prepared for:

National Aeronautics and Space Administration
Contract NAS 9-15114

Contract Period September 1, 1976 to September 30, 1979

Total Award $50,000

A. E. S. Green, Principal Investigator
University of Florida
Gainesville, Florida 32611

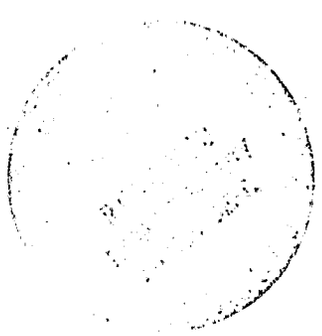

I. Summary of Work

The original objective of the work was to obtain radiometric measurements of cloud influence on UV-B and define mathematical models of the influence so as to lay the groundwork for later construction of the global UV-B climatology from satellite-determined ozone data. We believe we have made considerable progress towards these objectives as described in the attached papers.

The related radiometric work first undertaken by the group used all-sky photographs in conjunction with an Eppley radiometer and a Robertson-Berger meter. This particular study, initiated under the auspices of the CIAP program of the Department of Transportation but completed during the period of the grant, is described in Attachment 1. This work represents our best attempts at the broken cloud problem. More refined measurements comparing UV-B radiation with total solar radiation were carried out somewhat later in conjunction with the theoretical analyses given in Attachment 2. In Attachment 3 the cloudy case is referred to the cloudless sky irradiance and convenient "transmission" ratios are given. Attachment 4 summarizes an approach to the inversion of scattering data which should eventually facilitate the final objective of this work. Attachment 5 presents an improved characterization of the UV-B radiation from a cloudless sky. Such a result is not only of use in itself but also should facilitate further cloudy sky analyses. Attachment 6 extends these results to include actinic flux.

These studies along with studies undertaken by the writer in connection with his work as a member of the Nimbus-7 SBUV/TOMS experimental team have laid the groundwork for the later construction of a global UV-B

climatology from satellite-determined ozone data. We hope eventually to obtain funds to attempt to satisfy this final objective with the aid of Nimbus-7 UV data when it becomes available.

Not the least contribution of our program of UV studies has been our output of trained manpower, many of whom received their first exposure to atmospheric radiation research in our group. Dr. An Ti Chai is now at the NASA Lewis Research Center working on solar radiation and solar cells. Dr. Tsan Mo is now working at Goddard Space Flight Center. Dr. Janusz Borkowski has returned to the Institute of Geophysics at the University of Warsaw, and continues to be involved in stratospheric problems. Dr. James Spinhirne and Dr. Richard McPeters who received his Ph.D. degree during this period are also at NASA Goddard Space Flight Center working on atmospheric radiation problems. Dr. Kenneth Klenk now with System and Applied Sciences heads a project on the processing of Nimbus-4 and Nimbus-7 SBUV/TOMS data. Mr. Kenneth Cross is now working in industry as a program analyst. Mr. L. R. Smith, an undergraduate completing his B.S. degree, has undertaken a senior project in atmospheric sciences. Mr. David D. Doda and Dr. Dale Brabham should be completing their programs with us by next summer. Mr. Paul Schippnick has recently been initiated into theoretical atmospheric radiation studies. We hope to add an experimental graduate student with industrial experience in the next two months.

This Final Report of our study on the "Influence of Clouds on UV-B Penetration to the Earth's Surface" for NASA Contract NAS9-15114 covers the entire contract period. This was originally intended to be from September 1, 1976, through August 31, 1978. However, because of scientific manpower shortages the program was stretched out and extended to September 30,

1979, with no additional funds beyond the original $50,000 award. The stretch-out was also facilitated by the fact that during the period of this contract, the principal investigator was also supported by other grants and contracts, some of which overlapped the coverage of this contract in various ways. Section II contains a list of publications of the principal investigator since 1976. The items encircled represent works closely related to the topic of this grant. The items encircled and surrounded by hexagons are directly related to this contract. Copies of these publications are attached. Also attached is the Summary Chapter of a forthcoming book on a national problem of potential interest to NASA. The book concerns a topic which potentially has greater climatic and health consequences than the UV-ozone problem which has been the focus of this study.

We trust that this Final Report fulfills the requirements of this contract and look forward to future collaborations with NASA-Houston.

II. Publications, A. E. S. Green, 1976 to present

212. "Analytic Atomic Form Factors for Atoms and Ions with $A \leq 54$", with R. H. Garvey. Phys. Review A, 13, 3, 931-935 (1976).

213. "Latitudinal Variation in Biologically Effective Ultraviolet Radiation" with F. S. Johnson & T. Mo. Photochemistry and Photobiology, 23, 179-188 (1976)

214. "Multiple Elastic Scattering of Slow Electrons: A Parametric Study for H_2 with G. J. Kutcher., J. of Applied Physics, 47, 2175-2183 (1976).

215. "Measurement of the Ratio of Diffuse to Direct Solar Irradiances in the Middle Ultraviolet" with A.T. Chai. Applied Optics, 15, 1182-1187 (1976).

216. "Multistream and Monte Carlo Calculations of the Sun's Aureole", with D. R. Furman and T. Mo, Journal of the Atmospheric Sciences, 33, 3, 537-543 (1976).

217. "The Ultraviolet Dose Dependence of Non-Melanoma Skin Cancer Incidence" with G.B. Findley, Jr., Kenneth F. Klenk, W.M. Wilson and T. Mo, Photochem. and Photobiol., 24, 353-362(1976).

218. "Efficiencies for Production of Atomic Nitrogen and Oxygen by Relativistic Proton Impact in Air", H.S. Porter, C.H. Jackman, Journal of Chemical Physics, 65,1,154-167(1976).

219. "The Problem of Auroral NO^+ Concentration and the Intensity of 1.27μ Bands of O_2", with S.S. Prasad and D.R. Furman, Planet. Space Sci., 23, 1341-1343 (1975).

220. "Photographic Aureole Measurements and the Validity of Aerosol Single Scattering", McPeters, R.D. and A.E.S. Green, Applied Optics, 15, 10, 2457-2463(1976).

221. "Some Observations on Atomic Independent Particle Models", Green, A.E.S. and G.J. Kutcher, International Journal of Quantum Chemistry, Symp. 10, 135-140 (1976).

222. "A Model for Energy Deposition in Liquid Water, with G.J. Kutcher, Radiation Research, 67, 3, 408-425 (1976).

223. "Comment on Independent-Particle-Model Form Factors for Atoms and Ions with $Z \leq 54$," with R.H. Garvey, Phys. Rev. A, 14, 4, 1566-1568 (1976).

224. "Cloud Effects on Middle Ultraviolet Global Radiation," with J. Borkowski, A. T. Chi, and T. Mo. Acta Geophysica Polonica, 25, 4, 287-301 (1977).

225. "Energy-Apportionment Techniques Based Upon Detailed Atomic Cross Sections," with R. H. Garvey, Phys. Rev. A, 14, 3, 946-953 (1976).

226. "Solar Spectral Irradiance Reaching the Ground," published in the Proceedings on Nonbiological Transport and Transformation of Pollutants on Land and in Water: Processes and Critical Data Required for Predictive Description, May 11-13, 1976.

227. "A Comment on Skin Cancer Melanoma and Sunlight," American J. of Public Health, 67, 1, 59-60, (1977).

228. "An Analytic Degradation Spectrum for H_2*" with R. H. Garvey and H. S. Porter, J. of Applied Physics, 48, 1, 190-193, (1977).

229. "Further Comments on Atomic Central-Potential Models" with R. H. Garvey and D. D. Doda, Phys. Rev. A., 15, 1322-1325, (1977).

230. "Analytic Yield Spectra for Electrons on H_2" with R. H. Garvey and C. H. Jackman, International J. of Quant. Chem., Quant. Chem. Symposium 11, 97-103, (1977).

231. "Analytic Model Approach to the Inversion of Scattering Data" with Kenneth F. Klenk, published in the proceedings of the Interactive Workshop on Inversion Methods in Atmospheric Remote Sounding-Williamsburg, Va., December 15-17, 1976, Academic Press, (1977).

232. "Influence of Ground Level SO_2 on the Diffuse to Direct Irradiance Ratio in the Middle Ultraviolet" with Kenneth F. Klenk, Proceedings of the Eleventh International Symposium on Remote Sensing of Environment, Ann Arbor, Michigan, (1977).

233. "Models Relating Ultraviolet Light and Skin Cancer Incidence," Photochem. and Photobiol., 28, 283-291, (1978).

234. "Electron Impact on Atmospheric Gases, I. Updated Cross Sections" with Charles H. Jackman and Robert H. Garvey, J. of Geophysical Research, 82, 32, 5081-5090, (1977).

235. "Electron Impact on Atmospheric Gases, II. Yield Spectra" with Charles H. Jackman and Robert H. Garvey, J. of Geophysical Res. Research, 82, 32, 5104-5111, (1977).

236. "Noise vs Time, The pulse of a Community, NoiseExpo, Natl. Noise and Vibration Control Conf., Chicago, Ill., March 14-17, 1977, pp. 101-108, Acoustical Publications (1977).

237. "Yield Spectra and the Continuous Slowing Down Approximation" with Charles H. Jackman and Robert H. Garvey, J. of Applied Physics,B: Atom Molec. Phys., 10, 14, 2873-2882, (1977).

238. "Relativistic Yield Spectra for H_2" with Robert H. Garvey and Hayden S. Porter, J. of Applied Physics, 48, 10, 4353-4359, (1977).

239. "Diffuse/Direct Ultraviolet Ratios with a Compact Double Monochromator" with L. M. Garrison, L. E. Murray, D. D. Doda, Applied Optics, 17, 827-836, March 1978.

240. "Airglow from the Inner Comas of Comets", T. E. Cravens and A. E. S. Green, International Journal of Solar System Studies (ICARUS) Vol. 33, 612-623, March 1978.

241. "N-N GOBEP Meson Field Theory" with T. Ueda, F. E. Riewe, American Institute of Physics (1978) in the Proceedings of The Second Intl. Conf. on the Nucleon-Nucleon Interaction held on June 27-30, 1977, University of British Columbia, Vancouver, Canada.

242. "Spectral Sunphotometer Using a Compact Spectrometer", D. D. Doda and A. E. S. Green, Remote Sensing of Environment, 7, 97-104, (1978).

243. "Ultraviolet Skin Cancer and Response" American Journal of Epidemiology, 107, 4, 277-280, (1978)

244. "Ultraviolet Limit of Solar Radiation at the Earth's Surface with a Photon Counting Monochromator" with L. M. Garrison, L. E. Murray, Appl. Opts., 17, 683-684, (1978).

245. "N-N one-boson-exchange potentials based on generalized meson field theory" with T. Ueda and F. E. Riewe, Phy Rev C, 17, 1763-1773, May 1968.

246. "Cloud Effects on/Photoclimatology" with J. D. Spinhirne to appear in the Proceedings of the Twelfth International Symposium on Remote Sensing of Environment, April 20-26, 1978, Manila, Philippines.

247. "Ultraviolet Aureole Around a Source at a Finite Distance" with Fred Riewe, Applied Optics, 17, 1923-1929, 1978.

248. "Energy Deposition in a Gaseous Mixture" with L. R. Peterson and R. H. Garvey, J. of Geophysical Research, 83, A11, 5315-5317, (1978).

249. "Yield Spectrum for Protons Impacting on Helium" with R. A. Hedinger, J. Quantum Chem., to be published.

250. "Relativistic N-N One-Boson-Exchange Potentials with Asymptotic Power-Law Energy Dependence" with T. Ueda, Physical Review, 18, 1, 337-348, (1978).

251. "Calculation of the Relative Influence of Cloud Layers on Received UV and Integrated Solar Radiation" with J. D. Spinhirne, Atmospheric Environment, 12, 2449-2454, 1978.

252. "Florida's Air Quality, Present and Future," with D. E. Rio, and R. A. Hedinger, Florida Scientist, 41, 3, 182-190, (1978).

253. "Total Ozone Determination by Spectroradiometry in the Middle UV," with L. M. Garrison and D. D. Doda, Appl. Optics, 18, 6, 850-855, (1979).

254. "Remote Sensing of Atmospheric Aerosols," University of Florida Press, with D. A. Lundgren, Ed., 635-650, (1977).

255. "Distributional Analysis of Regional Benefits and Cost of Air Quality Control," with E. T. Loehman, S. V. Berg, A. A. Arroyo, R. A. Hedinger, J. M. Schwartz, M. E. Shaw, R. W. Fahien, V. H. De, R. P. Fishe, D. E. Rio, and W. F. Rossley, J. Environmental Economics and Management, 6, 3, 222-243, (1979).

256. "Electron Impact Excitation of the Beryllium Isoelectronic Sequence," with P. S. Ganas, Physical Review, 19, 6, 2197-2205, (1979).

257. "Remote Sensing of Ozone in the Middle Ultraviolet," with J. D. Talman, to be published in Proceedings of Workshop on Interpretation of Remotely Sensed Data, Williamsburg, Virginia, May 23-25, 1979, Academic Press, (1980).

258. "Electron Impact on Atmospheric Gases 3. Spatial Yield Spectra for N_2," with C. H. Jackman, J. of Geophysical Research, 84, A6, 2715-2724, (1979).

259. "Comparative Studies of Atomic Independent Particle Potentials," with J. D. Talman and P. S. Ganas, International Journal of Quantum Chemistry, in press.

260. "Pollution Dispersal Modeling and Regional Public Policy Implications," with E. T. Loehman, S. V. Berg, R. W. Fahien, M. E. Shaw, M. J. Jaeger, H. Wittig, A. A. Arroyo, J. M. Schwartz, R. A. Hedinger, V. H. De, D. E. Rio, T. J. Buckley, R. P. Fishe, W. F. Rossley, and D. Trimble, to be published in Proceedings of Symposium held in Williamsburg, April 17-19, 1979, on Environmental and Climatic Impact of Coal Utilization, Academic Press, (1980).

261. "Microplume Model of Spatial Yield Spectra," with R. P. Singhal, Geophysical Research Letters, 6, 7, 625-628, (1979).

262. "Factor of Safety Method Application to Air and Noise Pollution, with T. J. Buckley, D. E. Rio, A. MacEachern and R. Makarewicz, to be published in Atmospheric Environment.

263. "Improved Analytic Characterization of Ultraviolet Skylight," with K. R. Cross and L. A. Smith, to be published in Photochemistry and Photobiology.

264. "Correlation Between Noise and Air Pollution," with R. Makarewicz, to be published in Sound and Vibration.

265. "Vertical Transport of NO_2 Through the Tropopause," with J. Borkowski, published in ACTA GEOPHYSICA POLONICA, 26, 4, (1978).

266. "Aerosol Effects on Atmospheric Radiation," with P. F. Schippnick, to be published in Proceedings of Workshop on Atmospheric Aerosols: Their Formation, Optical Properties and Effects, held at Baltimore, Maryland, November 6-8, 1979, Academic Press,(1980).

267. "Spatial Aspects of Low and Medium Energy Electron Degradation in N_2," with R. P. Singhal and C. H. Jackman, to be published in Jour. Geophysical Research, (1980).

268. Coal Burning Issues, edited by A. E. S. Green, to be published by University Presses of Florida, 400 pp (1980).

269. "Atmosphere Modification," with K. E. Taylor and W. L. Chameides, Chapter 11 of Coal Burning Issues (see Number 268), 203-230 (1980).

270. "Quantitative Public Policy Assessments," with D. E. Rio, Chapter 15 of Coal Burning Issues (see Number 268), 303-330 (1980).

III. Recent Contracts and Grants

NATIONAL AERONAUTICS AND SPACE ADMINISTRATION

1. Aurora and Airglow Phenomena in Planetary Atmospheres, NGL-10-005-008.

   Fundamental investigations of airglow and auroral phenomena in planetary atmospheres. $50K, 5/1/79-4/30/80.

2. Science support for the Nimbus-7 Sensor, NAS-5-22908.

   As member of the Nimbus-7 Experiment Team (NET) for the Solar and Backscattered Ultraviolet and Total Ozone Mapping System (SBUV/TOMS) the P.I. assists in the determination of solar ultraviolet irradiance, ozone profiles, and global maps of total ozone. We provide experimental measurements of the ultraviolet levels reaching the ground, UV reflectivity measurements and total ozone values for correlation with the satellite measurements. $208K, 12/19/75-10/1/80.

3. Influences of Clouds on UV-B Penetration to the Earth's Surface, NAS-9-15114.

   Define mathematical model of UV-B irradiance reaching the ground and the influence of clouds. $50K, 9/1/76-9/30/79 - expired.

NATIONAL SCIENCE FOUNDATION

1. Atmospheric Radiative Transfer and Atomic Processes, NSF-ATM-75-21962.

   Theoretical and experimental atmospheric radiative transfer studies and atomic calculations for aeronomical applications. $39K, 5/26/78-10/31/79 - expired.

U. S. DEPARTMENT OF ENERGY GRANT

1. Biophysical Studies Related to Energy Generation, DE-AS05-76EV03798.

   Investigation of the physical stage of the interaction of the radiation with the inert matter and living organisms and on dose-response relationships especially related to energy generation. $50.3K, 6/1/79-5/31/80.

ENVIRONMENTAL PROTECTION AGENCY

1. The Impact of Stratospheric Ozone Depletion upon Tropospheric Ultraviolet, Photochemistry and Smog, EPA-R806373010. (With W. L. Chameides) $50K, 5/1/79-4/30/80.
   Radiative transfer calculations and modeling studies are used to determine the impact of stratospheric ozone depletions upon the tropospheric UV radiation field and photolysis rates, tropospheric photochemistry and smog formation.

UNIVERSITY OF FLORIDA (GATORADE), ICAAS

1. Comprehensive Coal Burning Issues Study (with 30 U.F. faculty members).

   ICAAS is conducting a detailed examination of energy and environmental issues facing the state and the country during the next quarter century, particularaly as it relates to coal burning and its atmospheric impacts. $150K, 7/1/79-9/30/80.

FLORIDA BOARD OF REGENTS

1. Impact of Increased Coal Use in Florida, ICAAS, STAR grant 79-064.
   $67K, 7/1/79-9/30/80 (with 15 U.F. faculty members).
   ICAAS is studying the major economic, social, environmental and technological issues involved in the anticipated increased use of coal in Florida.

ACTA GEOPHYSICA POLONICA
Vol. XXV, no. 4 1977

Janusz BĄRKOWSKI
Institute of Geophysics, University of Warsaw, Poland
An-Ti CHAI
NASA Lewis Research Center, Cleveland, USA
Tsan MO
Goddard Institute for Space Studies, New York, USA
Alex E. O. GREEN
Dept. of Physics and Astronomy, University of Florida, Gainesville, USA

CLOUD EFFECTS ON MIDDLE ULTRAVIOLET GLOBAL RADIATION*

Abstract

An Eppley radiometer and a Robertson-Berger sunburn meter are employed along with an all-sky camera setup to study cloud effects on middle ultraviolet global radiation at the ground level. Semi-empirical equations to allow for cloud effects presented in previous work are compared with our experimental data. Our study suggests a means of defining eigenvectors of cloud patterns and correlating them with the radiation at the ground level.

1. Prior work. The influence of clouds upon total solar irradiance at the ground has been the concern of many studies (Green, et al. 1974, Matveev 1967, Goody 1964, Barry and Chorley 1970). However, only a few studies (Nack and Green 1974, Mo and Green 1974, Buttner 1938, Bener 1964) have been devoted to the influence of clouds upon the ultraviolet radiation reaching the ground. The present work is an exploratory attempt to devise a detailed methodology for characterizing the influence of a cloud field upon ground level irradiance in the ozone absorbing region.

A simple equation in common use for the global irradiance $G(C)$ is

$$G(C)=(1-FC)G(0), \tag{1}$$

where C is the time averaged percent cloud cover, $G(0)$ represents the clear sky global flux at the ground level, and F is a parameter adjusted to give the best fit to experimental results. While generally speaking, F depends on cloud conditions; values of 0.56 and 0.65 are quoted in the literature (Nack and Green 1974). The factor F also has been written $F=a+bC$ which is equivalant to using

$$G(C)=[1-(a+bC)C]G(0), \tag{2}$$

where $0.14\leqslant a\leqslant 0.4$, $b\cong 0.38$, and C again is the time averaged cloud cover.

The magnitude of cloudiness is usually expressed in tenth's of the sky actually over-

* Research supported in part by U.S. Department of Transportation.

cast. The fractional cloud cover viewed from an observation point located on the earth's surface, is the fraction of an imaginary hemisphere, centered at an observation point, covered by clouds, and is called relative cloudiness. The relative cloudiness is greater or equal to absolute cloudiness which is a cloud covered fraction of the imaginary sphere centered at the center of the earth, or the fraction of area of the plane covered by projections of clouds on it, if a plane-parallel model of the atmosphere is considered. The absolute cloudiness may be identified with the cloud cover of the zenith's part of the sky or the cloud cover as viewed from a satellite. The difference between absolute and relative cloudiness is the greatest for convective type clouds. Niylisk (1972) found the relationship between relative and absolute cloudiness, for cumuliform clouds, in the form:

$$C_r = C + 0.8(1-C)C^{0.8}, \tag{3}$$

where C=absolute cloudiness and C_r=relative cloudiness.

In the present work we compare the previous empirical equations dealing with the cloud effect on middle ultraviolet sky radiation with our experimental data. Our work suggests a procedure for correlating the eigenvectors of cloud patterns with the radiation at the ground level.

2. Effects of clouds on the wavelength – integrated global UV fluxes. The global solar UV fluxes (in W/m²nm) for clear sky have been investigated by Shettle and Green (1974) using a multiple scattering formalism. Nack and Green (1974) extended these results by introducing a layer of clouds of various optical depths, τ_C, into the multiple scattering formalism, and they calculated the ratio of $G(\tau_C, \theta, \lambda)$, the global UV flux for a sky covered uniformly with clouds of optical depth τ_C, to the $G(0, \theta, \lambda)$ of clear sky. Their results are given as functions of τ_C, θ (the zenith angle) and λ (the wavelengths in nm). However, our experimentally measured quantities (see Section 3) include all the contributions from the wavelength interval of λ=280–340 nm. For direct comparison of the calculated quantities with the experimental results, one must also calculate the correspondingly wavelength-integrated quantities. For such purposes, we evaluate the quantity

$$R(\tau_C, \theta) = \int G(\tau_C, \theta, \lambda)\,d\lambda \Big/ \int G(0, \theta, \lambda)\,d\lambda, \tag{4}$$

where integration with respect to λ is from 280 to 340 nm. The numerator on the right hand side of Eq. (4) corresponds to the total global UV flux from 280 - 340 nm, at a cloudy sky of cloud optical depth τ_C, and the denominator corresponds to that of clear sky. The ratio $R(\tau_C, \theta)$ can be employed to study the effect of clouds of optical depth τ_C on the global UV flux at zenith angle θ.

The calculated values of $R(\tau_C, \theta)$ for various values of τ_C and θ are given in Table 1. The values of $G(0, \theta) = \int G(0, \theta, \lambda)\,d\lambda$ are also listed in the last column of Table 1. Figure 1 exhibits the typical τ_C-dependence of $R(\tau_C, \theta)$ for angles of 0 - 85°. This table shows that $R(\tau_C, \theta)$ is rapidly varying function of τ_C, but it only decreases slightly (less than 8%) as θ varies from 0° to 85° (see also Table 1). In practical application, this small θ-dependence of $R(\tau_C, \theta)$ can be ignored, if the values of $R(\tau_C, \theta)$ corresponding to mid-value of θ say θ=50°, is adopted (see Table 1).

Table 1

The calculated values of $R(\tau_C, \theta)$ as functions of τ_C and θ

θ (deg)	τ_C 0.1	0.2	0.5	1.0	2.0	5.0	10.0	20.0	50.0	100	$G(0, \theta)$* (W/m²)
0	0.995	0.990	0.975	0.951	0.904	0.778	0.622	0.441	0.230	0.124	13.539
30	0.994	0.988	0.9713	0.943	0.890	0.757	0.603	0.427	0.224	0.120	10.611
50	0.992	0.984	0.961	0.926	0.865	0.729	0.580	0.412	0.216	0.116	6.299
70	0.990	0.981	0.955	0.919	0.859	0.725	0.578	0.411	0.216	0.116	2.016
80	0.991	0.983	0.959	0.924	0.864	0.729	0.581	0.412	0.216	0.117	0.626
85	0.990	0.980	0.955	0.917	0.855	0.719	0.571	0.405	0.212	0.115	0.211

* $G(0, \theta) = \int_{280}^{340} G(0, \theta, \lambda)\,d\lambda$

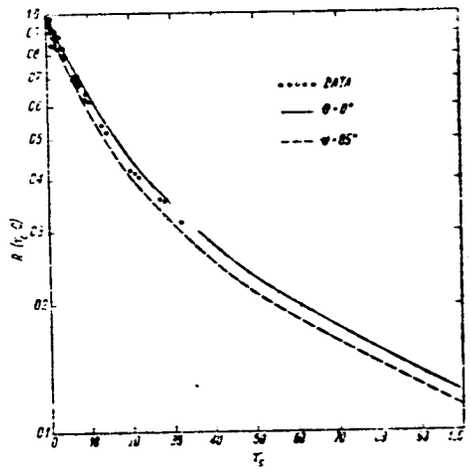

Fig. 1. The $R(\tau_C, \theta) = \int \varepsilon(\lambda) G(\tau_C, \theta, \lambda)\,d\lambda / \int \varepsilon(\lambda) G(0, \theta, \lambda)\,d\lambda$ versus the cloud optical depth τ_C. The $\varepsilon(\lambda)$ is spectral response of the Robertson-Berger sunburn meter. The dots are the values of $R(\tau_C, \theta)$ extracted from Eq. (8), using the measured data of $\int \varepsilon(\lambda) G(C, \tau_C, \theta, \lambda)\,d\lambda$ and $\int \varepsilon(\lambda) G(0, \theta, \lambda)\,d\lambda$.

In the above calculations, the $G(0, \theta, \lambda)$ and $G(\tau_C, \theta, \lambda)$ were calculated with an ozone thickness of 0.32 cm and a standard atmosphere as described by (Shettle and Green 1974).

The ratio $R(\tau_C, \theta)$ calculated from Eq. (4) can be employed to obtain the global UV flux $G(C, \tau_C, \theta)$ under the condition of fractional sky cover C and clouds of optical depth τ_C. The time-average global flux $G(C, \tau_C, \theta, \lambda)$ at wavelength λ is given by Nack and Green (1974)

$$G(C, \tau_C, \theta, \lambda) = (1-C)G(0, \theta, \lambda) + CG(\tau_C, \theta, \lambda). \tag{5}$$

If we integrate both sides of Eq. (5) with respect to the wavelength λ, we obtain

$$G(C, \tau_C, \theta) = [(1-C) + CR(\tau_C, \theta)]\,G(0, \theta), \tag{6}$$

where

$$G(C, \tau_C, \theta) = \int G(C, \tau_C, \theta, \lambda) d\lambda, \quad (7)$$

and $G(0, \theta)$ is the wavelength-integrated clear sky global flux, and values of $G(0, \theta)$ at various θ are given in Table I.

In principle, Eq. (6) can be used to calculate the quantity $G(C, \tau_C, \theta)$ if $R(\tau_C, \theta)$ and $G(0, \theta)$ are known. Unfortunately, the data of cloud optical depth τ_C are unavailable at the present time. Alternatively, we can use Eq. (6) to determine $R(\tau_C, \theta)$ and thus τ_C, since $G(0, \theta)$ and $G(C, \tau_C, \theta)$ can be measured with an instrument. Measurements with instruments, e.g. the Robertson-Berger sunburn meter, usually involve the spectral response $\varepsilon(\lambda)$ of the instrument, therefore the $\varepsilon(\lambda)$ should be folded into the integral of the global flux. From Eq. (5) we obtain,

$$\int \varepsilon(\lambda) G(C, \tau_C, \theta, \lambda) d\lambda = (1-C) \int \varepsilon(\lambda) G(0, \theta, \lambda) d\lambda + C \int \varepsilon(\lambda) G(\tau_C, \theta, \lambda) d\lambda. \quad (8)$$

The quantity $\int \varepsilon(\lambda) G(0, \theta, \lambda) d\lambda$ for the Robertson-Berger meter under a clear sky has been calculated and discussed elsewhere by Mo and Green (1974), and the integral on the left hand side of Eq. (8) can be measured from the instrument. Therefore, Eq. (8) can be used to obtain the integral $\int \varepsilon(\lambda) G(\tau_C, \theta, \lambda) d\lambda$, which contains the information of cloud optical depth τ_C. The integral $\int \varepsilon(\lambda) G(\tau_C, \theta, \lambda) d\lambda$ can also be calculated if the atmospheric conditions (i.e. ozone, aerosol, and cloud thicknesses) are known, then Eq. (8) can be used to check the accuracy between the measurement (the left hand side) and the calculations (the right hand side).

The ratio $R(\tau_C, \theta) = \int \varepsilon(\lambda) G(\tau_C, \theta, \lambda) d\lambda / \int \varepsilon(\lambda) G(0, \theta, \lambda) d\lambda$, (where $\varepsilon(\lambda)$ is the RB meter response) is calculated for $\tau_C = 0 - 100$, and the results are shown in Fig. 1.

3. Description of Experimental Apparatus. A. *All-Sky Camera.* In view of the large uncertainty in determining cloud cover in previous work (Bener, 1964) we have used an all-sky camera technique which records fairly accurately the cloud cover of the sky. The system consists of a 35 mm single lens reflex camera and a 30 cm diameter hub cap. The camera equipped with a 135 mm telephoto lens is located approximately 152 cm above the hub cap which serves as a hemispherical reflector. When properly focused, the image of the whole sky as reflected from the hub cap should fill the entire frame of the 35 mm film. The system can be operated either manually or by a motor drive. A motor drive which advances the film and releases the shutter once every twelve minutes automatically, has been built specifically for this purpose. This all-sky camera system is used in conjunction with two ultraviolet radiometers in the present study.

B. *Eppley Ultraviolet Radiometer.* The radiometer manufactured by the Eppley Laboratory essentially consists of selenium barrier-layer photoelectric cell which is protected by a quartz window. A bandpass interference filter restricts the wavelength response of the instrument to 295 - 330 nm, and a specially shaped diffusing disc of opaque quartz assures adherence of the instrument to the Lambert cosine law. The terminals of the photocell are connected through a precision resistor (1500 Ω) and the signal measured as a voltage drop across this resistor. The unit is housed in an internally blackened brass tube, assembled to be completely weatherproof. A Keithley 150 Microammeter and a Heathkit chart recorder were used to amplify and plot the global UV flux as a function of time (EST). The output of this instrument (in millivolts) is given by

$$I = k_e \int_{295}^{330} C_e(\lambda) G(\lambda) d\lambda, \quad (9)$$

where $C_e(\lambda)$ is the relative spectral response of the radiometer (see Fig. 2), $G(\lambda)$ is the global UV flux. The conversion factor $k_e = 30$ millivolts per mW/cm² has been provided by the manufacturer.

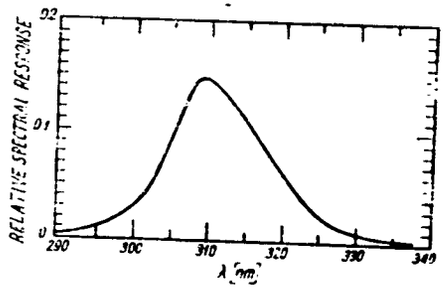

Fig. 2. Relative spectral response of the Eppley radiometer

C. *Robertson-Berger Sunburning Ultraviolet Dosimeter.* The sunburning dosimeter, manufactured by the Skin and Cancer Clinic of Temple University, has already been described by Berger et al. (1975). In essence a sensor unit housed in a weatherproof enclosure with a hemispherical quartz window is connected to an amplifier-digital recorder unit located at an inside site. The digital output in counts per half hour is given by

$$D = k_r \int_0^T \int_{290}^{330} \varepsilon_R(\lambda) G(\lambda) d\lambda dt, \quad (10)$$

where $G(\lambda)$ is again the global UV flux, and $\varepsilon(\lambda)$ denotes the sunburning meter relative response. For our instrument the constant k_r was found by using a calibrated standard lamp to be $0.164 \pm 5.6\%$ count/J/m² (Mo et al. 1974).

4. Observations. Our complete instrumental set-up is located on the roof of our solar research laboratory which is on top of the Space Sciences Research Building on the campus of the University of Florida. The Robertson meter has been operated continuously on a 24-hour basis; the Eppley meter is turned on at 6 : 00 AM and off at 6 : 00 PM each day automatically by a timer.

Between December 19, 1974 and January 20, 1975, we took all-sky pictures manually at a fifteen-minute interval whenever there was visible cloud variations. During February and March our motor drive unit was set up to take all-sky pictures automatically at twelve-minute intervals. A red filter and a gray scale were used to help distinguish cloud cover from the clear sky. After processing, the negatives were projected with an enlarger, on a grid made of concentric circles and radial lines. The distances between concentric circles were calibrated in such a way that the areas between two successive circles represent equal areas in the sky. Therefore, ten concentric circles and ten radial lines divide the entire

sky into 100 equal parts. To measure the percentage cloud cover of the sky, it is convenient to count the number of intersections covered by clouds on the grid. To insure accuracy, each picture was counted at least twice. Occasionally a picture had to be counted four or five times if the cloud could not be easily identified. We found the accuracy of this method to be usually within a few percent.

The correlation between the all-sky picture and the Eppley recording gives the instantaneous effect of clouds on the solar ultraviolet radiation reaching the ground. It is crucial to match the time of the two recordings accurately. A mark was made on the Eppley recording within a few seconds whenever a picture was taken. For reference and comparison, the local weather report was acquired from a nearby aviation station, which gave a description of visual observation on cloud cover and its base height.

5. Results and Discussion. The Eppley radiometer readings at the time all-sky camera pictures were taken were compared with nearby clear sky recordings at corresponding zenith angles. The ratio $R(C)$ of these two quantities for the all-sky camera pictures is plotted against relative cloud cover in Fig. 3.

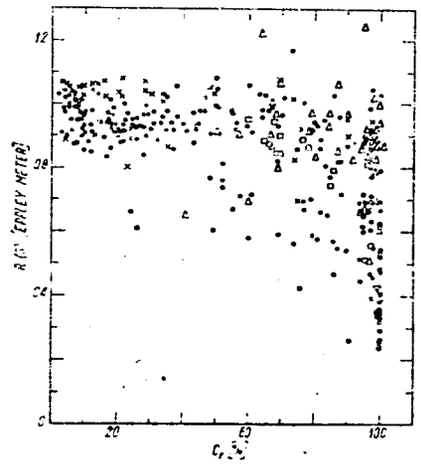

Fig. 3. The ratio $R(C)$ derived from the Eppley radiometer reading versus cloud cover. Symbols ○, ×, ●, △, and □ are used for high, middle, low, middle+high, and all types, respectively

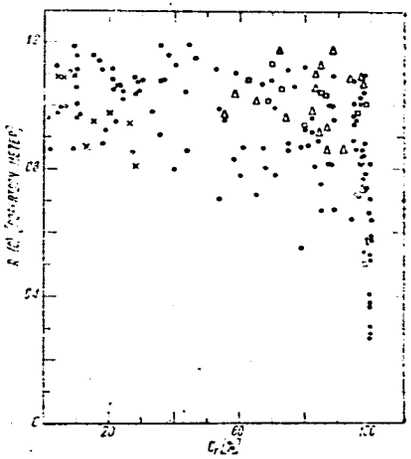

Fig. 4. The ratio $R(C)$ derived from the Robertson-Berger sunburn meter versus cloud cover. Symbols ○, ×, ●, △, and □ are used for high, middle, low, middle+high, and all types, respectively

Similarly, the quantity $R(C)$ can be derived from the Robertson-Berger Sunburning Meter counts. Since each printout represents an accumulation of the sunburning ultraviolet radiation in a half-hour period, two or three all-sky camera pictures are needed to get the average cloud cover for that period of time. The results are shown in Fig. 4.

Although the data we have collected in this pilot study are not numerous, certain features appear to be fairly evident. First of all, the linear dependence of $R(C)=G(C)/G(0)$ on C as prescribed by the empirical equation

$$G(C)=(1-FC)G(0) \tag{11}$$

is not quite clear from our data. Besides, the magnitude of the factor F quoted in the literature seems to be too high.

One should perhaps notice that all the low values of the ratio $R(C)$ are due to the blocking of the direct sunlight by low or cumuliform clouds. High clouds have much less effect on the sky ultraviolet radiation at the ground level.

Effort was made to fit our data points with the $R(\tau_C, \theta)$ curve calculated in Sec. 2, and to find qualitative estimates of cloud thickness for various kind of clouds. Considerable ranges of thickness variation were found for low and middle clouds, which probably suggested that some factors other than the optical thickness of clouds needed to be taken into consideration. The fitting of data points for thin and high clouds was quite good. According to the $R(\tau_C, \theta)$ curve, the optical thickness of those clouds should be in the neighborhood of 2; this is in agreement with our estimate by measuring the attenuation of direct sunlight with a sunphotometer.

Our measurements suggest that to study the influence of cloud cover on radiation phenomena in the atmosphere, it is necessary to have some quantitative characterization of the cloud cover. In routine meteorological observations, the only measured or estimated quantities associated with cloud cover are amount of clouds (relative cloudiness) and cloud base altitude; most previous work concerning the cloud effects on radiation are based on such quantities. Considering the pertinent cloud conditions discussed in *Appendix I*, it is not surprising that these quantities cannot represent adequately the complex structure of the cloud field in their influence upon the radiation field. Apparently we need a more realistic physical and statistical approach to deal with this problem. The next section outlines such an approach.

6. The Empirical Orthogonal Function Analysis. The empirical orthogonal functions or eigenvectors method can be used to analyze temporal variations and the spatial structure of the cloud pattern. The method allows us to represent the cloud pattern as a composition of basic patterns to which a definite physical meaning can be attached. The eigenvectors and their coefficients can be correlated with variables describing the radiation field, to determine the influence of clouds on the temporal and spatial variations of the radiation field. The advantage of the method is that it describes the random structure of the cloud field using only a few parameters. The basic properties of the eigenvectors method were described in the literature (Lorenz 1956, Alishouse et al. 1967) so that we shall give only a brief outline of the method.

Preliminary quantification of cloud pattern is made by photometric measurements of cloud photograph, so that the optical density at n points of the photograph is obtained. The complete set of observed data can be displayed as $m \times n$ (m photographs $\times n$ points) matrix. If the matrix is denoted by A then a_{ij} is the optical density at j^{th} point on i^{th} photograph. The observation matrix A can be expressed as a product of the eigenvector

matrix E and a matrix of associated coefficients C

$$A=EC. \tag{12}$$

In order to determine E and C, the eigenvalues of the symmetric matrix AA' are to be found by solving the equation

$$\det(AA'-\lambda I)=0, \tag{13}$$

where A' is the transpose of A and I is the indentity matrix. Eigenvectors Y_j are obtained from the equation:

$$AA'(Y_j)=\lambda_j(Y_j), \tag{14}$$

where Y_j is the j^{th} eigenvector corresponding to λ_j, and $j=1 \dots m$. After normalization of Y, the $m \times m$ matrix of orthogonal normalized vectors E is given.

The ratio of the particular eigenvalue to the sum of all eigenvalues represent the fraction of the total variance associated with the corresponding eigenvector. Usually several eigenvectors account for a majority of the total variance and the original pattern can be reproduced with great accuracy with the use of only the first few eigenvectors. The $m \times n$ matrix of coefficients C is:

$$C=E'A, \tag{15}$$

where E' is the transpose of E.

The eigenvectors represent the temporal variation of observed pattern, while the rows of C are associated eigenvectors coefficients which represent the spatial structure of the pattern. Thus the distribution of coefficients of the first eigenvector is governed by the major distribution of clouds on the sky, while the distribution of other eigenvector coefficients might be related to the thickness of the clouds.

The eigenvectors analysis technique has been applied to ten individual cloud patterns over the Gainesville area. The pictures of cloud cover were taken by our all-sky camera on March 13, 1974 at 12 minute intervals starting at 10h 27m EST. Initially the clouds covered all the sky but gradually clearance took place and at the end of the observation period cloud cover was only 56%.

The density of the film was determined in 100 points of each picture according to a 5 level gray scale, giving a 10 (picture) × 100 (points) array of data. The number 1 on this scale corresponded to the clear sky and number 5 to darkest thick clouds. The eigenvector analysis was performed on normalized set od data. The data were normalized by calculating the mean darkness of the film for every picture, subtracting the mean values from the data and dividing by the corresponding standard deviation.

The analysis yielded ten eigenvectors with components as a function of time, and 10 × 100 coefficients matrix with elements as a function of space.

The eigenvalues arranged in order of magnitude and cumulative percentage variance explained by the first six eigenvectors are shown in Table 2.

Table 2

Eigenvalues	3.842	1.349	1.092	0.821	0.702	0.601
Explained variance in %	38	52	63	72	78	84

The first two eigenvectors account for more than half of the variance of the total 10 × 100 array. The first three eigenvectors are displayed in Fig. 5 and the spatial distribution of coefficients associated with this three eigenvectors is shown in Figs 6a - 6c. The mean pattern of cloud field is shown on Fig. 7.

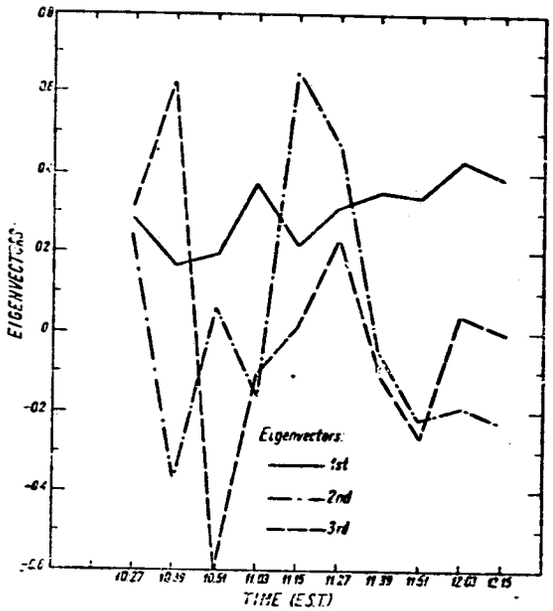

Fig. 5. Values of the first three eigenvectors

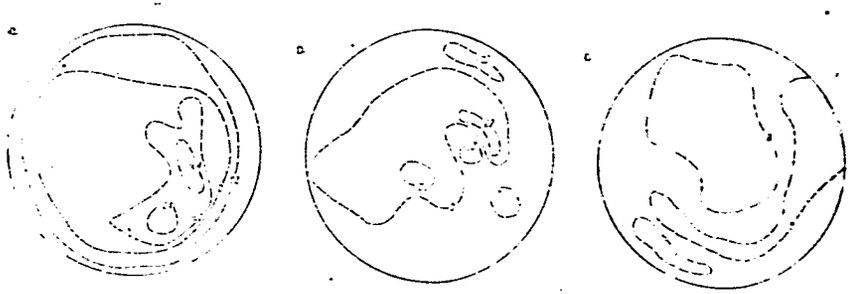

Fig. 6: a. Spatial distribution of coefficients of first eigenvector, b. Spatial distribution of coefficients of second eigenvector, c. Spatial distribution of coefficients of third eigenvector

The spatial distribution of the first eigenvector coefficients shows a close resemblance to the mean cloud pattern, with the majority of clouds gathered near the horizon and large patches of relatively lighter sky in the vicinity of zenits. The values of the components of the first eigenvector increase in time indicating the increasing contribution of the first pattern. This is in agreement with the fact of decreasing cloud cover during the observation period. The correlation coefficient between the components of the first eigenvector and the amount of cloud cover has the value −0.73. Thus the components of the first eigenvector exhibit the general tendency in the development of cloud field. In the spatial distribution of the second eigenvector coefficients, the largest values of coefficients are in the central area of the pattern, and components of the second eigenvector associated with this pattern vary substantially in time, with relatively smaller absolute values at the end of the observation period. This reflects the highly variable cloud cover of the area close to zenith, with clouds of different thickness. The distribution of the third eigenvector coefficients does not exhibit any features that can be easily associated with the physical situtation.

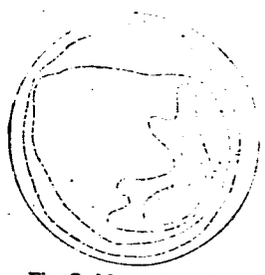

Fig. 7. Mean cloud field

As it was mentioned previously, the components of the eigenvectors and their coefficients can be correlated with the intensity of UV radiation to determine which aspects of the cloud pattern influences most of the UV radiation. In the present study only global solar UV flux as a function of time was measured, so that only correlations with time dependent components of the eigenvectors could be found. The correlation coefficients are 0.78, −0.41, 0.12 respectively. The negative value of the correlation coefficient for the second eigenvector confirms the supposition that the second pattern represents the variability in thickness of clouds.

Although the amount of data used in our analysis does not permit us to draw definite conclusions concerning the influence of a particular pattern on UV radiation, it indicates that not only the fraction of the sky covered by clouds but also their distribution determine the intensity of UV radiation. Moreover, the eigenvector analysis technique allows us to evaluate this influence in a quantitative way. Thus, this work suggests the undertaking of more intensive studies correlating higher resolution cloud photographic analysis with UV radiation measurements.

Acknowledgement: The authors wish to express their appreciation for the valuable consultation provided generously by R. D. McPeters on photographic photometry. Helpful assistance from J. Miller and G. B. Findley, Jr. are also acknowledged.

Appendix I. It is usually assumed that if the absolute cloudiness is C, then the probability that sun is obstructed by the clouds is also equal C. This assumption is valid for stratiform thin clouds, but can lead to considerable error when applied to convective clouds. Consider a cloud field in the from of cumulus clouds scattered uniformly over the sky. We assume that the clouds are in the form of inverted truncated paraboloid of revolution with the radius of the base R and vertical thickness T. It is also assumed that the bases of all the clouds are at the same level. The probability of a clear line of sight (PCLS) in direction of the sun, that is the probability that a solar ray will not meet with the cloud, depends on the cloudiness C, and the inclination of the solar rays to the plane of the horizon α (see Fig. Ia).

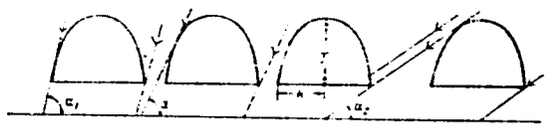

Fig. Ia. Geometry of cloud field

If the angle α is greater than α_1 − the angle between tangent to the cloud at its base, and the plane of the horizon, then the obstructed area is equal to the area of the base of the cloud, and PCLS does not depend on α. If absolute cloudiness is C, we have

$$P(C,\alpha)=1-C \quad \text{for} \quad \alpha>\alpha_1, \qquad \text{I (1)}$$

where $P(c,\alpha)$ is the probability of clear line of sight. The angle α_1 may be found from simple geometrical consideration as:

$$\alpha_1=\tan^{-1}\frac{2T}{R}. \qquad \text{I (2)}$$

According to Plank (1969), the ratio of cloud thickness to cloud diameter is fairly constant during the cloud development time and close to 1. In this case, we have $\alpha_1=75°$. The comparison of calculated probability with experimental data of Lund and Shanklin is presented on Fig. Ib. Lund and Shanklin estimated PCLS for different values of relative cloudiness reported by National Weather Service. Equation (3) is used for the conversion of relative cloudiness into absolute values.

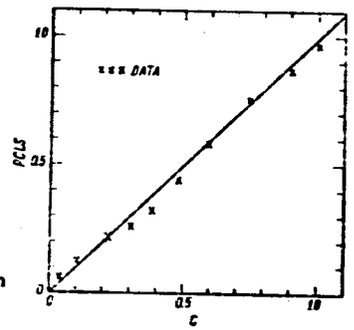

Fig. Ib. Probability of clear line of sight as a function of absolute cloudiness C for $\alpha>75°$

The second extreme case is when $\alpha<\alpha_2$, where α_2 is the smallest angle at which solar ray tangent to one cloud will not meet the neighboring cloud. The value of α_2 depends on distance S between clouds and satisfies the relation

$$4T(R+S)\tan\alpha_2-R^2\tan\alpha_2=4T^2. \qquad \text{I (3)}$$

The above relation reflects the condition that the solar ray inclined at angle α_2 and tangent to the cloud will graze the base of neighboring cloud at distance S. With the use of the simplifying assumption that the absolute cloudiness is represented by

$$C=\frac{4R^2}{(S+2R)^2} \qquad \text{I (4)}$$

equation I (3) becomes

$$C=\frac{(8TR\tan\alpha_2)^2}{(2T+R\tan\alpha_2)^4}, \qquad \text{I (5)}$$

and if $T/2R=1$

$$C=\frac{(16\tan\alpha_2)^2}{(4+\tan\alpha_2)^4}. \qquad \text{I (6)}$$

Value of C given by I (b) may be interpreted as the minimal absolute cloudiness at particular value of α_2 at which the solar ray tangent to one cloud will meet other cloud. The plot of C and C_r vs α_2 is shown on Fig. Ic. So if $\alpha<\alpha_2(C)$ the ratio of obstructed area to the total area is:

$$\frac{2R}{2R+S}=\sqrt{C}, \qquad \text{I (7)}$$

and

$$P(C,\alpha)=1-\sqrt{C}, \quad \alpha<\alpha_2(C). \qquad \text{I (8)}$$

For $\alpha_2<\alpha<\alpha_1$ the obstructed area is:

$$A=\frac{\pi R^2(4T^2-R^2\tan^2\alpha)^{3/2}}{6T^2R\tan\alpha}+\pi R^2\left(1-\frac{\beta}{2\pi}+\sin\frac{\beta}{2\pi}\right), \qquad \text{I (9)}$$

where

$$\beta=2\sin^{-1}\left(1-\frac{\tan^2\alpha}{16}\right)$$

and

$$P(C,\alpha)=1-C\left(1-\frac{\beta}{2\pi}+\frac{\sin\beta}{2\pi}\right)-\frac{C(16-\tan^2\alpha)^{3/2}}{24\pi\tan\alpha}. \qquad \text{(I (10)}$$

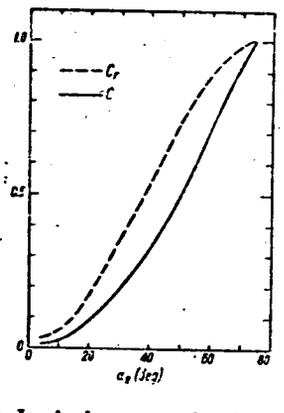

Fig. Ic. Angle α_2 as a function of C and C_r

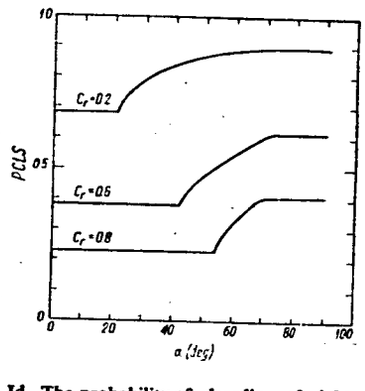

Fig. Id. The probability of clear line of sight as a function of α and relative cloudiness

Derivation of formulas are given in *Appendix II*. Thus, with aid of Eqs I (1), I (4), and I (10) we can calculate probability of clear line of sight for any given pair of values α and C. Figure Id presents the probability of clear line of sight as a function of the angle α, for relative cloudiness 0.2, 0.6 and 0.8. It shows that identification of probability of having the sun blocked by clouds with relative cloudiness is justified only if at specified value of C_r the angle α is smaller than α_2.

Appendix II. Assume that there is only one piece of cloud in the sky in the form of the inverted paraboloid of revolution with its vertex in the origin of the system of coordinates with Z axis directed downward (see Fig. IIa). The equation of the side surface of the cloud is:

$$Z=\frac{T}{R^2}(x^2+y^2); \quad Z<T. \qquad \text{II (1)}$$

The shade of the cloud in the plane $Z=T$, whose area is equal to the obstructed area on the earth surface consists of parabola with vertex in point A, and a segment of circle of radius R, Fig. IIb. Point A is the point of intersection of the X axis with the plane inclined at angle α and tangent to the cloud.

$$\alpha_A=\frac{4T^2+R^2\tan^2\alpha}{4T\tan\alpha}. \qquad \text{II (2)}$$

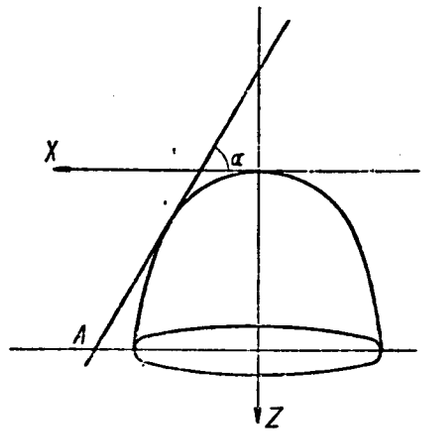

Fig. IIa. Geometry of a cloud

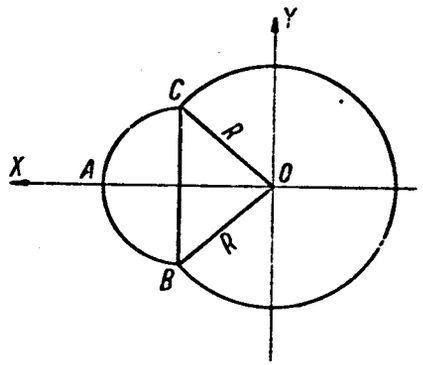

Fig. IIb. The shape of shade of cloud in horizontal plane

The chords of the parabola parallel to the Y axis are projections of the diameters of the circles, obtained by intersection of paraboloid with family of plains inclined at angle α to the horizon, on the plain $Z=T$. After simple consideration the equation of parabola may be obtained in the form

$$y^2=-\frac{xR^2\tan\alpha}{T}+\frac{4R^2T^2+R^4\tan\alpha}{4T^2}; \quad x_B<x<x_A, \qquad \text{II (2)}$$

where x_B is x^{th} coordinate of the centers of circles of intersection; $x_B=R^2\tan\alpha/2T$, the area limited by parabola and the chord BC is equal:

$$A_1=\frac{R(4T^2+R^2\tan^2\alpha)^{3/2}}{6T^2\tan\alpha}. \qquad \text{II (3)}$$

The length of the chord BC is

$$BC=R\left(1-\frac{R^2\tan^2\alpha}{4T^2}\right)^{1/2}, \qquad \text{II (4)}$$

so the angle between radii OB and OC is

$$\beta=2\sin^{-1}\left(1-\frac{R^2\tan^2\alpha}{4T^2}\right)^{1/2}, \qquad \text{II (5)}$$

and the area of the segment of the circle is:

$$A_2=\pi R^2-\frac{R^2\beta}{2}+\frac{R^2\sin\beta}{2} \qquad \text{II (6)}$$

where β is in radians. The sum A_1+A_2 gives the total obstructed area A. The fraction of a given area P on the earth surface obstructed by the cloud is then

$$f=\frac{A}{P}=\frac{R(4T^2+R^2\tan^2\alpha)^{3/2}}{P6T^2\tan\alpha}+\frac{\pi R^2}{P}+\frac{R^2\sin\beta}{2P}-\frac{R^2\beta}{2P}, \qquad \text{II (7)}$$

and because $\pi R^2/P=C$, and $T/2R=1$, f becomes

$$f=C\left(1-\frac{\beta}{2\pi}+\frac{\sin\beta}{2\pi}\right)+C\frac{(16-\tan^2\alpha)^{3/2}}{24\pi\tan\alpha}. \qquad \text{II (8)}$$

Probability of the clear line of sight is equal to $(1-f)$, which is given in Eq. I (10). It is easily seen that the assumption that there is only one piece of cloud in the sky does not have any influence on the final result I (10) which is valid in general case with any number of clouds.

Manuscript received by Editor: April 14, 1977.

REFERENCES

Alishouse J. C., Crone L. J., Fleming H. E., Van Cleef F. L., Work D. Q., 1967, *A discussion of empirical orthogonal functions on the application to vertical temperature profile*, Tellus, 19, 477 - 482.

Barry R. G., Chorley R. J., 1970, *Atmosphere, weather and climate*, Holt, Rinehart and Winston, Inc.

Berger D., Robertson D. F., Davis R. E., Urbach R., 1975, *Field measurements of biollogically effective UV radiation*, C.I.A.P. Monograph 5, 233 - 262, U.S. Dept. of Transportation.

Bener P., 1964, *Investigation on the influence of clouds on the ultraviolet sky radiation*, Contract AF61 (052) - 618, Technical Note 3, Davos.

Buttner K., 1938, *Physikalische Bioklimatologie*, Leipzig.

Goody R. M., 1964, *Atmospheric radiation*, Oxford, Clarendon Press.

Green A. E. S., Sawada T., Shettle E. P., 1974, *Photochemistry and photobiology*, 19, 251 - 259.

Lorenz E. N., 1956, *Empirical orthogonal functions and statistical weather prediction*, Sc. Rep. No. 1, Contract AF19 (604) - 1566, Dept. of Meteorology, MIT.

Lund T. A., Shanklin M. D., 1972, *Photogrammetrically determined cloud free lines of sight through atmosphere*, J. Appl. Meteor, 11, 773 - 785.

Matveev L. T., 1967, *Physics of the atmosphere*, U.S. Dept. of Commerce, Washington.

Mo T., Green A. E. S., 1974, *A climatology of solar erythema dose, photochemistry and photobiology*, 20, 483 - 496.

Mo T., Chai A. T., Green A. E. S., 1975, *An absolute calibration of the sunburn meter*, C.I.A.P. Monograph 5, 455 - 467, U.S. Dept. of Transportation.

Nack L. M., Green A. E. S., 1974, *Influence of clouds haze and smoke on the middle ultraviolet radiation reaching the ground*, Appl. Optics 13, 2405 - 2415.

Niylisk Kh. Yo., 1972, *On cloud characteristics in problems of radiational energetics in the Earth's atmosphere*, Atmospheric and Oceanic Physics 8, 270 - 276.

Plank W. G., 1969, *The size distribution of cumulus clouds in representative Florida population*, J. Appl. Meteor. 8, 46 - 67.

Shettle E. P., Green A. E. S., 1974, *Multiple scattering calculation of the middle ultraviolet reaching the ground*, Applied Optics, 13, 1567 - 1581.

WPŁYW ZACHMURZENIA NA NATĘŻENIE PROMIENIOWANIA ULTRAFIOLETOWEGO

Streszczenie

W celu zbadania wpływu zachmurzenia na natężenie promieniowania ultrafioletowego dochodzącego do powierzchni Ziemi zastosowano radiometr Eppleya i miernik Robertsona-Bergera przy jednoczesnym fotografowaniu nieba kamerą „all sky". Porównano wyniki badań z dotychczas stosowanymi zależnościami empirycznymi. Zastosowano metodę empirycznych funkcji ortogonalnych do badania rozkładu zachmurzenia i jego wpływu na natężenie promieniowania ultrafioletowego dochodzącego do powierzchni Ziemi.

Atmospheric Environment Vol. 12, pp. 2449–2454.

0004-6981/78/1201-2449 $02.00/0

CALCULATION OF THE RELATIVE INFLUENCE OF CLOUD LAYERS ON RECEIVED ULTRAVIOLET AND INTEGRATED SOLAR RADIATION*

J. D. SPINHIRNE and A. E. S. GREEN
University of Florida, Gainesville, Florida 32611, U.S.A.

(*First received* 1 *March* 1978 *and in final form* 6 *June* 1978)

Abstract–Discrete ordinate radiative transfer calculations are used to examine the relative influence of cloud layers on the received ultraviolet flux and the received solar energy for a plane parallel atmosphere. The wavelength dependence for the cloud influence on the integrated solar radiation is primarily a function of the interaction of the cloud layer with the surrounding atmosphere and the underlying surface. It is found that for u.v. wavelengths greater than 300 nm, the ratio of u.v. to solar energy flux transmission through the atmosphere is insensitive to changes of cloud height, cloud scattering parameters and surface albedo (for realistic values), but is dependent on cloud thickness. For wavelengths approaching and less than 300 nm, absorption by tropospheric ozone results in sensitivity to cloud height and surface albedo.

1. INTRODUCTION

Ultraviolet (u.v.) radiation is known to influence many biological processes and it is also known that the earth's ozone layer controls the amount of u.v. radiation which reaches the ground. In response to the great concern that anthropogenic modifications of the ozone layer might have significant health and agricultural impacts, there has been a rapidly expanding literature directed towards characterizing the u.v. spectral irradiance at the ground (Bener, 1972; Green *et al.*, 1974; Shettle and Green, 1974; Halpern *et al.*, 1974; Cutchis, 1974; Dave and Halpern, 1976; see also additional references listed in these works). As a result of these and subsequent works the problem of estimating the solar spectral irradiance at the ground under clear sky conditions is fairly well advanced. However, the problem of allowing for the influence of clouds upon the u.v. spectral irradiance has thus far received only limited attention (Halpern *et al.*, 1974 and Nack and Green, 1974) and much work remains to be done.

In this paper we will examine the relative effect of cloud layers on received u.v. and net solar radiation through use of radiative transfer calculations applied in the case of uniform, homogeneous cloud layers. The result of variation of cloud thickness, cloud height, droplet size distribution, surface albedo and the atmospheric ozone thickness upon u.v. and total solar radiation will be examined. The results presented will provide insight as to the relative influence of cloud cover on the u.v. and the net solar radiation. Our hope is that this insight will enable us to utilize the much larger body of information available on net solar radiation reaching the ground in the presence of clouds to predict the u.v. radiation reaching the ground for which only limited data is available.

2. COMPUTATIONAL PROCEDURE

Received radiation at the bottom of the atmosphere is both direct and diffuse. Whereas, the calculation of the direct component is a simple procedure, calculation of diffuse atmospheric radiation requires involved radiative transfer theory. A variety of radiative transfer methods have been applied for calculation of diffuse radiation in clear and cloudy atmospheres (Hunt, 1971). Both approximate calculation procedures and more exact methods involving much computational effort are possible. The discrete ordinate method for radiative transfer is an approximate solution, introduced originally by Chandrasekhar (1950), which gives good computational accuracy of fluxes with relatively minor computational labor. The discrete ordinate radiative transfer procedure has been applied in recent years to cloudy and hazy atmospheres (Yamamoto *et al.*, 1971; Nack and Green, 1974; Liou, 1976), and an adaptation of the discrete ordinate calculation described by Shettle and Green (1974) will be used in this study.

The solution is applied to a vertically inhomogeneous model atmosphere by dividing the atmosphere into horizontally homogeneous layers and applying appropriate boundary conditions between the solution for various layers. For each layer, the transfer properties are determined by the layer optical thickness, the single scattering albedo and the scatter-

* Supported in part by NASA Contract NAS9-15114.

ing phase function, all of which may be calculated through knowledge of the molecular and aerosol scattering and absorption within the layer.

Application of the discrete ordinate method as used in this study for calculation of u.v. spectral irradiance has been previously described by Shettle and Green (1974). Spectral irradiance values for a 2 nm band interval are determined at specific wavelengths with absorption coefficients for ozone appropriate to this band interval being used (Green, 1966). The influence of the atmosphere on the u.v. spectral irradiance may be defined in terms of a spectral flux transmission

$$T_{fuv}(\lambda_i, \mu_0) = \frac{F^{\downarrow}_{uv}(\lambda_i, \mu_0)}{\mu_0 f(\lambda_i)} \quad (1)$$

where $F^{\downarrow}_{uv}(\lambda_i, \mu_0)$ is the downward spectral irradiance received on a horizontal surface at the bottom of the atmosphere, $f(\lambda_i)$ the extraterrestrial solar spectral irradiance and μ_0 the solar zenith angle.

Determination of the total received solar energy requires integration over all solar wavelengths reaching the ground. By using broad spectral regions for the wavelength integration, computational effort can be decreased. Band weighted absorption parameters appropriate to the given spectral intervals must then be used. Fine wavelength integration intervals would be expected to produce more accurate results. However, for application of a more approximate radiative transfer solution such as the discrete ordinate method, the computation is intrinsically imperfect and the improvement of results by use of finer wavelength integration is limited. For this study the solar spectrum was divided so that the 0.7, 0.82, 0.94, 1.1, 1.38, 1.87 and 2.7 μm water vapor absorption bands were included as separate spectral regions. The region from 0.34 μm to 0.7 μm was further divided into four spectral regions of equal incident solar energy. For each spectral region, appropriate coefficients for molecular and aerosol scattering and gaseous absorption were determined. The coefficients for molecular and aerosol scattering in each spectral region were chosen to give values of scattering thickness equivalent to weighting by the spectral intensity of incident solar radiation. Absorption coefficients for ozone, water vapor, CO_2 and other gases in the visible region were computed from the data given by Selby and McClatchey (1975).

The flux transmission for the integrated solar energy may be given as

$$T_{fs}(\mu_0) = \frac{\Sigma_i F_s{\downarrow}(\Delta\lambda_i)}{\mu_0 S} \quad (2)$$

where $F_s{\downarrow}(\Delta\lambda_i)$ is the received downward energy in each spectral band for which a radiative transfer calculation is performed and S is the solar constant. In addition to the ten visible spectral intervals given above, the irradiance in the sub-340 nm region was determined by integrating over the spectral irradiance that was separately calculated for six u.v. wavelengths.

Since the integrated solar irradiance is being determined both with use of an approximate radiative transfer technique and with broad spectral integration, a comparison between the diffuse irradiance as calculated by the method of this study and the more exact solution of Dave and Braslau (1975) was undertaken. The results are given in Fig. 1. For the calculations shown, the model atmosphere used for the discrete ordinate solution was set up to be the same as in Dave and Braslau's (1975) Cl and Dl-ST models. The discrete ordinate calculation was applied with an eight layer atmospheric model. In the case of the cloud free Cl model, the values for diffuse transmission of solar energy through the atmosphere agreed for all zenith angles. For the Dl-ST model with a 3.57 optical thickness (0.55 μ) stratus cloud, the discrete ordinate calculation produced values of received diffuse solar energy that were a few per cent low for small zenith angles and a few per cent large for the extreme zenith angles.

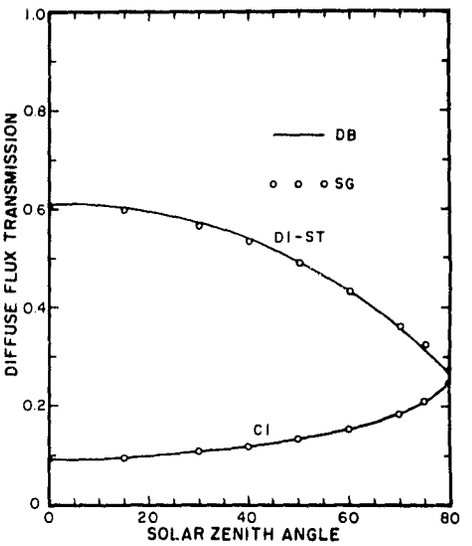

Fig. 1. Comparison of the received diffuse solar flux calculated by the wide wavelength interval, discrete ordinate method used in this study with the more exact calculations by Dave and Braslau (1975). Results for their Cl and Dl-ST models are shown. Model Cl is a cloud free atmosphere with nonabsorbing particulates, and for Model Dl-ST there is a stratus cloud layer and absorbing particulates.

3. MODEL

For all calculations in this study, aerosol scattering parameters were determined using the "Haze L" size distribution by Deirmendjian (1969). Unless otherwise noted, an aerosol refraction index of 1.50–0.01i and a total particulate optical depth of 0.125 at 590 nm were used. The particulate height distribution was that given by Shettle and Green (1974).

The water vapor and mixed gas profiles for the model atmosphere is the representation given by McClatchey *et al.* (1970) for midlatitude summer

conditions. The ozone vertical profile given by Shettle and Green (1974) with a total ozone thickness of 0.318 cm is used unless otherwise noted.

Cloud layers will be defined by the total optical thickness at 590 nm and by the height for the top and bottom of the cloud layer. The phase function for cloud scattering was computed using the C1 cloud size distribution of Deirmendjian with a refraction index of $1.34+0.0i$. Legendre polynomial coefficients for use in the discrete ordinate transfer solution were calculated directly from the cloud scattering phase function. Unless otherwise defined, a cloud with a base at 3 km and top at 4 km will be used for model calculations.

4. RESULTS

The relative influence of cloud cover on received u.v. and total solar energy will be presented in terms of the ratio of u.v. and total solar energy flux transmission through the atmosphere.

$$R_l(\lambda_l, \mu_0) = \frac{T_{fuv}(\lambda_l, \mu_0)}{T_{fs}(\mu_0)}. \quad (3)$$

Values of R_l were calculated as a function of cloud thickness, cloud height and surface albedo. Results for five u.v. wavelengths are to be presented — 290, 300, 310, 320 and 330 nm.

The behavior of the u.v. to total energy transmission ratio as a function of solar zenith angle in the case of zero surface albedo is shown in Fig. 2. The decrease of u.v. spectral irradiance as the zenith angle increases is primarily due to ozone absorption. The actual values of the u.v. total energy transmission ratio will be strongly dependent on the atmospheric ozone thickness, and the values given in Fig. 2 apply only for a thickness of 0.318 cm of ozone.

As seen in Fig. 2, the presence of a cloud layer of increasing thickness acts to increase the ratio of the u.v. to solar energy flux transmission through the atmosphere. One possible factor is that both the cloud optical thickness decreases and the droplet scattering phase function becomes more sharply forward-peaked for shorter wavelengths. Values of cloud optical thickness, τ_c, and the asymmetry factor of the cloud scattering phase function, g, are given in Table 1 as a function of wavelength. The transmission through an isolated cloud layer is thus greater for shorter wavelengths. However, it was found that changes in the cloud droplet distribution did not appreciably effect the ratio of u.v. to solar energy flux transmission through a cloudy atmosphere. Even when the values given in Fig. 2 are recomputed using a constant cloud optical thickness and scattering phase function with wavelength, the results are not significantly changed.

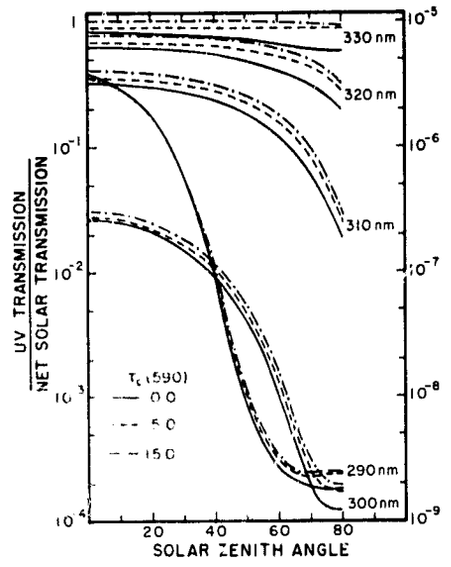

Fig. 2. The ratio of total transmission, diffuse plus direct, for u.v. radiation and total solar energy as a function of solar zenith angle. Values for three different cloud thicknesses, τ_c, at each of five wavelengths, 290, 300, 310, 320 and 330 nm are shown. The scale on the left applies for all wavelengths except 290 nm for which the scale on the right is used. In this case a surface albedo of 0.0 was assumed. The values shown are for an ozone thickness of 0.318 cm.

The behavior of the u.v. to solar energy flux transmission ratio with increasing cloud thickness is due primarily to the interaction of the cloud layer scattering with that of the surrounding atmosphere. The scattering thickness of the cloud-free atmosphere is much greater at u.v. wavelengths than for visible wavelengths. In the case of zero surface albedo as in Fig. 2, there will be significant reflectivity by molecular scattering beneath the cloud layer for the shortwave radiation but very little reflectivity under the cloud when considering the integrated solar radiation. A doubling interaction between the cloud layer reflectivity and scattering by the underlying atmosphere results in a smaller decrease of the surface u.v. irradiance with increasing cloud thickness. The effect is moderated by the u.v. radiation incident on the cloud top being more diffuse than the integrated solar radiation, but not sufficiently moderated to give a relatively greater decrease of the surface u.v. irradiance with increasing cloud thickness.

It can also be seen from Fig. 2 that the behavior of

Table 1. Cloud optical thickness τ_c and scattering phase function asymmetry factor g as a function of wavelength

λ	290	310	330	405	490	590	690	790	920	1110	1400	1900	3050
τ_c	4.56	4.69	4.78	4.91	4.96	5.00	5.03	5.07	5.11	5.16	5.25	5.38	5.79
g	0.860	0.860	0.859	0.858	0.856	0.853	0.850	0.846	0.841	0.834	0.823	0.802	0.768

Realistic cloud cover, however, is not uniform and homogeneous. For broken cloud cover, the ratio of the instantaneous received u.v. and net solar radiation will change rapidly. Since the u.v. radiation incident on a cloud layer is much more diffuse than the visible radiation, a partial coverage cloud which blocks the direct solar radiation will decrease the total received visible flux to a greater extent than the total received u.v. flux. Over time periods sufficiently long to average such fluctuations, however, it might be expected that the relative decrease of the received u.v. and net solar radiation would be similar to that predicted for uniform cloud cover of an appropriate thickness. Either much more elaborate radiative transfer calculations or a body of experimental data would be required to determine if this is the case.

REFERENCES

Bener P. (1972) Technical Report, European Research Office, U.S. Army, London, Contract DAJA 37-68-C-1017.

Chandrasekhar S. (1950) *Radiative Transfer*. Dover, New York, p. 393.

Cutchis P. (1974) Stratospheric ozone depletion and solar ultraviolet radiation on earth. *Science* **184**, 13–19.

Dave J. V. and Braslau N. (1975) Effect of cloudiness on the transfer of solar energy through realistic model atmospheres. Report RC 4869, IBM Scientific Center, Palo Alto, CA.

Dave J. V. and Halpern P. (1976) Effect of changes in ozone amount on the ultraviolet radiation received at sea level of a model atmosphere. *Atmospheric Environment* **10**, 547–555.

Deirmendjian D. (1969) *Electromagnetic Scattering on Spherical Polydispersions*. Elsevier, New York, p. 290.

Furukawa P. M. and Heath D. F. (1973) The apparent spectral ultraviolet reflectances of various natural surfaces. NASA-NCAR Solar u.v. Measuring Program (unpublished).

Green A. E. S. (1966) *The Middle Ultraviolet: Its Science and Technology*. John Wiley, New York.

Green A. E. S., Sawada T. and Shettle E. P. (1974) The middle ultraviolet reaching the ground. *Photochem. Photobiol.* **19**, 251–59.

Halpern P., Dave J. V. and Braslau N. (1974) Sealevel solar radiation in biologically active spectrum. *Science* **186**, 1204–1280.

Hunt G. E. (1971) A review of computational techniques for analysing the transfer of radiation through a model cloudy atmosphere. *J. Quant. Spectrosc. Radiat. Transfer* **11**, 655–90.

Liou K. N. (1976) On the absorption, reflection and transfer of solar radiation in cloudy atmospheres. *J. atmos. Sci.* **33**, 789–805.

McClatchey R. A., Fenn R. W., Selby J. E. A., Garing J. S. and Volz F. E. (1970) Optical properties of the atmosphere. Report AFCRL-70-0527, Air Force Cambridge Research Laboratories, Bedford, MA.

Nack M. L. and Green A. E. S. (1974) Influence of clouds, haze and smog on the middle ultraviolet reaching the ground. *Appl. Opt.* **13**, 2405–2415.

Selby J. E. A. and McClatchey R. A. M. (1975) Atmospheric transmittance from 0.25 to 28.5 μm: Computer code LOWTRAM 3. Report AFCRL-TR-75-0255, Air Force Cambridge Research Laboratories, Bedford, MA.

Shettle E. P. and Green A. E. S. (1974) Multiple scattering calculation of the middle ultraviolet reaching the ground. *Appl. Opt.* **13**, 1567–1581.

Yamamoto G., Tanaka M. and Asano S. (1971) Radiative heat transfer in water clouds by infrared radiation. *J. Quant. Spectrosc. Radiat. Transfer* **11**, 697–708.

CLOUD EFFECTS ON ULTRAVIOLET PHOTOCLIMATOLOGY

A. E. S. Green and J. D. Spinhirne

Interdisciplinary Center for Aeronomy and
Other Atmospheric Sciences

University of Florida, Gainesville, FL 32611

ABSTRACT

The purpose of this study is to quantify for the needs of photobiology the influence of clouds upon the ultraviolet spectral irradiance reaching the ground. Towards this end we first develop analytic formulas which approximately characterize the influence of clouds upon total solar radiation. These may be used in conjunction with a solar pyranometer to assign an effective visual optical depth for the cloud cover. We also develop a formula which characterizes the influence of the optical depth of clouds upon the UV spectral irradiance in the 280-340 nm region. Thus using total solar energy observations to assign cloud optical properties we can calculate the UV spectral irradiance at the ground in the presence of these clouds. As incidental by-products of this effort, we have found convient formulas for the direct and diffuse components of total solar energy.

1. INTRODUCTION

There is now great concern that anthropogenic modifications of the ozone layer might alter the ultraviolet (UV) radiation reaching the ground. This concern has led to a rapid expansion of the literature on the biological impacts of UV radiation and on the quantitative aspects of the UV spectral irradiance reaching the ground [Bener (1972), Green, Sawada and Shettle (1974) (GSS), Shettle and Green (1974), Halpern et al., (1974), Dave and Halpern (1976)]. Unfortunately clouds are a large source of uncertainty in such work. Nack and Green (1974), Halpern, Dave and Braslau (1974), and Spinhirne and Green (1978) have carried out radiative transfer calculations of the influence of cloud cover on the received UV irradiance for wavelengths in the 280-340 nm range, at various solar zenith angles, and various ground reflectivities. To facilitate the practical use of such calculations in photobiological applications, we attempt, in the present work, to express the results of these earlier works and our supplementary calculations in terms of convenient analytic forms.

The strategy of the present effort is to use observations of total solar energy to infer the optical properties of clouds. Thus the reduction of total solar irradiance from the expected cloud-free levels can be used to estimate the effective cloud optical depth, the critical parameter needed to improve UV calculations. Characterizations of total solar energy will be discussed in Section 2.

2. CLEAR SKY TOTAL IRRADIANCES

For reference in our cloudy sky work, it is valuable to have approximate representations of the clear sky irradiances for various sun angles and ground reflectivities. Using Beer's law the monochromatic downward component of the transmitted (t) solar irradiance may be calculated using

$$B_t(\theta,\lambda) = \mu H(\lambda)\exp - \Sigma_i\, w_i(y)k_i(\lambda)/\mu_i \qquad (1)$$

where $H(\lambda)$ is the extraterrestrial solar spectral irradiance, θ is the solar zenith angle, i = 1, 2, 3 denote air, particulates and other absorbing components, $w_i(y)$ denote the altitude dependent vertical thickness and $k_i(\lambda)$ the wavelength dependent attenuating coefficient. To allow approximately for the fact that the earth is round, we will use a generalization of $\mu = \cos\theta$ given by

$$\mu_i = [(\mu^2 + \kappa_i)/(1 + \kappa_i)]^{\frac{1}{2}} \tag{2}$$

where κ_i are species dependent dimensionless parameters. The equivalent generalization of $\sec\theta = \mu^{-1}$ is $\sigma = \text{seq}\theta = \mu_i^{-1}$ (GSS, 1974).

To calculate the "transmission" for the downward component of the total transmitted (t) solar irradiance, we use

$$T_{Tt} = \frac{\mu \sum \Delta\lambda_j H(\lambda_j) e^{-\sum_i w_i k_i/\mu_i}}{\mu S} \tag{3}$$

where $S = \sum \Delta\lambda_j H(\lambda_j)$. The wavelength intervals used in the present calculations are given in Spinhirne and Green (1978).

We may represent the results of our total solar transmission calculations to a good approximation by the "random" model which Mayer (1947) and Goody (1952) developed for infrared band transmission. Thus we may use

$$T_{Tt} = \exp - \frac{\alpha\sigma}{(1+\beta\sigma)^{\frac{1}{2}}} \tag{4}$$

where the κ parameter used in σ has been determined by the rule

$$\bar{\kappa} = (\kappa_r\tau_R + \kappa_p\tau_p)/(\tau_R + \tau_p) \tag{5}$$

where $\kappa_R = 1.8\text{x}10^{-3}$, $\kappa_p = 0.3\text{x}10^{-3}$ and τ_R and τ_p are the Rayleigh and particulate optical depths at 550 nm. Figure 1 shows the calculated values (points) using Eq. (3) and the analytic representations (solid lines) using Eq. (4) for the various aerosol optical depths with parameters given by

$$\alpha = \alpha_1 + \alpha_2\tau_p \tag{6}$$

with $\alpha_1 = 0.2138$ $\alpha_2 = 0.8848$ and $\beta = 0.1717$. It is seen that the random model transmission formula with this assignment of parameters works quite well. The result is not entirely unexpected if one considers the physical analogies involved in the calculation of infrared band model transmission and the calculation of total solar energy transmission (see Green and Wyatt, 1965).

To calculate the downward diffuse (d) irradiance (skylight!) we adapted the discrete ordinate radiative transfer code of Shettle and Green (1974) to obtain the "diffuse transmission" for total solar radiation given by

$$T_{Td} = \frac{\sum \Delta\lambda_j F\downarrow(\lambda_j)}{\mu S} \quad . \tag{7}$$

We have represented the calculated results analytically using

$$\mu T_{Td} = K \exp - \frac{\gamma\sigma}{(1+\delta\sigma)^{\frac{1}{2}}} \tag{8}$$

with the parameters given by

$$K = K_1 + K_2\tau_p \tag{9}$$

and

$$\gamma = \delta = \gamma_1 + \gamma_2\tau_p \tag{10}$$

with $K_1 = 0.0716$ $K_2 = 0.8642$ $\gamma_1 = 0.283$ $\gamma_2 = 1.302$. The lower curves in Fig. 1 show the fits to the numerical calculations (points). The fits are surprisingly good considering the fact that the physical processes are so different from those implied in the random model. The fits can be adjusted to well within 1% if we relaxed the specification that $\gamma = \delta$.

To allow for the influence of ground albedo (Lambertian reflectivity) we may use a device of Shettle and Green (Eq.43). This is based upon the assignment of a reflectivity parameter r which is the fraction of the total radiation reflected by the surface which is scattered back to the surface by the atmosphere. Thus for any albedo the global transmission for solar radiation may be represented approximately by

$$T_{Tg} = \frac{T_{Tt} + T_{Td}}{1 - Ar} \tag{11}$$

where $r = 0.124$ and T_{Tt} and T_{Td} are given by Eqs. (6) and (8) respectively.

3. CLOUD EFFECTS UPON TOTAL SOLAR RADIATION

Dave and Braslau (1975), Liou (1976), and Spinhirne and Green (1978) have calculated the total solar radiation penetrating various cloud thicknesses. Here we consider the ratio of the downward component of solar radiation in the presence of a homogeneous cloud layer of optical thickness τ (at 550 nm) to the total downward solar radiation for a cloudless sky. Thus we characterize the transmissivity of the cloud layer by the ratio

$$R(\tau,\mu) = \frac{\Sigma_j F_j{\downarrow}(\Delta\lambda_j,\mu,\tau)}{\Sigma_j F_j{\downarrow}(\Delta\lambda_j,\mu,0)} \tag{12}$$

where $F_j{\downarrow}(\Delta\lambda_j,\mu,\tau)$ is the total received downward energy in each spectral band used in the radiative transfer calculation.

We have obtained good fits to the results of our radiative transfer calculations with the surprisingly simple formula

$$R_T(\tau,\mu,A) = \exp - \frac{\tau(1-r_1A)}{[a^2(\mu-\mu_o)^2 + c\tau(1-r_2A)]^{\frac{1}{2}}} \tag{13}$$

where $a = 16.0$, $\mu_o = 0.240$, $c = 9.13$, $r_1 = 0.922$ and $r_2 = 0.952$. Figure 2 illustrates the fits of R_T vs. μ for $\tau = 2$, 10, and 30 when $A = 0.1$ and $A = 0.5$.

We see that Eq. (13) provides an analytic representation of the three dimensional hypersurface $R_T(\tau,\mu,A)$ which expresses the variation of the total solar radiation with sun angle (through μ) ground albedo (A) and cloud thickness (τ) in terms of only five adjusted parameters. Let us next consider the corresponding representations for spectral irradiance in the 280 to 340 nm region.

4. ULTRAVIOLET SPECTRAL IRRADIANCES FOR CLEAR SKY

The ultraviolet spectral irradiance problem has the wavelength (λ) and the ozone optical depth (τ_3) as important additional degrees of freedom. The downward transmitted spectral irradiance at the ground may be computed simply using

$$B_t(\lambda,0) = \mu H(\lambda) \exp\left[-\frac{\tau_1}{\mu_1} - \frac{\tau_2}{\mu_2} - \frac{\tau_3}{\mu_3}\right] \tag{14}$$

where $H(\lambda)$ is the extraterrestrial solar irradiance, τ_1, τ_2, and τ_3 denote the wavelength dependent Rayleigh, aerosol and ozone optical depths, respectively, and μ, μ_1, μ_2 and μ_3 denote the $\cos\theta$ and generalized cosine functions for these species. If we now specify the optical depths of the three components at a standard wavelength ($\lambda_o = 300$ nm) and their dependence on wavelength, we can

simply calculate the downward transmitted component of the sun's UV irradiance. The spectral dependence of the optical depths for ozone, air and a representative aerosol model in the wavelength region of interest may be represented analytically by

$$\tau_1 = \tau_a(\lambda_o/\lambda)^{\nu_a} \ , \ \tau_2 = \tau_p(\lambda_o/\lambda)^{\nu_p} \ ,$$

and

$$\tau_3 = \tau_{30}\left[\frac{\beta + 1}{\beta + \exp(\lambda-\lambda_o)/d}\right] \tag{15}$$

where λ_o = 300 nm, τ_a = 1.221, ν_a = 4.27, τ_p = 0.365, ν_p = 0.58, β = 0.0439, d = 8 nm, and τ_{30} = 3.2. Of course, τ_p and τ_{oz} are dependent upon atmospheric conditions.

Skylight or the diffuse irradiance is particularly important in the ultraviolet. Dave and Furukawa (1966) have calculated UV skylight for the case of a purely molecular atmosphere. To deal with the turbid atmosphere, Green, Sawada and Shettle (GSS, 1974) developed a semi-empirical analytic representation to fit the synthesis of 10 years of UV spectral irradiance measurements by Bener (1972). In addition, Shettle and Green (1974) have used a fast and inexpensive radiative transfer calculational technique to obtain the UV diffuse component in a turbid atmosphere. Dave and Braslau (1975) have also completed UV radiative transfer calculations using a much more refined computation which can serve as a standard of accuracy in atmospheric radiative transfer calculations. These sets of calculations can also be approximately represented by the GSS empirical formulas with minor parameter adjustments.

The GSS semi-empirical formula for the diffuse spectral irradiance has appeared in the literature with several minor variations and with somewhat differing parameter sets. It is believed that their analytic representations of radiative transfer calculations or experimental data can be improved from the 25% level of accuracy to the 5% level by using molecular band models (Green and Wyatt, 1965) rather than Beer's law as a point of departure. However, pending the completion of this work, we recommend using the version and parameters of the GSS formula in Green, Mo and Miller (1974). To correct for ground reflectivity upon clear sky global spectral irradiance, we use the ground-air ground-reflectivity function of Shettle and Green (Eq. 46).

5. CLOUD EFFECTS UPON UV SPECTRAL IRRADIANCES

To represent cloud effects upon UV spectral irradiances we use the same basic methodology as that used to represent cloud effects on total solar radiation. Thus we assume that the ratio of the global cloudy sky spectral irradiance to the global clear sky spectral irradiance (for A = 0) may be represented by a slight generalization of the form

$$R_{uvg} = \exp - \frac{\tau}{\{a^2[(\mu-\mu_o)^2 + \kappa^2\tau_r^2] + c\tau\}^{\frac{1}{2}}} \tag{16}$$

where $a = a_o[\tau_R/(\tau_R + \tau_{oz})]^2$ and a_o = 25.14, μ_o = 0.4181, κ = 0.732, c = 16.26. Figure 3 illustrates the fits of R_{uvg} vs. μ for τ = 2, 10 and 30 and for several wavelengths. The magnitudes of the results are quite good although the small variations with μ are not precisely described. However, the simplified radiative transfer calculations themselves might not be accurate on such fine points.

We have explored the dependence of the R_{uvg} upon ground reflectivity. We have had reasonable success with the simple device of replacing τ in Eq. (16) by $\tau(1-rA)$ with r = 0.69 [see Eq. (13)]. Undoubtedly we can do better by letting r be wavelength dependent but since UV ground reflectivities are low (Furukawa and Heath, 1973) this simple correction should handle many situations.

6. APPLICATIONS

The basic strategy of this applied study is to take advantage of the large body of solar radiation measurements to assess the optical property of clouds. Thus the local user would use observations of ground level total solar irradiances together with T_{Tg}, given by Eq. (11), and R_T, given by Eq. (13), to establish the τ values of clouds in the visible region. Here we can take advantage of the fact that Eq. (13) is algebraically invertible. First we cast Eq. (13) to the random model form

$$R = \exp - (\tau/\tau_1)/[1 + (\tau/\tau_2)]^{\frac{1}{2}} \quad . \tag{17}$$

Then by algebra we find the visible optical depth, τ, using

$$\tau = (\gamma nR)^2 \frac{\tau_1^2}{2\tau_2} 1 \mp \left[1 + \frac{4}{(\gamma nR)^2}\left(\frac{\tau_2}{\tau_1}\right)^2\right] \tag{18}$$

Next we translate visible ground albedo into UV ground albedo using the data of Heath and Furukawa (1973). Then using the CSS formula for the clear sky, together with Eq. (16), we calculate the UV spectral irradiance at the ground from a cloudy sky. We hope in time to relate our results to spectral irradiance observations from satellites (Heath, Mateer and Krueger, 1973).

It should be noted that at $\lambda \sim 300$ nm the cloud transmission ratio [Eq.(16)] is sensitive to the ozone concentration in the cloud (Spinhirne and Green, 1978). The characterization of this sensitivity remains to be established.

When the cloud thicknesses are not uniform we must first establish a distribution function for the optical depth. This can be done by using a time trace of the total solar radiation to infer [via Eq. (13)] the time variation of τ over the observing site. Then using these τ in conjunction with Eq. (16) and GSS formula for the clear sky UV spectral irradiance we may determine a distribution function for the UV spectral irradiance for a cloudy sky.

We are currently involved in practical tests of the foregoing procedures by independent measurements of total solar irradiances and UV spectral irradiances when clouds are present. From our preliminary investigations we are confident that the procedure should work reasonably well when the horizontal scale of inhomogeneities is small compared to the vertical scale. It is not yet clear how the method would work for the case of widely scattered clouds but such studies are also underway.

7. SUMMARY AND CONCLUSIONS

We have defined a procedure for translating observations of total solar irradiances when clouds are present into estimates of UV spectral irradiances. The procedure can be implemented with the aid of a modern desk top computer. The essential aspect of our procedure is the use of semi-empirical representations of diffuse radiative transfer obtained by outputs of complex radiative transfer calculations made with large computers. Our work indicates that these outputs lend themselves to analytic representations which are far more convenient in application than the tabular outputs themselves. For example, once the analytic representations of the UV spectral irradiance vs. λ, θ, etc. are available, one can by the methods described by GMM calculate daily UV dose, monthly dose, annual dose, etc. One can also integrate over various measured or assumed spectral response function (action spectra). The present work is a feasibility study which indicates that it is possible to implement such methodology.

ACKNOWLEDGMENT

The authors would like to thank J. M. Schwartz, K. R. Cross, L. A. Smith and Dr. F. Riewe for their valuable assistance in the calculations reported here.

This work was supported in part by the National Aeronautics and Space Administration under Grant No. NAS9-15114.

REFERENCES

Bener, P., 1972, Final Technical Report", European Research Office, U.S. Army, London, Contract DAJA 37-68-C-1017.

Dave, J. V. and Braslau, N., 1975, "Effect of cloudiness on the transfer of solar energy through realistic model atmospheres", Report RC 4869, IBM Scientific Center, Palo Alto, CA.

Dave, J. V., and Furukawa, P. M., 1966, "Scattered radiation in the ozone absorption bands at selected levels of a terrestrial, Rayleigh atmosphere, Meteorological Monographs, 7, 29.

Dave, J. V., and Halpern, P., 1976, "Effect of changes in ozone amount on the ultraviolet radiation received at sea level of a model atmosphere." Atmospheric Environment, 10, 547-555.

Furukawa, P. M., and Heath, D. F., 1973, "The apparent spectral ultraviolet relectances of various natural surfaces. NASA-NCAR Solar UV Measuring Program, 9/17/73.

Goody, R. M., 1952, Quant. J. Roy. Met. Soc., 78, 165.

Green, A. E. S., Mo, T. and Miller, J. H., 1974, "A study of solar erythema radiation doses, Photochem. and Photobiol. 20, 473-482.

Green, A. E. S., Sawada, T., and Shettle, E. P., 1974, "The middle ultraviolet reaching the ground", Photochem. and Photobiol. 19, 251-259.

Green, A. E. S., and Wyatt, P. J., 1965, Atomic and Space Physics, Addison-Wesley Publishing Co., Inc., Reading, MA.

Halperin, P., Dave, J. V., and Braslau, N., 1974, "Sealevel solar radiation in the biologically active spectrum, Science, 186, 1204-1280.

Heath, D. F., C. L. Mateer, and Krueger, A. J., 1973, The Nimbus-4 backscatter ultraviolet (BUV) atmospheric ozone experiment: Two years operation, Pure Appl. Geophys., 1238, 106-108.

Liou, K. N., 1976, "On the absorption, reflection and transfer of solar radiation in cloudy atmospheres, J. Atmos. Sci., 33, 798-805.

Mayer, H., 1947, "Methods of opacity calculations, Los Alamos Scientific Laboratory, LA-647.

Nack, M. L. and Green, A. E. S., 1974, "Influence of clouds, haze and smog on the middle ultraviolet reaching the ground, Appl. Opts. 13, 2405-2415.

Shettle, E. P. and Green, A. E. S., 1974, "Multiple scattering calculations of the middle ultraviolet reaching the ground, Appl. Opts., 13, 1567-1581.

Spinhirne, J. D. and Green, A. E. S., 1978, Submitted for publication.

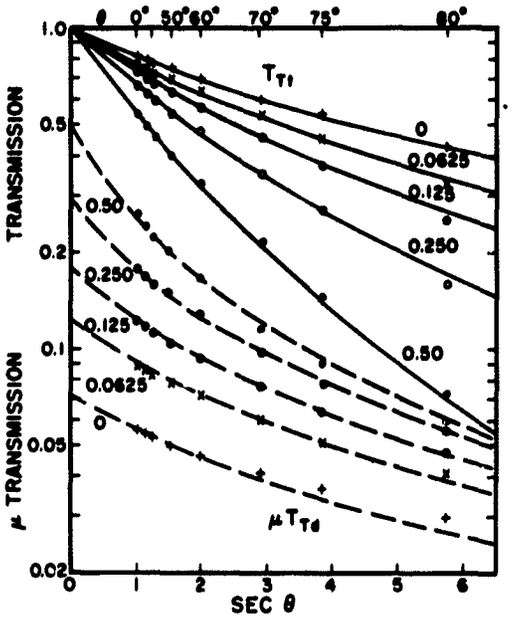

Figure 1. DIRECT TRANSMISSION AND μ x TRANSMISSION FOR DIFFUSE SOLAR RADIATION

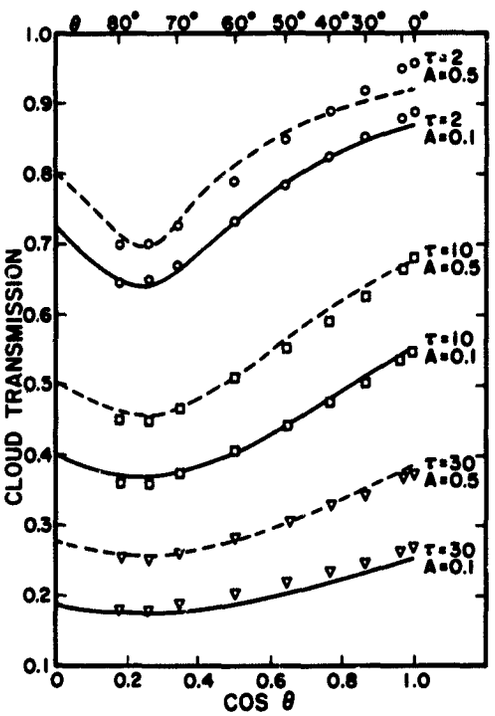

Figure 2. RATIO OF CLOUDY TO CLEAR SKY SOLAR IRRADIANCES

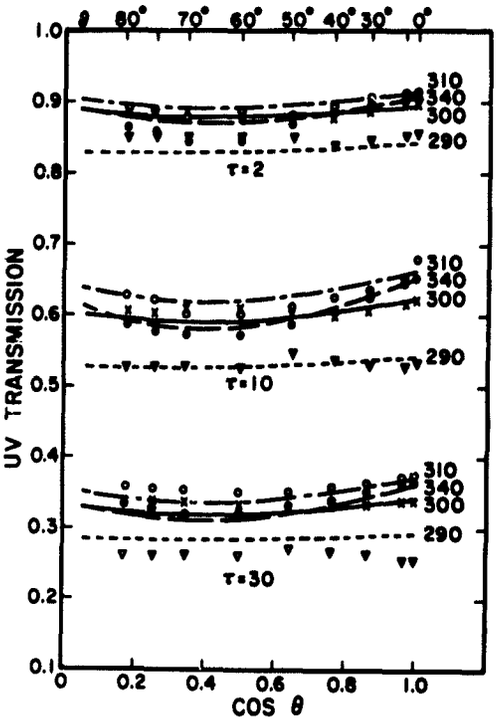

Figure 3. RATIO OF CLOUDY TO CLEAR SKY UV SPECTRAL IRRADIANCES

Reprinted from,
Inversion Methods in
Atmospheric Remote Sounding

ANALYTIC MODEL APPROACH TO THE INVERSION OF SCATTERING DATA

Alex E. S. Green and Kenneth F. Klenk
University of Florida

We apply an analytic model approach which has been developed in nuclear studies to several simple atmospheric inversion problems. We illustrate by past work on the solar aureole that this method gives a sharp determination of aerosol size distribution parameters. We show that this analytic approach, together with ground level point sampling data measurements, may be used to infer information on the tropospheric ozone profile.

I. ATMOSPHERIC AND NUCLEAR OPTICS

Many of us who are now involved in atmospheric inversion problems were previously involved in analogous problems in other disciplines. As is natural, we try to bring to bear the experience, sense of aesthetics, or prejudices, if you will, which we have acquired in these other fields. The beauty of this conference as it is developing following some of the earlier papers is the sense of open-mindedness which has emerged. It is as if this conference has said, "Let a thousand flowers blossom."

In my own (Green) case, my main prior involvement with inversion problems has been in connection with two nuclear physics endeavors based largely upon scattering data--(1) inferring the nature of the fundamental interaction between neutrons and protons, and (2) inferring the detailed nature of the nuclear potential manifest in the shell and optical models of the nucleus. Let me use

the first problem as an illustration of how understanding is advanced in scattering inversion problems.

When the neutron was discovered in 1932, the fundamental problem in nuclear physics became that of inferring the basic force between neutrons and protons. The approach followed has been to perform scattering experiments, i.e., fire neutrons or protons on hydrogen targets, and examine the emerging angular distributions (phase functions) and polarizations at various energies (wavelengths) of the outgoing particles. The hope was to be able to test various proposed two-body potentials which when inserted into the Schrödinger equation or Dirac equation might account for these data within statistical error. This was the main line of approach in nuclear physics until the early 1960s when the only phenomenological models which could fit the 0 to 400 MeV array of scattering data and auxiliary data such as the properties of the bound two-body system (the deuteron) were exceedingly complex, requiring as many as 40 adjustable parameters in their description.

A breakthrough came in the mid-1960s when the discovery of the ω, ρ and η mesons by particle physicists led to the revival of meson theory of nuclear forces initiated by Yukawa in 1935. With the additional physical constraints of meson theory, it suddenly became possible to fit the scattering data with one boson exchange model requiring only five to ten adjustable parameters, rather than the 40 parameters of purely phenomenological models. Although the final story is not yet told, the nuclear physics community, since 1967 (Refs. 1 and 2), has felt a great aesthetic sense of relief that the fundamental law of nuclear physics is not as monstrous as it had appeared to be in the early sixties.

Thus, as some of the earlier speakers have already suggested, it is the additional physics, physical judgment, and physical information which one brings to bear with the scattering data which will often determine the success and utility of an inversion scheme.

Studies leading to the nuclear shell and optical models (Ref. 3) are even more analogous to the atmospheric inversion problem. For over 40 years, experiments have been performed in which various nuclear particles accelerated from 1 MeV to 100 GeV energy range are scattered from various nuclear targets. Many lead to optical-type angular distributions (phase functions), polarizations, scattering, and absorption cross sections. Many of these data patterns can be accounted for by assuming a complex energy dependent nuclear potential (complex wavelength dependent index of refraction). Even the terminology of this subject, such as "the cloudy crystal ball model," reflects the light scattering analogy. Now nuclear opticians, like atmospheric opticians, divide up into a school concerned with average gross properties and a school concerned with statistical fluctuations. Both groups have greatly enriched the subject, although, as in the light scattering case, the communications between the schools has not always been the best.

My own specialized pursuits of atmospheric optics (apart from a stint in World War II) began in 1959 just after an intensive involvement with nuclear optics (Ref. 4). In these pursuits, I have mostly used the gross structure-nuclear optical modelers approach. The style here has been to use analytic models whose parameters are determined by nonlinear least square adjustment to experimental data. Then we look at the systematics of the parameters with the ultimate objective of relating them to more fundamental physical parameters, e.g., those in the basic nuclear force. I would like now to illustrate this nuclear optical approach with a few simple-minded attacks on some atmospheric optics problems.

II. AUREOLE STUDIES

Deirmendjian and Sekera (Refs. 5 and 6) very early recognized the importance of Mie particles in the theory of the solar aureole. Their work was motivated by an attempt to account for some reported

anomalously high transmission of the ultraviolet part of direct sunlight. It is interesting to note that D. S. Saxon, who collaborated with Deirmendjian and Sekera on scattering from dielectric spheres (Ref. 7) during the same time frame, played an important role in the development of the nuclear optical model.

Our work, on determining aerosol size distributions from solar aureole intensities, has used a type of atmospheric modeling and single scattering theory which we first used in a satellite ozone sounding analysis (Ref. 8). That the skylight in the neighborhood of the sun can be used to good advantage may be surmised from the optical theorem of nuclear and atomic scattering theory and bistatic radar analysis (Ref. 9). These works indicate that whereas backscatter cross sections (180° scatter) vary in a complex manner with particle shape and index of refraction, forward scatter cross sections are primarily determined by the volume of the particle. This property was first utilized in the doctoral theses of Adarsh Deepak (Ref. 10) and Barton J. Lipofsky (Ref. 11) which, among other things, involved photographic and photoelectric studies of the solar aureole in the visible region (Ref. 12). More recently, these studies have been extended into the ultraviolet (Refs. 13 and 14).

Dr. Deepak has already described some of the features of this work in his talk on the Aureole Isophote Method and in connection with his Stratospheric Aerosol Photographic Experiment (SAPE) proposal. Let me add some words here on the advantages of this type of experiment.

In Fig. 1, we show the densitometric traces of a measured photographic aureole made with the obscuring disc technique. The traces labeled r and l are through the solar almucantar whereas the traces labeled b and t are below and above the sun in the solar meridian. The beauty of this experiment is the reference intensity provided by the solar disc, so in essence we have on our measuring medium a comparison between diffuse sky intensity and the direct

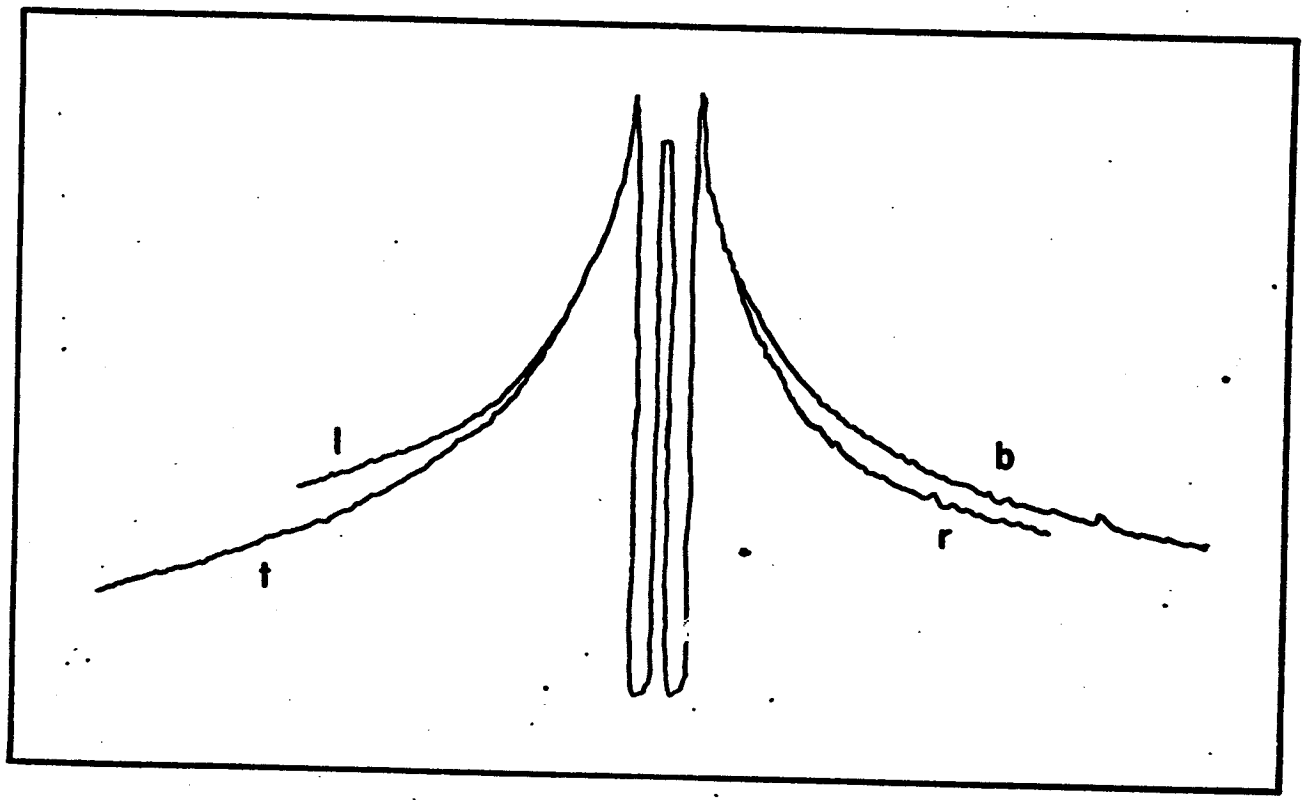

Fig. 1. Densitometric trace of aureole photograph with obscuring disc for horizontal and vertical scans with l, r, t, and b denoting positions of scans on the left, right, top, and bottom sides of the disc, respectively.

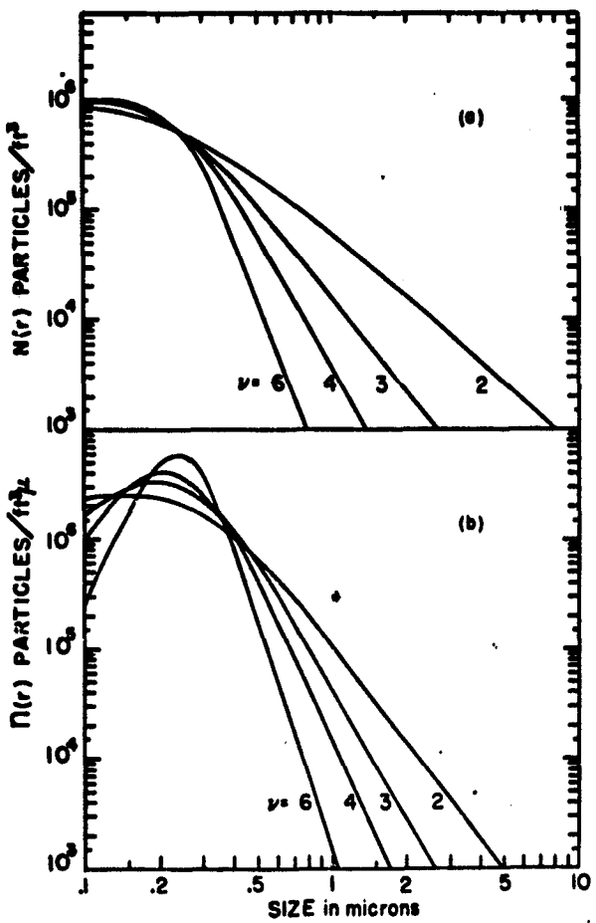

(1 ft³ = 2.831 × 10⁻²m³)

Fig. 2a. Examples of oversize distribution.

Fig. 2b. Corresponding examples of distribution.

solar intensity, attenuated by 10^4 by a Neutral Density 4 (ND4) filter. Thus far, in our work at the University of Florida, we have only exploited the information content in the almucantar trace of the solar aureole.

For the convenience of analysis, we use an analytic size distribution characterized by the cumulative distribution function (see Fig. 2).

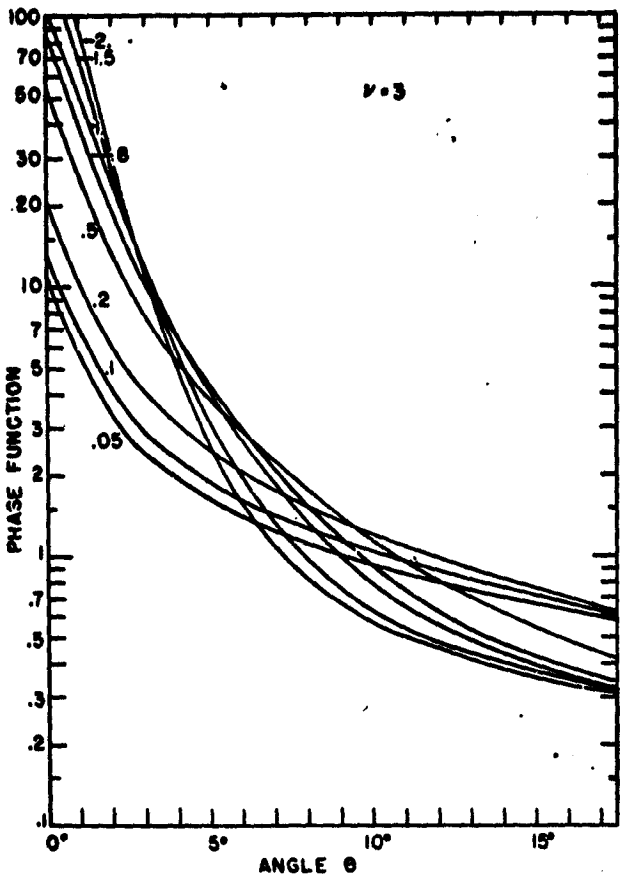

(a) ν = 3.

Fig. 3. Phase functions for model distribution.

$$N(r) = N_o / [1 + (r/a)^{\nu}] \tag{1}$$

where N_o, ν and a are adjustable parameters. This corresponds to the differential size distribution

$$n(r) = \frac{dN}{dr} = N_o \frac{\nu}{a^{\nu}} \frac{r^{\nu - 1}}{[1 + (r/a)^{\nu}]^2} \tag{2}$$

This analytic size distribution is a generalization of the Junge power law which is well behaved as $r \to 0$.

We have calculated a library of normalized phase function for this two-parameter size distribution function. Figure 3 illustrates several examples. Figure 4 illustrates some recent work at 640 nm showing the sharpness in the determination of ν obtained by this type of analysis (Ref. 14).

Spectral turbidity measurements, such as determined by a multi-channel Sun photometer, also give information about the particle size distribution (Ref. 15). Green and Sawada (Ref. 16) have determined the relative spectral turbidities associated with

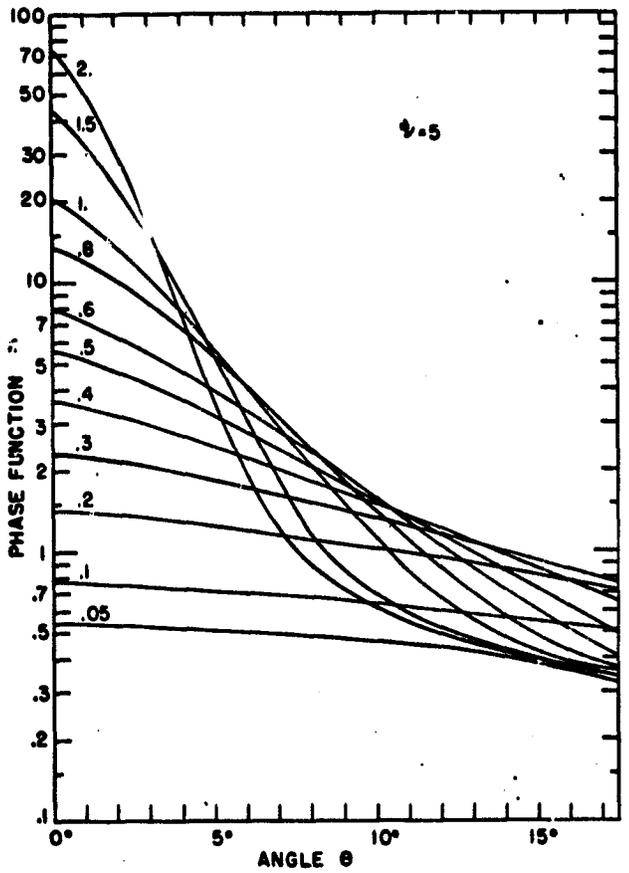

(b) ν = 5.

Fig. 3. Concluded.

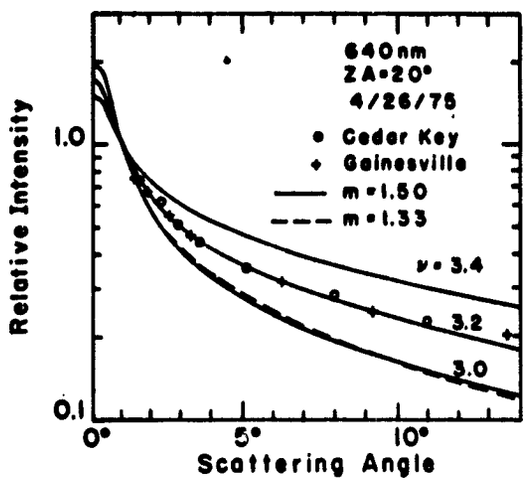

Fig. 4. Measured aureole intensity along the almucantar compared with calculations for three ν variations in the aerosol size distribution. (From Ref. 14.)

aerosol size distributions characterized by Eqs. (1) and (2). Thus, aureole data augmented by spectral turbidity data can lead to a very sharp determination of ν, as well as N_o.

We have considered the problem of multiple scattering in the solar aureole (Ref. 17), particularly in the ultraviolet where Rayleigh scattering becomes so important. Figure 5 shows an intercomparison of three calculations (Ref. 18): (1) a single scattering treatment, (2) a multiple scattering calculation using Monte Carlo techniques, and (3) a multi-channel calculation. The calculation indicates that multiple scattering can be quite significant, particularly in the ultraviolet.

In subsequent work, McPeters and Green (Ref. 14) have found that Rayleigh scattering is the source of most of this multiple scattering in the solar aureole except at high particulate optical depths. Accordingly, they have proposed an analysis technique which uses single aerosol and Rayleigh scattering augmented by

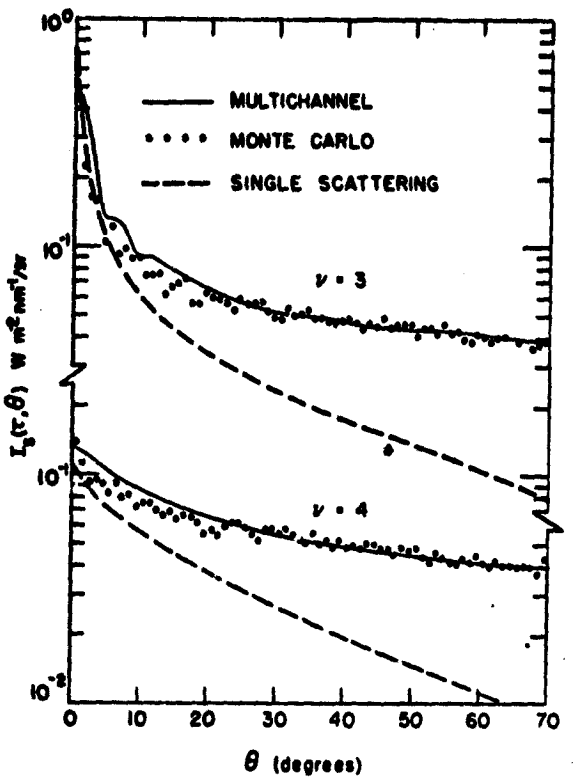

Fig. 5. Absolute intensity as a function of detector zenith angle for two different Mie scattering functions as calculated by three separate methods. The solid lines represent the results of the multi-channel calculations, the dots are the Monte Carlo results, and the dashed curves are the single scattering calculations. Note the break in the scale to avoid superposition of the two sets of results. (From Ref. 18.)

multiple Rayleigh scattering as determined by the use of the tables of Coulson, Dave, and Sekera (CDS) (Ref. 19). Figure 6 is an illustration of a fit to data based upon such an analysis.

III. DIFFUSE TO DIRECT RATIO MEASUREMENTS

In connection with our ultraviolet studies in support of the Climatic Impact Assessment Program (Ref. 20), we have attempted to realistically characterize the diffuse solar radiation or sky radiation in the ultraviolet. As it turns out, sky radiation in the ultraviolet is often of greater biological consequence than direct sunlight. Green, Sawada and Shettle (Ref. 21) have developed an approximate analytic formula which describes the diffuse spectral irradiance in the ultraviolet region by adapting a single scattering analysis to the systematics of Bener's experiments (Ref. 22) and to theoretical calculations of Shettle and Green (Ref. 23).

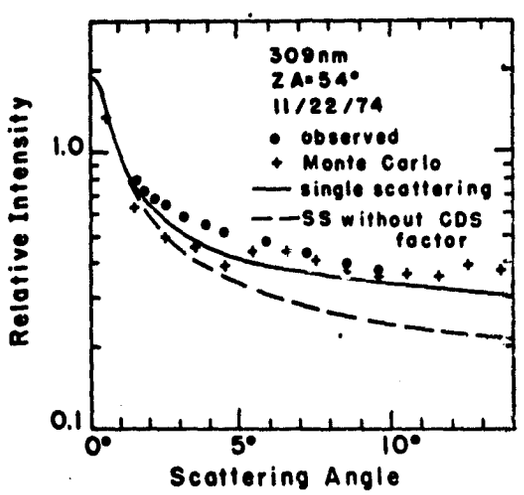

Fig. 6. Normalized ultraviolet aureole intensities along the almucantar compared with modified single scattering calculation, with and without the CDS Rayleigh multiple scattering correction factor, and compared with a Monte Carlo full multiple scattering calculation. (From Ref. 14.)

More recently, Chai and Green (Ref. 24) have recognized the merits of measurements of the ratio of diffuse to direct spectral irradiance as a simple indicator of atmospheric optical properties. The ratio method is analogous in some respects to our aureole method except that there we must attenuate the direct solar intensity by four orders of magnitude to compare it to the sky intensity. Figure 7 is an example of measurements of the total sky irradiance, the direct irradiance, and the ratio. The diffuse and direct both vary very markedly, and reflect the fluctuations in the extraterrestrial solar spectral irradiance and in the ozone extinction coefficients as well as in the wavelength dependence of instrumental sensitivity. However, the diffuse to direct ratio is only slowly varying but still sensitively depends upon such interesting characteristics as atmospheric particulate loading, ground albedo, and sky cover. This ratio method avoids problems associated with the difficulty of absolute spectral irradiance measurements which, at this time, are limited to about 8% in the ultraviolet region.

It should be remarked that Herman, et al. (Ref. 25) have theoretically examined such a ratio method in the visible region in an attempt to estimate the imaginary part of the index of refraction of atmospheric aerosols.

We shall next consider another example of inverting of optical data with the aid of the analytic modeling approach and auxiliary information, such as may be obtained with simple ground-based instruments.

IV. THE INVERSION OF THE LOW ALTITUDE OZONE PROFILE

Tropospheric ozone is a constantly varying atmospheric component which changes with the season of the year, location, and time of day. Both photochemical and stratospheric transport processes are important sources of tropospheric ozone and are responsible for the strong diurnal, seasonal, and spatial variations.

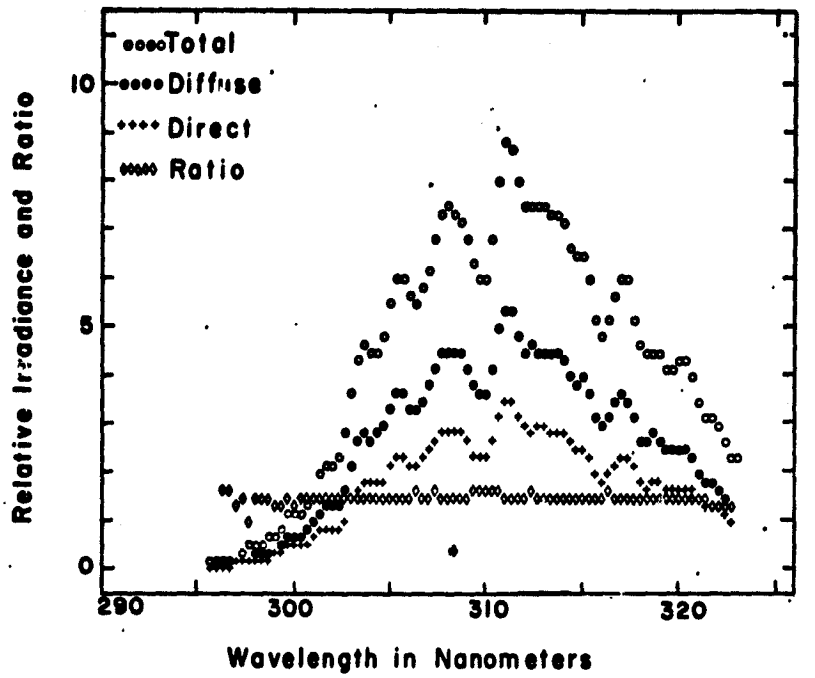

Fig. 7. Total, diffuse, direct, and the ratio of diffuse to direct components of solar irradiances as a function of wavelength as recorded on 31 July 1975 at around 13:50 EST. The magnitudes of the irradiances are in relative scale; they are proportional to the photomultiplier output in 100 μV. (From Ref. 24.)

A systematic program of balloon-borne ozonesonde observations has provided valuable data on the altitude structure of ozone which can be used as a guide in constructing a versatile analytic model (Ref. 26). We consider in what follows the possibility of inferring the tropospheric ozone profile from diffuse to direct ratio measurements in the middle ultraviolet in conjunction with ozone point-sampling at the ground. We model the altitude profiles of the atmospheric components with analytic functions because such

a technique simplifies data inversion and provides a convenient way of communicating the resulting profiles.

Green (Ref. 8) has modeled the stratospheric ozone column density as a function of altitude y with a distribution used extensively in the nuclear studies (the so-called Wood-Saxon function)(Refs. 3 and 4)

$$w(y) = \frac{w_o(1 + e^{-y_o/h})}{1 + e^{(y - y_o)/h}} \tag{3}$$

Here w_o is the total ozone thickness and y_o and h are parameters. The density profile $\rho(y)$ is given by

$$\rho(y) = -\frac{dw}{dy} = \frac{w_o}{h} \quad \frac{(1 + e^{-y_o/h}) e^{(y - y_o)/h}}{(1 + e^{(y - y_o)/h})^2} \tag{4}$$

The parameter y_o is the altitude at which the density function peaks and h scales the width of the distribution. Green (Ref. 2) shows how y_o, h and w_o can be approximately inferred from solar backscatter ultraviolet (UV) measurements.. In their recent analysis on ground level UV, Shettle and Green (Ref. 23) add an exponential term to this function to allow for the tropospheric ozone component. Here to characterize tropospheric ozone profiles which are concave, i.e., the density decreases with altitude above the ground and then increasing at the tropopause, we add a second term of the form of Eq. (3) or (4) with the parameters y_o' and h' and where w_T is now the sum of $w_o + w_o'$.

In Fig. 8, several profiles corresponding to various values of h' and $\rho(0)$ are shown. Here $y_o' = 0$ and $w_o = 0.29$ atm-cm; and y_o and h are set to 23 km and 4 km, respectively. Extreme concave profiles can be obtained as well as curves of almost constant density. Furthermore, convex profiles can be generated with two distributions by setting y_o' to be a positive number. Convex profiles are observed with greatest frequency in the summer months at latitudes above 40°N.

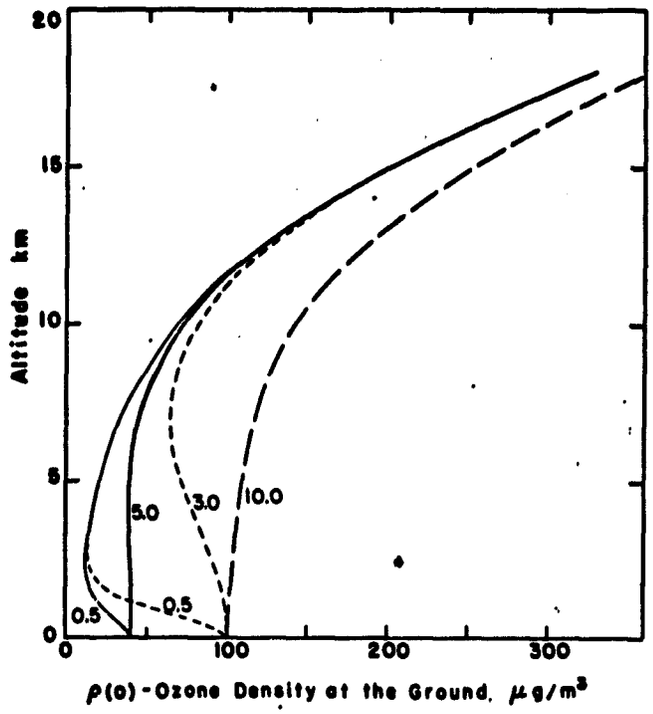

Fig. 8. Ozone density profiles for a number of different values of the parameter h_1' and ground density, with y_o = 23 km, h = 4 km and y_o = 0.

Assuming we know the ground level ozone density and also that the ozone profile can be represented by a two component model with y' = 0, we can test the sensitivity of the diffuse to direct ratio to the parameter h'. In Fig. 9, we plot the ratio versus h' for ρ(0) = 40, 70, 100 (μg/m³) for a wavelength of 300 nm. We take y_o = 23 km and h_o = 4 km. Furthermore, we have assumed the air and aerosol profiles of Shettle and Green (Ref. 23) which are based on Elterman's 1964 data (Ref. 27). The total aerosol optical depth is 0.411; the aerosol is characterized by the cumulative size distribution given by Eq. (1) with ν = 3 and a = 0.03 μm; the

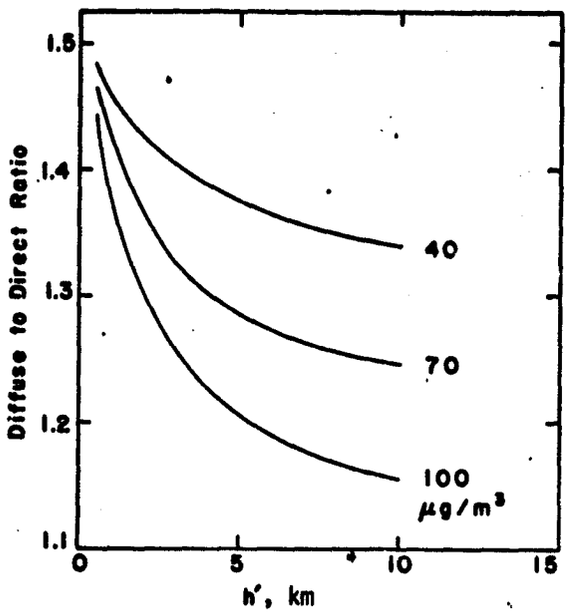

Fig. 9. Diffuse to direct ratio dependence on the scale parameter h' for ground ozone densities of 40, 70, and 100 μg/m³.

aerosol index of refraction is 1.5 + .01i; a ground albedo of 0.05 is assumed; and the Sun is directly overhead. The ratios are calculated by using the multiple scattering technique of Shettle and Green (Ref. 23).

The diffuse to direct ratio then can be used to infer a value of h' from a set of curves as in Fig. 9 when used with point sampling measurements which give the ozone concentration at the ground.

Other simple and inexpensive measurements can be made simultaneously with the ratio and point-sampling measurements in order to further delimit the inversion and reduce the uncertainties. For example, aureole photography can be employed to infer the aerosol size distribution parameters (Refs. 10, 12, and 14). Also,

multi-wavelength photometry provides valuable information on the aerosol optical thickness and its wavelength dependence (Refs. 15 and 16).

The two most nebulous parameters are the aerosol single scatter albedo and the ground albedo. It is important to know how uncertainties in these parameters propagate through the inversion. The aerosol single scatter albedo will depend on the aerosol index of refraction and size distribution. By using aureole photography to pin down the size distribution, one can draw on experience from previous investigations to fix the aerosol index of refraction within a range of confidence. For example, bistatic laser and aureole photography methods (Ref. 28) indicate that the index of refraction of a typical Gainesville aerosol is 0.005 ± 0.005 for the imaginary part and 1.50 ± 0.05 for the real part. The diffuse to direct ratio is found to be relatively insensitive to this range of possible error. Similar considerations apply to the ground albedo. In the theoretical model a ground albedo of 0.05 was assumed which is compatible with measurements by Furukawa and Heath (unpublished reports, 1973) of various natural surfaces for the wavelength region 310 to 380 nm. For example, they found that for scrub desert the ground albedo was 0.04 over the 310 to 380 nm region. For farmland, 70% tilled and 30% covered with vegetation, the ground albedo was found to be 0.07 to 0.08 for the 310 to 340 nm region.

Small errors in the ground albedo (≈ 0.02) do not significantly affect the calculations. Furthermore, once the ground albedo is known for a given location, the daily variations of h' can be determined, unless, of course, the surface changes because of snow cover, cultivation, or the like.

If the true optical depth is used in the inversion, then underestimating the ground albedo or the aerosol single-scatter albedo will lead to calculated ratios which are too small. Overestimation will lead to calculated ratios which are too large. Diffuse to direct ratio measurements in the 320 to 340 nm region

can be used to infer effective aerosol optical depths here since in this region the ratios are rather insensitive to tropospheric ozone. The effective optical depths can be extrapolated to smaller wavelengths. These effective optical depths will be somewhat different from the true aerosol optical depths and will tend to compensate for errors in the ground albedo and aerosol single-scatter albedo. The diffuse to direct ratio around 300 to 320 nm is insensitive to the altitude distribution of the aerosols so long as the ozone profile near the ground is not changing too rapidly. Also, detailed knowledge of the stratospheric ozone structure or thickness is not required.

V. CONCLUDING REMARKS

Strictly numerical methods of inversion are becoming predominant in remote sensing these days. These are, of course, valuable to infer the irregularities and statistical fluctuations in atmospheric properties. The analytic model method which we have illustrated can be a valuable supplement to such numerical methods. They are particularly useful when used in conjunction with dynamical models of atmosphere structure because of the additional physical input of such models. When the models are joined to ground-based point sampling data, this remote-sensing-analytic model approach gives approximate answers to important questions involved in many public policy decisions on atmospheric pollution.

SYMBOL

a	size distribution parameter, corresponds approximately to the size of particle where n(r) peaks
h	ozone distribution parameter which is proportional to width of ozone density function; prime denotes another value of h
m	real part of aerosol refractive index

I_s	absolute scattered intensity
n(r)	differential aerosol size distribution
N(r)	cumulative aerosol size distribution
N_o	size distribution parameter which is equal to total number of aerosol particles
r	aerosol particle radius
w_o	total ozone thickness; prime denotes another value of w_o
w(y)	the ozone thickness function
y	altitude
y_o	altitude at which ozone density peaks; prime denotes another value of y_o
ZA	zenith angle
θ	scattering angle
ν	size distribution parameter which determines power law dependence of n(r) at large r
$\rho(y)$	ozone density function
τ	optical depth

ACKNOWLEDGMENT

Supported in part by the Atmospheric Sciences Programs of the National Science Foundation and National Aeronautics and Space administration.

REFERENCES

1. A. E. S. Green, M. H. MacGregor and R. Wilson (Eds.), Proceedings of International Conference on N-N interaction, *Rev. Mod. Phys. 39*, 495 (1967).

2. A. E. S. Green, The fundamental nuclear interaction, *Science, 169*, 933 (1970).

3. A. E. S. Green, T. Sawada and D. S. Saxon, "The Nuclear Independent Particle Model, The Shell and Optical Models. Academic Press, Inc., 1968.

4. A. E. S. Green, C. E. Porter and D. Saxon (Eds.), *Proc. of the International Conference on the Nuclear Optical Model, Florida State University Studies, Tallahassee, Florida*, 1959.

5. D. Deirmendjian and Z. Sekera, Theory of the solar aureole, Part I; Scattering and radiative transfer, *The Rand Corporation, Santa Monica, California*, November 1957 [Internal Report.]

6. D. Deirmendjian and Z. Sekera, Atmospheric turbidity and the transmission of ultraviolet sunlight, *J. Opt. Soc. Am. 46*, 565 (1956).

7. D. S. Saxon, Z. Sekera, D. Deirmendjian and R. S. Fraser, On the scattering of plane electromagnetic waves by dielectric spheres, *University of California, Los Angeles*, 1957 [Internal Report.]

8. A. E. S. Green, Attenuation by ozone and the Earth's albedo in the middle ultraviolet, *Appl. Opt. 3*, 203 (1964); see also A. E. S. Green, The middle ultraviolet and its space applications, *Convair General Dynamics, San Diego, California*, ERR-AN-185, July 1962.

9. K. M. Siegal, Bistatic Radar Cross Sections, *Proc. IEEE, 45*, 1137 (1960).

10. Adarsh Deepak, "Second and Higher Order Scattering of Light in a Settling Polydispersed Aerosol," Ph.D. Dissertation, University of Florida, Gainsville, 1969. [Available from Xerox Univ. Microfilms, Ann Arbor, Michigan 48106.]

11. B. J. Lipofsky, "Single Scattering of Light by Polydispersed Aerosols," Ph.D. Dissertation, University of Florida, Gainsville, 1970. [Available from Xerox Univ. Microfilms, Ann Arbor, Michigan 48106.]

12. A. E. S. Green, A. Deepak and B. J. Lipofsky, Interpretation of the sun's aureole based on atmospheric aerosol models, *Appl. Opt. 10,* 1263 (1971).

13. R. D. McPeters, "Scattered Sunlight in the Atmosphere from the Middle Ultraviolet through the Near Infrared," Ph.D. Dissertation, University of Florida, Gainsville, 1975. [Available from Xerox Univ. Microfilms, Ann Arbor, Michigan 48106.]

14. R. D. McPeters and A. E. S. Green, Photographic aureole measurements and the validity of aerosol single scattering, *Appl. Opt. 15,* 2457 (1976).

15. G. E. Shaw, "An Experimental Study of Atmospheric Turbidity Using Radiometric Techniques," Ph.D. Dissertation, University of Arizona, Tucson, 1971. [Available from Xerox Univ. Microfilms, Ann Arbor, Michigan 48106.]; see also G. E. Shaw, J. A. Reagan and B. M. Herman, "Investigations of atmospheric extinction using direct solar radiation measurements made with a multiple wavelength radiometer, *J. Appl. Meteorol. 12,* 374 (1973).

16. A. E. S. Green (Ed.), Report of the coordinated program for the remote sensing of atmospheric aerosols clean air preservation and enhancement research, *University of Florida, Gainesville, Report,* September 10, 1971.

17. A. Deepak, Double scattering corrections to the theory of the sun's aureole, NASA TM X-64800, December 1973; see also Ref. 16.

18. D. R. Furman, A. E. S. Green and T. Mo, Multistream and Monte Carlo calculations of the sun's aureole, *J. Atmos. Sci. 33,* 537 (1976).

19. K. L. Coulson, J. V. Dave and Z. Sekera, "Tables Related to Radiation Emerging from a Planetary Atmosphere with Rayleigh Scattering." University of California Press, Berkeley, California, 1960.

20. Alan J. Grobecker, (Ed.), Impacts of climatic change on the biosphere, *Dept. of Transportation Climatic Impact Assessment Program*, DOT-TST-75-55, September 1975.

21. A. E. S. Green, T. Sawada and E. P. Shettle, The middle ultraviolet reaching the ground, *Photochem. Photobiol. 19*, 251 (1974).

22. P. Bener, *Technical Report, European Research Office, U.S. Army, London*, Contract No. DAJA37-68-C-1017, 1972.

23. E. P. Shettle and A. E. S. Green, Multiple scattering calculation of the middle ultraviolet reaching the ground, *Appl. Opt. 13*, 1567 (1974).

24. A. T. Chai and A. E. S. Green, Measurement of the ratio of diffuse to direct solar irradiances in the middle ultraviolet, *Appl. Opt. 15*, 1182 (1976).

25. B. M. Herman, P. S. Browning and J. J. DeLuisi, Determination of the effective imaginary term of the complex refractive index of atmospheric dust by remote sensing: The diffuse-direct ratiation method, *J. Atmos. Sci. 32*, 918 (1975).

26. W. S. Hering and T. R. Borden, Jr., Ozonesonde observations over North America, AFCRL-64-30II, July, 1964.

27. L. Elterman, *Environmental Research Paper No. 46, Air Force Cambridge Research Laboratories*, AFCRL-64-740.

28. G. Ward, K. M. Cushing, R. D. McPeters and A. E. S. Green, Atmospheric aerosol index of refraction and size-altitude distribution from bistatic laser scattering and solar aureole measurements, *Appl. Opt. 12*, 2585 (1973).

DISCUSSIONS

Deirmendjian: With regard to the importance of multiple scattering in the aureole, I don't want to blow my horn, but I certainly wish to protect Professor Sekera's memory. In my 1956 doctoral thesis, I looked at the problem of the solar aureole at his suggestion. The method used was essentially Sekera's idea and consisted of treating the aureole as a perturbation on the Rayleigh multiple scattered skylight. And that is precisely what I did. Have you seen my original 1957 paper on the aureole?

Green: Yes, we have seen your paper.

Deirmendjian: It was exactly that. You increase the optical thickness of the Rayleigh atmosphere by adding a perturbation optical thickness due to the aerosols. When you do that, it is a kind of hybrid method where single scattering on the aerosols produces the aureole, but multiple scattering, mainly on the Rayleigh particles, produces the rest of the background skylight. I thought you didn't make that clear.

Green: We weren't aware of that aspect of your paper back then. We were aware of your work on the aureole and we have quoted it in our work.

Deirmendjian: I think that was the principal point. I have since reexamined this method in 1970. I did not publish the results in the open literature due to lack of funds. But they are available in a formal 1970 Rand Corporation report, in which I introduced new phase functions. Indeed, the curves that are obtained look very much like some of the measurements I have seen. Subsequently, I intended to compare them with the measurements and look into their use to get information about the aerosol size distribution. At the time, I was unable to do this for lack of support.

Green: Well, there was no intention to slight you or Professor Sekera. We have in our work in this area acknowledged this. The UV problem has a new interest in light of its biological aspects. So part of this work was directed toward answering some particular questions about the radiance of the UV aureole where some serious problems remained. My point about the low altitude ozone distribution is that you can take advantage of the extra scattering associated with aerosols to extend the path and the absorption in the low altitude ozone layer. Thus, you can actually drag out a little information about the high altitude distribution, but little about the low altitude profile.

Weinman: While I agree with the previous speaker that the aureole technique is a powerful one for determining size distributions, I should point out that invisible cirrus clouds can plague this

technique. While there are frequent cases where you can get nice smooth functions to which you can apply the theory, this hazard always exists. If one looks at this data, one can pick up cirrus clouds which are not at all visible to the naked eye. I think that it takes a certain amount of judicious discrimination to get cases to which you can apply the radiative transfer theory.

Green: I think Adarsh has shown some results where contours of isodensity on a film show distortions that are suggestive of a thin cloud layer. In some of our work, we have noted some problems of that nature, which one can, perhaps, use as information content.

Deepak: Yes, we have been looking at the shapes of the solar aureole isophotes rather carefully and we see small bumps. The isophote curves are not very smooth. That could be due to the presence of thin clouds. In fact, we have an airport nearby; when aircraft take off we can easily detect the presence of contrails from the systematic distortion in the shape of the isophotes over the region of the contrail image.

Fymat: I was very interested in your conclusion in determining the scale height for the troposphere.

Green: For the tropospheric ozone distribution.

Fymat: Yes, but you need, as you say, the ozone distribution at the lower altitudes. However, it seemed to me, and Dr. Mateer may care to comment on it, that the actual ground-based Dobson measurements are really being phased out in view of the fact that they produce different results on inversion using different methods. So, if we cannot get the distribution at the lower altitudes, how practical is your conclusion?

Green: Well, insofar as profile, the Umkehr method (not the Dobson method) relies, and Carl can correct me since he is much more expert, on the setting of the sun and inverting sky radiances. Our method could be worked at high noon since it is instantaneous. We would use wavelength information and we have, in effect, shown by simulated tests that the diffuse to direct ratio is only sensitive to the addition of extra ozone below about 10 kilometers. So that while it is not a complete profile, if you use it in conjunction with ground level chemical measurement, it gives you information which relates to the lower atmospheric ozone and it is insensitive to the stratospheric ozone which is far more abundant. Now am I correct that the Umkehr method more or less gives you the most information about the higher atmospheric ozone? So there is no real contradiction with anything previously known.

Mateer: The Umkehr measurement is a different kind of measurement. It is a ratio measurement of two wavelengths as opposed to what you are doing--a ratio of diffuse to direct sunlight.

Green: Yes. We also are helped if we use two wavelengths as well. It eliminates a little bit of the absolute radiometry problem. It gives us another check.

OPEN DISCUSSIONS I

King: Alex, what do you think we can learn about solving the atmospheric temperature inversion problem from the similar type inversion problem in inferring nuclear potential in nuclear physics?

Green: Well, I was discussing this type of thing with Dr. Wark, and the analogy would be if we brought to bear to the problem all the physical dynamics data, not only at one location but at adjacent locations. Thus, if we had relatively few questions that we posed to the radiative transfer problem, for example, to get horizontal gradients in temperature profile, and perhaps include such facts that there tends to be a tropopause and we are mainly interested where the temperature break occurs, and ask questions which embody all of our experience as to reasonable temperature profiles. Then when we apply this external information to an inversion problem, it is usually much easier to come to a physically reasonable answer. Now I don't know if that's a good paraphrase of the analogy. We do have one problem which I have to confess compromises the analogy. In the case of the nuclear force problem we think all neutrons and protons are the same, and unfortunately the atmosphere takes on so many different states that we do have that extra complication. Thus, if you tried to unfold many, many details of the instantaneous atmosphere, you may be in trouble with this approach. On the other hand, if you are satisfied with answering the types of physical questions that our dynamical meteorologists, pollution experts, or biologists want answered, I think you get a lot of useful information by these modeling approaches.

Herman: Alex, I would like to ask you, what is the sensitivity of the direct diffuse--insofar as solving for ozone--to variations in aerosol contents? Because as you know we are trying to apply it to learn various parameters of the aerosol. Now you are using it to learn about the ozone but it still has a sensitivity to aerosols even at the ultraviolet wavelengths.

Green: Yes, I should, unless I commit another error of omission, mention that Ben has used the direct-to-diffuse ratio to infer the imaginary part of the index of refraction working at 500 nanometers. We were not aware of this work when we started ours, but were aware of it during its course. I think the trick in our case is to choose two wavelengths--one in the region where the ozone is absorbing and one where it is nonabsorbing. Then we take advantage of whatever we know about our aerosols, including a ground-level aerosol measuring device, plus an aureole measuring device. I would not go to anything expensive like a lidar. But I think if we bound our aerosol model somewhat we find by sensitivity analyses that we do get some information about the low level ozone. This is what we would pick up by using two wavelengths, just as Dobson does. We would go to about 320 nanometers and then to 305 nanometers. We

would expect that the aerosols do not change very much, so that we hold the aerosols confusion factor down.

Goulard: I am trying to apply inversion techniques to the field of combustion. I get the profiles of temperature or concentrations following the methods that Dr. Chahine has developed. But, I get them in terms of optical thickness. And when I want to convert it to physical thickness, which is what the combustion people want, I find that I cannot depend on the constant concentration of CO_2 as you do in the atmosphere. Could someone give me some help on how to get around this problem in frequency scanning only?

Chahine: Let me answer Professor Goulard's question on the solution in terms of the optical depth. You know, the independent variable in the radiative transfer equation is τ but we set $d\tau = (\partial\tau/\partial z)dz$ in the equation and obtain a solution as a function of the physical scale z. As you know $\partial\tau/\partial z$ is obtained on the basis of an atmospheric model. Thus, the solution is truly a function of τ although it is usually presented as a function of z. The transformation from the τ-scale to the z-scale is done through a model.

Goulard: You assume Laplace Law of the atmosphere and a constant mixing ratio?

Chahine: Yes, we have to do this.

Goulard: And for a flame?

Chahine: You would have to develop a model for your flame and correlate your optical depths with a physical scale.

Goulard: Is the concentration of CO_2 really constant throughout the atmosphere?

Green: Well, it is, yes, within a small period of time. There are some people who think it is growing.

Gille: The concentration of CO_2 in the troposphere is quite constant although not absolutely so. It varies seasonally by perhaps one part per million out of a background of 330 with a long-term trend of, perhaps, 0.7 ppm per year.

Photochemistry and Photobiology, Vol. 30, pp. [illegible]
© Pergamon Press Ltd 1979. Printed in Great Britain
0031-8655/79/[illegible]

IMPROVED ANALYTIC CHARACTERIZATION OF ULTRAVIOLET SKYLIGHT

A. F. S. Green, K. R. Cross and L. A. Smith
ICAAS, University of Florida Gainesville, FL 32611, U.S.A.

Abstract—We present an improved analytic characterization of diffuse spectral irradiance (skylight) for the wavelength range 280–380 nm and solar zenith angle range from 0 to 85°. The formulas achieve greater accuracy by (a) focusing on ratio representations and (b) adjusting the parameters to the more precise radiative transfer calculations of Dave Braslau and Halpern.

INTRODUCTION

There is a serious need for simple but accurate analytic characterizations of skylight, particularly in the UV where skylight sometimes has greater biological importance than direct sunlight. Previous work by Green *et al.* (1974) (GSS), Shettle and Green (1974), Green and Mo (1974) (GM), Mo *et al.* (1975) and Green (1976) have provided simple approximate phenomenological representation of the systematics of Bener (1972) and of numerically calculated diffuse spectral irradiances. However, experimental studies of Chai and Green (1976), and Garrison *et al.* (1978a, b) have focused attention on the diffuse/direct ratio which avoids problems with absolute radiometry which are particularly difficult in the UV region. Furthermore, this ratio depends more slowly upon wavelength than the diffuse spectral irradiance itself. Unfortunately the dependence upon angle of the diffuse/direct ratio can be large because the denominator (the direct irradiance) becomes so small at large solar zenith angles. In the present work we will use more elaborate ratio techniques to find an accurate analytic characterization of skylight which, for all angles and wavelengths of interest, will bring the fit to numerically generated diffuse irradiance from the 25% level of accuracy to about the 5% level. Toward this aim, rather than use the numerical output of the code available to us (Shettle and Green 1974) we will use the results of the more precise radiative transfer calculations of Braslau and Dave (1973) and Dave and Halpern (1975). Their results (to be referred to as DBH) for six models (B, C, D, Cl, Dl and Cl*, see Table 1) have kindly been made available to us in the form of magnetic tape output and readable hard copy. In effect, the objective of this paper is to make the results for the various DBH models available in analytic form for biological users. The form developed is more elaborate than those previously proposed but should be worthwhile if a precise knowledge of the state of the atmosphere is available.

ANALYTIC FORM FOR DIRECT IRRADIANCE

The problem we are involved with has many dimensions, λ, the wavelength, θ, the sun angle, w_3, the ozone thickness, w_2, the aerosol thickness, (both of which are dependent upon y, the altitude) and A, the ground albedo. In addition, the profile characteristics of the ozone and aerosol enter. Rather than begin at the beginning in this attempt to describe UV skylight as a function of these many degrees of freedom, we shall attempt to utilize the experience gained in our earlier studies.

The downward direct spectral irradiance at the ground may be placed in the basic form.

$$D(\lambda, \theta) = \cos\theta\, F(\lambda) \exp - \sum_j (\tau_j/\mu_j) \qquad (1)$$

where τ_1, τ_2 and τ_3 denotes the air, aerosol and ozone optical depths, respectively, and μ, μ_1, μ_2 and μ_3 denote $\cos\theta$ and generalized cosine functions which are appropriate to the three species in view of the roundness of the earth. We will express these functions in the form

$$\mu_i = \left(\frac{\mu^2 + t_i}{1 + t_i}\right)^{1/2} \qquad (2)$$

where the t_i's are small characteristic numbers which depend upon the altitude distribution of the species. (See GSS 1974 for a more complete discussion.)

CHARACTERIZATION OF SKYLIGHT

It would be time and space consuming to recount all the analytic forms, mathematical models and approaches we have examined during the course of this investigation. In addition to molecular band type

Table 1. Atmospheric models

Model	Gaseous absorption	Aerosols: Height distribution	Aerosols: Refractive index
A	No	No	—
B	Yes	No	—
C	Yes	Average	1.5-0.0i
D	Yes	Heavy	1.5-0.0i
Cl	Yes	Average	1.5-0.01i
Dl	Yes	Heavy	1.5-0.01i
Cl*	Yes	Average	1.5-0.01i

To be published in Jan 1980

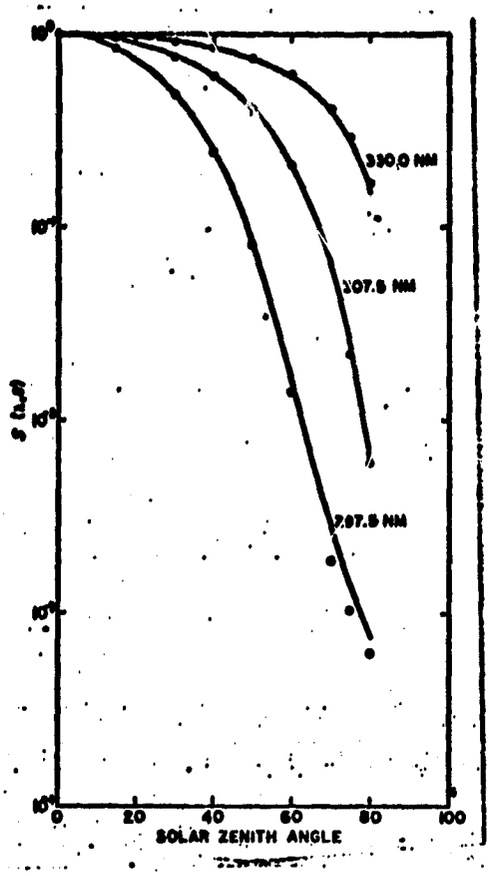

Figure 1. Shows our fits to $\mathscr{S}(\lambda, 0)$. The smooth curves are our analytic fits and the points represent the 'data'.

models we tried again to adapt the two stream model (Mo *et al.*, 1975) for the purpose at hand. However, inaccuracy or cumbersomeness led us to reject many approaches in favor of the analytical model which finally evolved. In this model our basic strategy is to represent the downward diffuse spectral irradiance (S) at the ground in terms of two ratios and the direct spectral irradiance for an overhead sun ($\theta = 0$, or $\mu = 1$). Thus for diffuse sky irradiance we use

$$S(\lambda, \theta) = \mathscr{S}(\lambda, \theta) M(\lambda) H(\lambda) \exp - \left(\sum_j \tau_j\right) \quad (3)$$

where

$$\mathscr{S}(\lambda, \theta) = S(\lambda, \theta^\circ)/S(\lambda, 0^\circ) \quad (4)$$

with

$$M(\lambda) = S(\lambda, 0^\circ)/D(\lambda, 0^\circ). \quad (5)$$

The virtue of this combination of ratios is that the dynamic range of M is less than one order of magnitude for the wavelength range of interest (280–380 nm) and for various aerosol optical depths and ozone thicknesses of interest. Furthermore, the dynamic range of $\mathscr{S}$ is also reasonable (1 order of magnitude above 320 nm, 2 above 300 nm, 3 orders above 290 nm and 4 orders of magnitude above 280 nm). Thus, representations at the few per cent level of accuracy should be feasible except possibly at the largest solar zenith angles and the shortest wavelengths.

The points in Fig. 1 illustrate variations of $\mathscr{S}$ with θ at $w_3 = 0.30$ using 'data' from Dave and Halpern (1975) Model C. Here the points are numerically generated results at 297.5, 307.5 and 330.0 nm. The smooth curves are derived from an analytic representation in the form

$$\mathscr{S}(\lambda, \theta) = [F + (1 - F)\exp - \gamma_3(\tau_3 + \tau_4)\phi]\exp - (\gamma_1\tau_1 + \gamma_2\tau_2)\phi \quad (6)$$

where

$$F = \frac{1}{1 + A_{03}[\tau_3 N_3(y) + \tau_4 N_2(y) + g k_3(\lambda)]^{m_3}}, \quad g = g_0 + g_a y, \quad (7)$$

$$\phi = \left(\frac{1 + t}{\mu^2 + t}\right)^{1/2} - 1 \Big/ \mu = \cos\theta, \Big/ t = t_0 + t_a y \quad (8)$$

where here τ_4 denotes the particulate absorption optical depth corresponding to τ_3 the particulate scattering optical depth, $k_3(\lambda)$ the ozone absorption coefficient. $N_1(y)$, $N_2(y)$, and $N_3(y)$ are the total thicknesses above the altitude (y) each normalized to unity at sea level ($y = 0$). The mathematical form we use for each of these is (see Fig. 2 and Table 2).

$$N_i(y) = f_i \frac{1 + \alpha_i}{\alpha_i + \exp(y/h_i)} + (1 - f)\frac{1 + \exp - y_i/\chi_i}{1 + \exp(y - y_i)/\chi_i} \quad (9)$$

where y_i denotes the altitude of the maximum *density* of species i, h_i and χ_i are scale height parameters, α_i is a shape parameter, and f_i is a fitting parameter. All of the parameters in Eq. 9 are dependent on the model distribution used. The first term in Eq. 9 controls the low altitude distribution, the second the high altitude distribution. With this representation the $\tau_i(\lambda)$ is the optical depth at sea level and $\tau_i(\lambda)N_i(y)$ is the optical depth above any altitude. The Rayleigh and ozone extinction coefficients used by DBH are given in Table 3. The spectral shape of the aerosol extinction coefficient over the range 280–350 nm depends upon the size distribution assumed. For the DBH models it appears adequate to use an average aerosol optical depth independent of wavelength. Table 4 gives the best fit parameters obtained for the DBH models.

Next we examine the ratio M. After trying a number of approaches, we obtained favorable results for the DBH models with the representation

$$M(\lambda) = \frac{A_{a1}\tau_1 N_1(y) + A_{a2}[\tau_2 N_2(y)]^{n_a}}{1 + A_{a3} w_3 N_3(y)[\tau_3 N_3(y) + \tau_4 N_2(y)]^{m_a}}. \quad (10)$$

Table 4 gives the M parameters for the DBH models. Figure 3a illustrates the fits as a function of wavelength for Model C1* with $w_3 = 0.2$, 0.3 and 0.4.

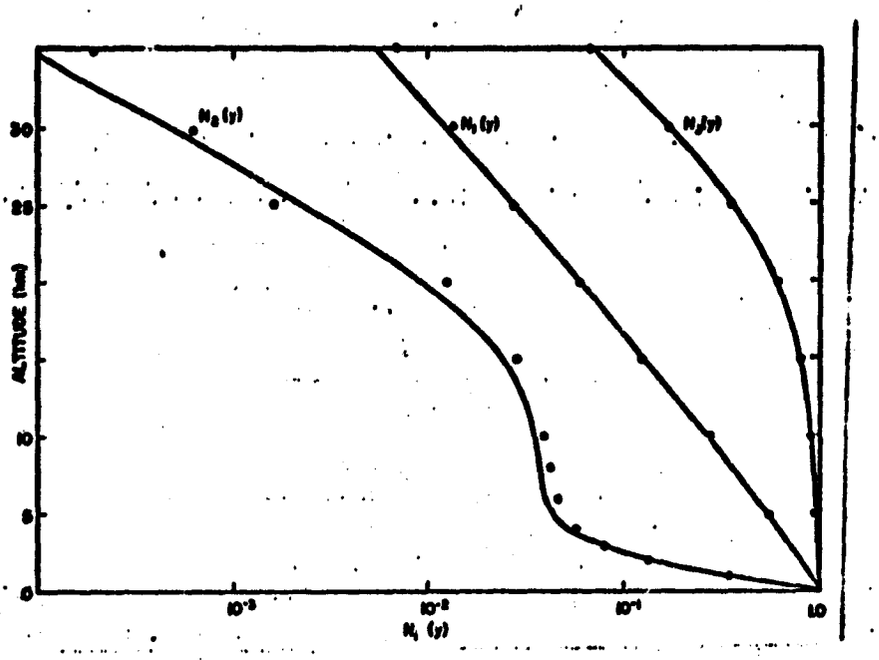

Figure 2. $N_i(y)$ functions.

Table 2. Adjusted parameters for $N_i(y)$.

	Average aerosols*		Heavy aerosols	
i	1	2(C)	3	2(D)
f_i	1.000	0.960	0.039	0.956
a_i	0.437	−0.145	2.350	−0.448
b_i	6.350	0.952	2.660	1.003
y_i	—	16.330	22.510	19.378
z_i	—	3.090	4.920	1.106
δ_i	1.8×10^{-3}	3.0×10^{-4}	7.4×10^{-3}	3.0×10^{-4}

Table 3. Wavelength dependent optical parameters as used in computations

λ Wavelength (μm)	$H(\lambda)$ Solar energy incident at top (mW cm^{-2} μm^{-1})	Nominal spectral bandwidth (μm)	$\tau_1(\lambda)$ Scattering optical thickness due to molecules	$k_3(\lambda)$ Ozone absorption coefficient (atm-cm)$^{-1}$	$\tau_2(\lambda)$ Scattering optical thickness due to aerosols	$\tau_4(\lambda)$ Absorption optical thickness due to aerosols
0.2975	54.90	0.005	1.2652	13.58	0.08012	0.01369
0.3025	55.85	0.005	1.1779	6.76	0.08052	0.01355
0.3075	64.60	0.005	1.0980	3.50	0.08091	0.01342
0.3125	72.65	0.005	1.0248	1.73	0.08129	0.01328
0.3175	79.70	0.005	0.9577	0.890	0.08166	0.01315
0.3225	90.25	0.005	0.8960	0.460	0.08203	0.01302
0.3300	105.90	0.010	0.8123	0.1730	0.08256	0.01282
0.3400	107.40	0.010	0.7164	0.0515	0.08324	0.01257
0.3500	109.30	0.010	0.6341	0.0086	0.08390	0.01233
0.3600	106.80	0.010	0.5634	0.0014	0.08452	0.01209
0.3750	115.70	0.020	0.4751	0.0000	0.08539	0.01175
					$t_2 = 0.081$*	$t_4 = 0.013$*

* For DI Model multiply t_2 and t_4 by 4.18.

Table 4a. Parameters for $\mathscr{S}$, M and $r(\lambda, w_3)$ for average model

Species parameter	Rayleigh $l = 1$	Particulate $l = 2$	Ozone $l = 3$
γ_l	0.5777	0.427	0.977
A_{al}	0.7879	2.9550	0.1978
A_{bl}	0.5399	0.0230	0.6710
A_{cl}			3.285

Table 4b.

Alpha parameter	$\alpha = 0$	$\alpha = a$	$\alpha = b$
q_α	1.104	1.0790	0.5866
p_α	—	1.5230	0.7847
β_α	1.433	0.067	
t_α	0.0199	-3.31×10^{-3}	

GROUND ALBEDO DEPENDENCE

It is possible to infer the global irradiance $G(A, \lambda, \theta)$ for any ground albedo (A) from the global irradiance $G(0, \lambda, \theta)$ for zero ground albedo by using the formula

$$G(A, \lambda, \theta) = \frac{G(0, \lambda, \theta)}{1 - r(\lambda)A} \quad (11)$$

where $r(\lambda)$ are the air reflectivities. The air reflectivity values of Shettle and Green have fit rather accurately by a similar equation as the analytic equation for $M(\lambda)$ above i.e.

$$r(\lambda, w_3) = \frac{A_{b1}\tau_1 N_1(y) + A_{b2}[\tau_2 N_2(y)]^{p_b}}{1 + A_{b3}[\tau_3 N_3(y) + \tau_4 N_2(y)]^{q_b}}. \quad (12)$$

Table 4 gives the corresponding parameters for the various DBH models. Figure 3b illustrates the fits for the models at $w_3 = 0.2$, 0.3 and 0.4.

The dependence of the diffuse spectral irradiance upon the height of the ground above sea level has been a source of confusion. Strictly speaking, one cannot use the downward diffuse spectral irradiance at an altitude y above the ground (at sea level) as equivalent to the downward spectral irradiance at ground which is at a height y_g above sea level. Yet this is the only data available to us at this time. We can, however, use such data to fill out our analytic representation in the following way.

First, we calculate the equivalent ground albedo associated with the air and aerosols below ground altitude y by using the altitude dependent irradiance S, D and U in

$$\hat{A}_{eq} = \frac{U(y)}{D(y) + S(y)} \quad (13)$$

where U is the upward diffuse irradiance when the sea level ground albedo vanishes. The albedos so obtained are slightly dependent upon the sun angle as might be expected from the fact that the backscatter from the air and aerosols would not strictly by Lambertian. However, using $\hat{A}_{eq}$ to correct the downward diffuse spectral irradiance to the equivalent ground level but for zero ground albedo we use

$$S(0, \lambda, y_g) = S(0, \lambda, y) - r(\lambda, y)U(0, \lambda, y) \quad (14)$$

where $r(\lambda, y)$ is the air reflectivity function. We would expect this function to fall off with altitude in a way dependent upon the air and aerosols above the ground. Since the backscatter of air is usually much greater than the backscatter of aerosols, we will let

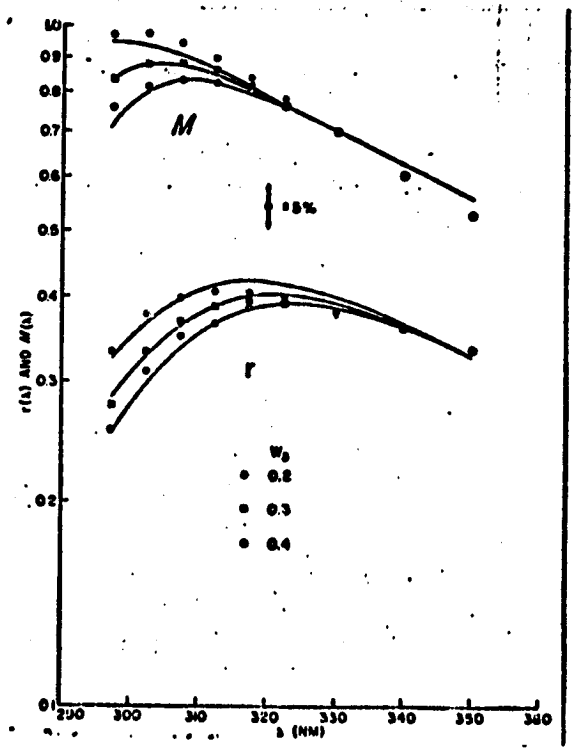

Figure 3a. Shows our fits to $M(\lambda)$. Again, the smooth curves are the fits and the points are the data.

Figure 3b. Shows analytic fits to $r(\lambda, w_3)$.

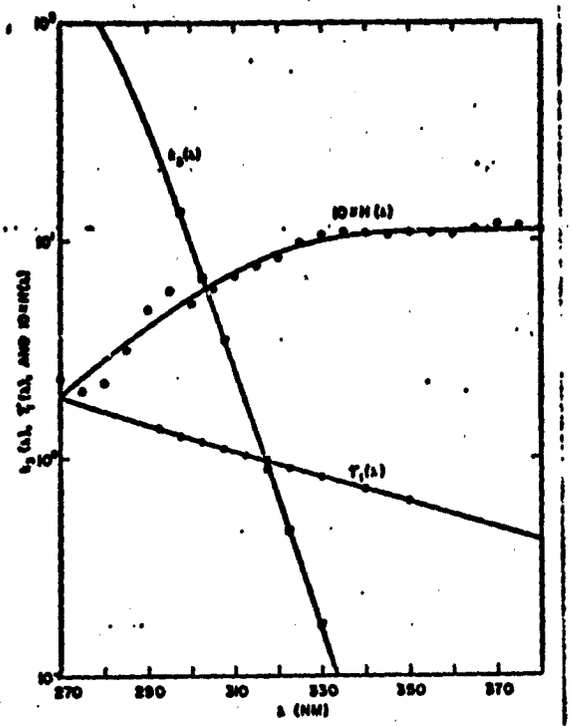

Figure 4. Spectral functions.

$r(\lambda, y)$ fall off with height above sea level according to the approximation

$$r(\lambda, y) = r(\lambda, 0)p(y)/p_0 = r(\lambda, 0)N_1(y). \quad (15)$$

This permits us to generate diffuse spectral irradiance values for ground level at an equivalent zero albedo. We next use the procedures in the previous section to analytically represent $S(0, \lambda, y_g)$. We have tested this procedure with model C. The altitude dependent coefficients are well characterized by Eq. 12.

WAVELENGTH DEPENDENT FUNCTIONS

Previously Green *et al.* characterized the extraterrestrial solar spectral irradiance $H(\lambda)$ by

$$H(\lambda) = K\left(1 + \frac{\lambda - \lambda_0}{d}\right). \quad (16)$$

This provides a reasonable representation in the interval 290 to 340 nm. However, to extend this we will use

$$H(\lambda) = K\left\{1 - \exp\left[-\kappa \exp\left(\frac{\lambda - \lambda_0}{\delta}\right)\right]\right\} \quad (17)$$

where $K = 1095$, $\kappa = 0.6902$, $\delta = 23.74$, $\lambda_0 = 300$ nm.

Figure 4 shows the fits in relationship to the data of Thekaekara (1971). It should be noted that the Planck function does not fit this spectral region no matter what temperature is chosen.

The Rayleigh optical depth can also be fit reasonably well in this spectral region by

$$\tau_1(\lambda) = \tau_{10}\left(\frac{\lambda_0}{\lambda}\right)^{4.27}$$

where

$$\tau_{10} = 1.221. \quad (18)$$

Figure 4 also shows this behavior.

Finally the ozone attenuation coefficient may be represented quite well by

$$k_3(\lambda) = k_0 \frac{\beta + 1}{\beta + \exp\left(\frac{\lambda - \lambda_0}{\delta}\right)} \quad (19)$$

where $k_0 = 2.517$, $\beta = 0.0445$ and $\delta = 7.294$.

Figure 4 also shows this function.

For the aerosol models chosen by Dave *et al.* it is sufficient to treat τ_2 as a constant, i.e. its value at $\lambda_0 = 300$ nm. For other models we could revert to the expression used earlier by GSS, i.e.:

$$\tau_2 = \tau_{20}(\lambda_0/\lambda)^{\nu_2} \quad (20)$$

DISCUSSION AND CONCLUSION

We have developed a mathematical expression for the diffuse spectral irradiance (skylight!) which has been adjusted simultaneously to the various models of DBH using their extinction and attenuation coefficients. The fits to these data are generally within 10% for the wavelengths (λ) zenith angles (θ), ozone thickness (w_3) and aerosol optical depths (τ_2) available as input data. The fits have been generalized to encompass several ground albedo (A) and ground altitude (y_g). The function of six variable (λ, θ, w_3, τ_2, A, y_g) so obtained can now reasonably be used for various interpolations and extrapolations between or somewhat beyond the data points used in adjustment process.

Our equations are capable of more precise fits to numerical data (5%) if one limits the number of models that are fit simultaneously and if one uses numerical inputs for $H(\lambda)$, $k_3(\lambda)$ etc. Thus we can describe the CI* model output, for example, with considerably greater precision and with fewer parameters than we can by fitting all the models simultaneously. Table 5 contains the parameter values for the individual fits to the various models. For some specialized purposes such representations might be useful as alternatives to the original tables.

For the purposes of most of the applications our generalized model adjusted to all of the cloudless DBH models should be most useful. Furthermore, if we replace the wavelength dependent inputs used by DBH by the smooth mathematical functions described in the Wavelength Dependent Functions section we can compute approximate spectral irradiances at arbitrary wavelength separation. This should be helpful to photobiologists who must convolute spec-

Table 5.

Model Parameter	B	C	CI	CI*	D	DI
(a) $M(\lambda)$ Parameters						
A_{o1}	0.7120	0.8869	0.7994	0.8628	0.8012	0.7994
A_{o2}	—	−0.7872≪⟨⟩⟨3.3274		14.614	3.6567	3.3274
A_{o3}	0.2333	0.3016	0.1918	0.2525	0.1556	0.1918
P_o	—	3.2873	1.6552	7.7010	1.6368	3.2873
q_o	1.0358	0.8909	1.0691	0.9257	1.0674	1.0691
(b) $r(\lambda, w_3)$ Parameters						
A_{b1}	0.5332	0.5640	0.5595	0.5608	0.4789	0.4375
A_{b2}	—	0.1000	−0.0127≪⟨⟩⟨0.1068		0.1470	0.07316
A_{b3}	0.5808	0.6470	0.6543	0.6428	0.5197	0.5829
P_b	—	1.0000	0.8118	0.9455	0.5165	0.2430
q_b	0.6539	0.6040	0.6020	0.6050	0.6334	0.6102
(c) $\mathscr{S}(\lambda, 0)$ Parameters						
γ_1	0.542	0.5842	0.5565	0.4758	0.5328	0.4840
γ_2	0.0	0.3968	0.5583	1.1383	0.6832	0.7779
γ_3	0.9833	0.9968	1.0046	1.0158	1.0234	1.0184
o	1.0712	1.1826	1.2010	1.0210	1.1510	1.2083
A_{o3}	8.0884	7.7196	1.0117	19.98	4.7746	0.6355
t_o	0.01992	0.02285	0.02091	0.02253	0.02892	0.02825
θ_o	0.5941	0.4123	3.0985	0.2701	0.5789	3.4702
θ_o	0	0	0	0	0	0
t_o	0	0	0	0	0	0

Table 6. Analytic models of $\mathscr{S}(\lambda, 0)$ tested*

Model	Formula	Fit
Exponential	$e^{-\alpha\phi}$	Poor
Double Exponential	$(1-F)e^{-\alpha\phi} + Fe^{-\beta\phi}$	Best
Mayer Goody ϕ	$e^{-\alpha\phi(1+\delta\phi)^{\frac{1}{2}}}$	Good
Verhulst ϕ	$F/(e^{\beta\phi} - 1 + F)$	Fair
Verhulst 0	$(\rho + 1)/(\rho + e^{\beta\theta})$	Poor
Verhulst 0^2	$(\rho + 1)/(\rho + e^{\beta\theta^2})$	Fair
Mayer Goody 0^2	$e^{-\alpha\theta^2/(1+\delta\theta^2)^{\frac{1}{2}}}$	Fair
Modified M-G 0^2	$e^{-\alpha\theta^2/(1+\delta\theta^2)}$	Fair
Gaussian −1	$e^{-\alpha\theta^2}$	Poor
Gaussian −2	$e^{-\alpha\theta^2-\delta\theta^4}$	Good
Gaussian −3	$(1-F)e^{-\alpha\theta^2} + Fe^{-\beta\theta^2}$	Fair
Fraction to Power	$[\alpha/(1-\mu+\alpha)]^\delta$	Fair
Malkmus	$\exp - 2\alpha/\beta[(1+\beta\phi)^{\frac{1}{2}} - 1]$	Good

* ϕ is defined by Eq. 8. The symbols β, α, δ, and F are wavelength dependent parameters.

tral irradiances with various types of action spectra to arrive at an equivalent dose rate for studies of dose response relationships. For such purposes the irregular structures in $M(\lambda)$, $k_3(\lambda)$ should average out for the most part.

Our analytic altitude distributions can also serve as a convenient way of inputting other possible atmospheric models. It is not unreasonable to expect that the spectral irradiances for somewhat varied altitude distributions will change in a fashion called for by our equations. It is also reasonable to allow for other absorbing components such as high SO_2 concentrations in an urban area into our model by incorporating an additional $w_5 k_5(\lambda) N_5(y)$ in parallel with the ozone term.

It might serve a useful purpose to inventorize the alternatives which we have examined during the course of this study. The GSS formula and the GM variation were first considered but set aside in favor of models which led to simpler expressions for the ratio $\mathscr{S}(\lambda, 0)$ (Eq. 4.) The two stream formula by Mo *et al.* (1974) was also considered but was found to be very cumbersome when modified to achieve accuracy. Table 6 lists some of the formulas which we have considered for the ratio $\mathscr{S}(0, \lambda)$ along with comments as to our fitting experience. While we cannot say that further data fitting will not change the overall rating the double exponential has the advantage of flexibility and simplicity. The ratios $M(\lambda)$ (Eq. 10) and $r(\lambda, w_3)$ (Eq. 12) were directly adapted from the GSS effort.

In final conclusion we trust that in addition to its usefulness to photobiologists our equation will serve as a frame of reference for charting experimental observations of diffuse UV spectral irradiances.

Acknowledgements—The writers would like to thank Dr. Norman Braslau and Dr. J. V. Dave for making available tapes and paper copy output of their original radiative transfer calculations. We would also like to thank Drs. Martyn Caldwell, Robert Rundel and Richard Zepp for their helpful comments.

This work was supported in part by the National Aeronautics and Space Administration Experiment Definition and Special Projects Branch (under Contract No. NAS9-15114) and the Nimbus 7 Data Application Office (under Contract No. ATM 75-21962).

REFERENCES

Bener, P. (1972) European Research Office, U.S. Army, London, Contract No. DAJA37-68-C-1017, p. 59.

Braslau, N. and J. V. Dave (1973) Effect of aerosols on the transfer of solar energy through realistic model atmospheres, Part III: Ground level fluxes in the biologically active bands, 12850-.3700 microns, IBM Research Report, RC 4308.

Dave, J. V. and P. Halpern (1976) *Atmos. Env.* 10, 547–555.

Chai, A. T. and A. E. S. Green (1976) *Appl. Opt.* 15, 1182–1187.

Garrison, L. M. L. E. Murray, D. D. Doda and A. E. S. Green (1978a) *Appl. Opt.* 17, 827–836.

Garrison, L. M., L. E. Murray and A. E. S. Green (1978b) *Appl. Opt.* 17, 683.

Green, A. E. S. (1976) Solar spectral irradiance reaching the ground, In *Proceedings on Nonbiological Transport and Transformation of Pollutants on Land and in Water.* National Bureau of Standards, New York.

Green, A. E. S., T. Sawada and E. P. Shettle (1974) *Photochem. Photobiol.* 19, 351–359.

Green, A. E. S. and T. Mo (1974) Proceedings of the 3rd Conference on CIAP, DOT-TSC-OST-74-15, 518–522.

Halpern P., J. V. Dave and N. Braslau (1974), *Science* 186, 1207.

Mo, T., G. P. Kezwer and A. E. S. Green (1975) *J. Geophys. Res.* 80, 2672–2676.

Shettle, E. P. and A. E. S. Green (1974) *Appl. Opt.* 13, 1567–1581.

Thekaekara, M. P. (1971) *Solar Electromagnetic Radiation.* NASA SP-8005.

AEROSOL EFFECTS ON ATMOSPHERIC RADIATION IN THE MIDDLE ULTRAVIOLET

A. E. S. Green and P. F. Schippnick
University of Florida[a]

The needs for an accurate characterization of ultraviolet (UV) skylight in several disciplines are sometimes better served by approximate analytic representations rather than by large masses of computer outputs. Towards this end we first review sources of numerical "data" for UV atmospheric radiation and prior attempts to characterize UV skylight analytically. After indicating the various formulas examined we present illustrations of fits of the Green, Cross and Smith formula to theoretical spectral irradiances calculated by Braslau and Dave. The degrees of freedom include wavelength, solar zenith angle, ozone thickness, aerosol content, ground albedo and altitude. Finally, we present a representation of Peterson's actinic UV flux in a form similar to that developed for spectral irradiance.

To be published in the Proceedings of
Atmospheric Aerosols Workshop
November 6-8, 1979

[a]*ICAAS, Gainesville, Florida 32611*

1. Introduction

Accurate characterizations of ultraviolet (UV) skylight are needed in several disciplines. These include photobiology, where UV plays an important role in vitamin D production, in skin cancer dose response studies and in agriculture where it adversely influences plant growth, and in biological oceanography where it influences phytoplankton. In addition, UV impacts upon air pollution, tropospheric chemistry in general and indirectly upon climate change questions. The need for accurate characterizations is probably better served by approximate analytic representations rather than by large masses of computer outputs. Towards this end we first review sources of numerical "data" on UV atmospheric radiation. Then we review a number of attempts by the Florida group to characterize UV skylight analytically. These began in 1973 with the Green, Sawada, and Shettle representation and continue with the 1979 formulation of Green, Cross and Smith. After indicating the various formulas examined we present illustrations of fits of these formulas to experimental and theoretical spectral irradiances. The degrees of freedom include wavelength, solar zenith angle, ozone thickness, aerosol content, ground albedo and altitude. Finally, we present a representation of actinic UV flux in a form similar to that developed for spectral irradiance. The purpose is to provide the user with convenient access to the massive body of radiative transfer calculations in the middle ultraviolet regions.

2. Prior Work and Sources of Data

Experimental and theoretical knowledge of atmospheric spectral

irradiance in the ultraviolet (UV), particularly the diffuse component (skylight) was at a very primitive state until the 1960s. From 1958 to 1969 Bener (1963, 1970a, b) conducted extensive series of measurements of solar ultraviolet (UV) radiation in Switzerland, which to this day provides the best available body of spectral data. The systematics of these measurements as functions of solar angle, wavelength, ozone thickness and other variables were gathered together in a final report (Bener, 1972).

The first major theoretical attempt to present UV spectral irradiances reaching the ground was by Dave and Furakawa (1966). They presented solutions to the radiative transfer equation for Rayleigh atmosphere having realistic levels of ozone. Serious attempts to allow for aerosol scattering came out first in 1973 in several parallel and independent efforts. Green, Sawada and Shettle (GSS, 1973, 1974) used a phenomenological modification of a formula based upon single Rayleigh and aerosol scattering adjusted to Bener's systematics as an analytic representation of the diffuse spectral irradiance (skylight). Simultaneously Shettle and Green (1974) developed a fast multiple scattering calculational method to predict UV spectral irradiance. Shotkin and Thompson also in 1973 used atmospheric models containing aerosols along with a Monte Carlo method and the two stream approximation to arrive at UV spectral irradiances. They compared their results with Bener's data and found some discrepancies of the order of 20%. Braslau and Dave (1973) also about the same time, used direct solutions of the spherical harmonic approximation to the basic radiative transfer equation to arrive at diffuse UV spectral irradiances. Thus by 1975 our knowledge

of UV radiation levels and the influence of aerosols upon it had advanced very greatly.

In connection with the applications mentioned in the introduction, there is a serious need for simple but reliable analytic characterizations of ultraviolet skylight which usually have greater biological importance than direct UV sunlight. The work along these lines by GSS and SG, by Green, Mo, and Miller (1974) Λ, Mo, Kezwer and Green (1975), and Green (1976) provide analytic representations of the systematics of Bener's 1972 work and of numerically calculated diffuse spectral irradiances of Shettle and Green. To overcome problems of assigning absolute irradiances, Chai and Green (1976), and Garrison et al. (1978a, b) focused attention on diffuse/direct ratios. These ratios depend more slowly upon wavelength than does the diffuse spectral irradiance itself. Unfortunately, because the direct irradiance becomes so small at large solar zenith angles, the dependence upon angle of the diffuse/direct ratio is very large. Green, Cross and Smith (1979) have recently found a more accurate analytic characterization of skylight which, for all angles and wavelengths of interest, will bring the fit to numerically generated diffuse irradiance from the 25% level of accuracy to about the 5% level. As input data they used the results of the more precise radiative transfer calculations of Braslau and Dave (1973) and Dave and Halpern (1975). This work summarizes the GCS effort particularly as it related to the influence of aerosols on skylight. In addition it describes some initial results of an attempt to represent actinic flux with a formula of the GCS type.

3. The GCS Representation of Diffuse Spectral Irradiance

The spectral irradiance problem has many dimensions; λ, the wavelength, θ, the sun angle, w_3, the ozone thickness, w_2, the aerosol thickness (both of which are dependent upon y, the altitude) and A, the ground albedo. In addition, the profile characteristics of the ozone and aerosol play a role.

The direct downward spectral irradiance reading the ground follows in a straightforward way using Beer's Law. It may be written in the form

$$D(\lambda,\theta) = \cos\theta\ H(\lambda)\exp - \sum_j \left(\tau_j / \mu_j\right) \qquad (1)$$

where τ_1, τ_2, τ_3 and τ_4 denotes the Rayleigh scattering, aerosol scattering, ozone absorbing and aerosol absorbing optical depths, and μ, μ_1, μ_2 and μ_3 denote $\cos\theta$ and generalized cosine functions of the form

$$\mu_i = (\mu^2+t_i)/(1+t_i)^{\frac{1}{2}} \qquad (2)$$

Here the t_i's are small characteristic numbers depending upon the altitude distribution of the species which allow approximately for the roundness of the earth. It would be time- and space-consuming to recount all the analytic forms, mathematical models and approaches which have been tried to analytically characterize the diffuse spectral irradiance. The most natural model to start with is the two stream model and attempts to use it have been made by Shotkin and Thompson (1973) and by Mo, Kezwer and Green (1975). However, inaccuracies or cumbersomeness have thus far favored empirical models over the two stream model. In the GCS model the basic strategy was to represent the downward diffuse spectral

irradiance (S) at the ground in terms of two ratios and the direct spectral irradiance for an overhead sun ($\theta = 0$, or $\mu = 1$). Thus diffuse sky irradiance is expressed in the form

$$S(\lambda,\theta) = \mathcal{S}(\lambda,\theta)\mathcal{M}(\lambda)H(\lambda)\exp -(\textstyle\sum_j \tau_j) \qquad (3)$$

where

$$\mathcal{S}(\lambda,\theta) = S(\lambda,\theta°)/S(\lambda,0°) \qquad (4)$$

with

$$\mathcal{M}(\lambda) = S(\lambda,0°)/D(\lambda,0°) \qquad (5)$$

The virtue of this combination of ratios is that the dynamic range of $\mathcal{S}(\lambda,\theta)$ and particularly $\mathcal{M}(\lambda)$ over the wavelength range of interest (280-380nm) and for various aerosol optical depths and ozone thicknesses of interest are relatively modest so that analytic representations at the few percent level of accuracy should be feasible except possibly at the largest solar zenith angles and the shortest wavelengths.

The numerically generated points in Figure 1 illustrate variations of $\mathcal{S}$ with θ at $w_{oz} = 0.30$ using "data" obtained from Dave and Halpern (1975). The dark smooth curves on Figure 1 are derived from the GCS analytic representation

$$\mathcal{S}(\lambda,\theta) = [\,F + (1-F)\exp-\gamma_3(\tau_3+\tau_4)\phi]\exp-(\gamma_1\tau_1 + \gamma_2\tau_2)\phi \qquad (6)$$

where

$$\phi = [(1 + t)/(\mu^2 + t)]^{\frac{1}{2}} - 1 \qquad (7)$$

Here τ_4 denotes the particulate absorption optical depth corresponding to τ_2 the particulate scattering optical depth and

$$F = \frac{1}{1 + A_{o3}[\tau_3 N_3(y) + \tau_4 N_2(y) + g\ k_3(\lambda)]^{q_o}} \tag{8}$$

with

$$t = t_o + t_a y \tag{9}$$

and

$$g = g_o + g_a y \tag{10}$$

The functions $N_1(y)$, $N_2(y)$, and $N_3(y)$ are the total thicknesses above the altitude each normalized to unity at sea level (y = 0). Following GSS, GCS and other works they are represented by the mathematical form

$$N_i(y) = f_i \frac{1 + \alpha_i}{\alpha_i + \exp\ (y/h_i)} + (1-f_i) \frac{1+\exp\ -\ y_i/\chi_i}{1+\exp\ (y-y_i)/\chi_i} \quad . \tag{11}$$

With these representations the $\tau_i(\lambda)$ are the optical depths at sea level.

Also shown on Figure 1 by light lines are the direct ratios

$$\mathfrak{D}(\lambda,\theta) = D(\lambda,\theta)/D(\lambda,0°) \tag{12}$$

Note that these fall off more rapidly at large solar zenith angles than do the corresponding $\mathcal{S}(\lambda,\theta)$. Thus, as the sun sets the diffuse irradiance increasingly becomes more important as compared to the direct irradiance.

For $\theta = 0$ the relative magnitudes of the direct and diffuse spectral components are fixed by the $\mathcal{M}(\lambda)$ function. The lower curve in Fig. 2 gives the $\mathcal{M}(\lambda)$ function for $w_3 = 0.3$cm.

$$\mathcal{M}(\lambda) = \frac{A_{a1}\tau_1 N_1(y) + A_{a2}[\tau_2 N_2(y)]^{p_a}}{1 + A_{a3} w_3 N_3(y)\,[\tau_3 N_3(y) + \tau_4 N_2(y)]^{q_a}} \quad . \tag{13}$$

Table 1 gives parameters for the GCS diffuse spectral irradiance formula for an average atmospheric model. The quantities in parentheses will be described in the next section. To complete an analytic representation it is necessary to specify $H(\lambda)$, $\tau_1(\lambda)$, $\tau_2(\lambda)$, $\tau_3(\lambda)$ and $\tau_4(\lambda)$. The wavelength dependence of $H(\lambda)$ in the interval 280-380mn may be represented as a smooth function

$$H(\lambda) = K \left\{1 - \exp[- \kappa \exp (\frac{\lambda - \lambda_o}{\Delta})]\right\} \qquad (14)$$

with $K = 1095$ W/m^{2}nm, $\kappa = 0.6902$, $\Delta = 23.74$, $\lambda_o = 300$nm. This empirical function fits much better than the Planck function no matter what temperature is chosen.

The Rayleigh optical depth and the ozone absorption coefficient may be represented by

$$\tau_1(\lambda) = 1.221(\lambda_o/\lambda)^{4.27} \qquad (15)$$

and

$$k_3(\lambda) = \tau_3(\lambda)/w_3 = k_o(\beta+1) \; / \; [\beta+\exp(\frac{\lambda - \lambda_o}{\delta})] \qquad (16)$$

with $k_o = 9.517$ (atm. cm)$^{-1}$, $\beta = 0.0445$ and $\delta = 7.294$. For most purposes it is sufficient to characterize the aerosol scattering depth τ_2 and the aerosol absorption depth τ_4 as independent of wavelength over the range 280nm to 380nm. While some variation would be expected, the usually uncertain differences between atmospheric models from the no-aerosol case $\tau_2 = \tau_4 = 0$ to an average aerosol case, $\tau_2 = 0.08$, $\tau_4 = 0.012$, to a heavy aerosol case, $\tau_2 \approx 0.34$, $\tau_4 \approx 0.05$, far outweigh these minor wavelength variations.

The foregoing equations apply to the case of zero ground albedo. One can use the methodology of Shettle and Green, and Green, Cross and Smith to correct for any ground albedo. This entails introducing an air reflectivity function, $r(\lambda,w_3)$ which may be represented by

$$r(\lambda,w_3) = \frac{A_{b1}\tau_1 N_1(y) + A_{b2}[\tau_2 N_2(y)]^{P_b}}{1 + A_{b3}[\tau_3 N_3(y) + \tau_4 N_2(y)]^{q_b}} \tag{17}$$

The complete model so constructed using the average parameters given in Table 1 provides a reasonably accurate representation of spectral irradiance for all of the Dave Braslau atmospheric models.

To correct the irradiance for non-zero albedo we use

$$G(A,\lambda,\theta) = \frac{G(0,\lambda,\theta)}{1 - r(\lambda,w_3)A} \tag{18}$$

where A is the ground reflectivity and

$$G(0,\lambda,\theta) = D(\lambda,\theta) + S(\lambda,\theta).$$

4. Analytic Representation of the Diffuse Actinic Spectral Flux

Peterson (1976) has used the Dave Braslau multiple scattering code to calculate values of the actinic flux as a function of altitude, wavelength, and solar zenith angle for an ozone thickness of 0.292 atm-cm, aerosol scattering depth of 0.204 at 302.5nm and an aerosol absorption depth of 0.034. He presents the values calculated for the ground level in two tables, one for zero albedo and the other for a best-estimate albedo. Starting with his zero albedo values, we subtracted off the corresponding direct actinic flux, $\tilde{D}(\lambda,\theta)$, to obtain the inferred downward (since at ground level with zero albedo) diffuse actinic flux, $\tilde{S}(\lambda,\theta)$, at ground level. For the direct actinic flux Beer's law gives

$$\tilde{D}(\lambda,\theta) = H(\lambda)e^{-\tau\sec\theta} \tag{19}$$

where $\tau = \sum_i \tau_i$, where the τ_i are previously defined. Here we do not differentiate the μ_i's since large solar zenith angles are not used.

The downward diffuse actinic flux at ground level for zero albedo is represented in a form completely analogous to that for the downward diffuse irradiance (see Eq.(3)). The ratio $\tilde{\mathcal{S}}(\lambda,\theta) = \tilde{S}(\lambda,\theta)/\tilde{S}(\lambda,0°)$ is defined likewise in complete analogy with the irradiance case (See Eq.(6)) as is $\tilde{\phi}$ (see Eq. (7)). It will be convenient to designate the actinic case values of the GCS fit parameters and functions by placing a tilde over the general symbol.

Now, instead of defining $\tilde{F}$ in strict analogy with F in Eq. (8) we have simplified $\tilde{F}$ a little to facilitate the fit to Peterson's data. The reason for this is that the parameter g in Eq. (8) controls the variation of F with w_3 and altitude and since we had only one value of w_3 to work with and one altitude, the purpose of the parameter g was nullified. Thus, in $\tilde{F}$ we simply set $\tilde{g} = 0$. $\tilde{M}(\lambda)$ is defined in exact analogy with the irradiance case (Eq. (13)).

The parameter values for this representation of the actinic flux are given in parenthesis in Table 1. Figure 3 displays graphs of $\tilde{\mathcal{S}}(\lambda,\theta)$ and $\tilde{\mathcal{D}}(\lambda,\theta)$ for selected values of λ. One sees a close similarity of the $\tilde{\mathcal{S}}(\lambda,\theta)$ with $\mathcal{S}(\lambda,\theta)$ in Fig. 1 in both shape and magnitude. The $\mathcal{D}(\lambda,\theta)$ and $\tilde{\mathcal{D}}(\lambda,\theta)$ are quite different, however, because of the $\cos\theta$ factor in Eq. (1).

A comparison of the parameters in Table 1 indicates that the γ's do not change much: γ_1 changes the most with a 35% decrease. F and $\tilde{F}$ are both relatively small throughout the wavelength region of interest. All in all, the normalized θ-dependence is not much changed.

The greatest difference between irradiance and actinic representations lies between $M(\lambda)$ and $\tilde{M}(\lambda)$ (see Fig. 2). We may first note the ratio $\tilde{A}_{a3}/A_{a3} = 7.95$. The large relative value of $\tilde{A}_{a3}$ causes $\tilde{M}(\lambda)$ to fall more steeply as λ decreases from 310nm than does $M(\lambda)$. Above 315nm the denominators of $M(\lambda)$ and $\tilde{M}(\lambda)$ are both nearly unity. Now turning our attention to the numerators, let us denote the Rayleigh and aerosol terms by R and A and take note of the following handy decomposition:

$$\frac{\tilde{R} + \tilde{A}}{R + A} = \frac{\tilde{R}}{R} \cdot \frac{1}{1 + A/R} + \frac{\tilde{A}}{A} \cdot \frac{1}{1 + R/A} \qquad (20)$$

Now note that $\tilde{R}/R = \tilde{A}_{a1}/A_{a1} = 2.19$, $\tilde{A}/A$ has the essentially constant value of .59, and R/A lies in the range 2.0-3.5. The ratio of the numerators is thus seen to lie in the range 1.6-1.8. Taking the effect of the denominator into account, one obtains that the ratio $\tilde{M}(\lambda)/M(\lambda)$ lies in the range 1.4-1.7, and in fact the ratio $\tilde{M}(\lambda)/M(\lambda)$ has a mean value of 1.62 over the wavelength interval 295nm-365nm (the wavelength region of interest) and median value of 1.64 there.

Going back to the normalized θ-dependence, we observe another interesting contrast in the parameter values between the actinic and irradiance cases, namely in the parameter A_{03}. The comparison of $\tilde{A}_{03}$ and A_{03} is complicated by the fact that we set $\tilde{g} = 0$. Noting that $\tau_3 >> \tau_4$ for $\lambda < 320$nm, it is clear after a little algebra that $\tilde{A}_{03}$ roughly corresponds to $A_{03}(1 + g_o/w_3)^{q_o}$ in this region. Noting that $\tau_4 >> \tau_3$ for $\lambda > 340$nm, it is then clear that $\tilde{A}_{03}$ roughly corresponds to A_{03} in this region. Thus one might expect the value of $\tilde{A}_{03}$ chosen by the fit to be some sort of average of the values of the above two expressions which are, respectively, 23.34 and 3.285. This is indeed the case, with $\tilde{A}_{03} = 12.02$.

5. Conclusions

In the work summarized in Section 3 it has been shown to be possible to represent diffuse spectral irradiance in the 280-380nm region to a reasonable level of accuracy by an analytic model which displays the explicit dependences upon the ozone parameter w_3 and the aerosol parameters τ_2 and τ_4. For a more precise representation of the Braslau Dave data, i.e. to the 5% level of accuracy, the work of Green, Cross and Smith suggests that some of the parameters should be particularized to the specific Braslau Dave atmospheric model. It might be remarked that with the adjustment of only one aerosol parameter ($A_{a2}^{*} = 12.8$) the average GCS model (see Table I) successfully represented a large body of irradiance data taken in the South Pacific by Baker and Smith (1980).

The work presented in Section 4 is based upon a much more limited data set. It suggests that actinic flux can also be represented by the same equations. A detailed comparison of the $\mathcal{S}(\lambda,\theta)$ and $\tilde{\mathcal{S}}(\lambda,\theta)$ in Figures 1 and 3 indicates that these two quantities are very close for all values of λ and θ. Thus the difference between $S(\lambda,\theta)$ and $\tilde{S}(\lambda,\theta)$ is largely manifested in the differences between $\mathcal{M}(\lambda)$ and $\tilde{\mathcal{M}}(\lambda)$. These quantities have essentially the same shape and the significant difference between them can be best expressed as a rough scaling factor of 1.62.

Our work on the actinic flux is not yet completed. We have yet to test our model with other values of ozone thickness or at varying altitudes. Such work, which requires the generation of additional "data" using a radiative transfer code is now in progress. However, it is not unreasonable to expect that the GCS dependencies upon w_3 and y for spectral irradiance will also be efficacious for representing the dependence of

actinic flux upon these same variables. As an interim measure to characterize the actinic flux as a function of all independent variables including w_3 and y, it is not unreasonable to use $\tilde{\mathcal{I}}(\lambda,\theta) = \mathcal{I}(\lambda,\theta)$, $\tilde{M}(\lambda) = 1.62M(\lambda)$ and $\tilde{r}(\lambda,w_3) = r(\lambda,w_3)$. The interim and the final actinic formulae should be applicable in models of smog reaction, tropospheric chemistry and other important photochemical problems.

6. Acknowledgment

This work was supported in part by Grant R 806373010 from the United States Environmental Protection Agency.

References

Bener, P., The diurnal and annual variations of the spectral intensity of ultraviolet sky and global radiation, Switzerland, Technical Note No. 2, Jan. (1963).

Bener, P., Measured and theoretical values of the spectral intensity of ultraviolet zenith radiation and direct solar radiation at 316, 1580 and 2818 m, a.s.l, AFCRL, Contract F 61052-67-C-0029, (1970).

Bener, P., Solar intensity and intensity and polarization of sky radiation for 347.0, 488.0 and 533.5nm at selected points along the sun's vertical and other meridians measured at 2818 m a.s.l., August, (1970).

Bener, P., Technical Report, European Research Office, U.S. Army, London, Contract No. DAJA 37-68-C-1017 (1972).

Baker, K. R., and R. A. Smith, private communication.

Braslau, N., and J. V. Dave, Effect of aerosols on the transfer of solar energy through realistic model atmospheres, Part III: Ground level fluxes in the biologically active bands, 12850-.3700 microns, IBM Research Report, RC 4308 (1973)

Chai, A. T., and A. E. S. Green, Measurement of the ratio of diffuse to direct solar irradiances in the middle ultraviolet, Applied Optics, 15:1182 (1976).

Dave, J. V., and P. M. Furukawa, Meteor. Monographs, 7:1-10 (1966).

Dave, J. V., and P. Halpern, Atmos. Env., 10:547-555 (1976).

Garrison, L. M., L. E. Murray, D. D. Doda, and A. E. S. Green, Diffuse-direct ultraviolet ratios with a compact double monochromator, Applied Optics, 17:(5), March (1978)

Garrison, L. M., L. E. Murray, and A. E. S. Green, Ultraviolet limit of solar radiation at the earth's surface with a photon counting monochromator, Applied Optics, 17(5), March (1978).

Green, A. E. S., Solar spectral irradiance reaching the ground, Proceedings on Nonbiological Transport and Transformation of Pollutants on Land and in Water, May (1976).

Green, A. E. S., K. R. Cross, and L. A. Smith, Improved Analytic characterization of ultraviolet skylight, Photochemistry and Photobiology, (to be published).

Green, A. E. S., T. Mo, and J. H. Miller, A Study of Solar Erythema Radiation Doses, Photochemistry and Photobiology, 20: (473) (1974).

Green, A. E. S., T. Sawada, and E. P. Shettle, The middle ultraviolet reaching the ground, Photochemistry and Photobiology, 19:(251) (1974).

Mo, T., G. P. Kezwer, and A. E. S. Green, The use of the modified two-stream approximation to represent a multistream numerical solution of the radiative transfer equation, Journal of Geophysical Research, 80:(18) June (1975).

Peterson, James T., Calculated Actinic Fluxes (290-700nm) For Air Pollution Photochemistry Applications, EPA-600/4-76-025, June 1976. U.S. Environmental Protection Agency, Office of Research and Development.

Shettle, E. P., and A. E. S. Green, Multiple scattering calculation of the middle ultraviolet reaching the ground, Applied Optics, 13:(7) July, (1974).

Shotkin, L. M., and J. F. Thompson, Jr., Use of an atmospheric model with aerosols to examine solar UV data, Journal of the Atmospheric Sciences, 30:1699, Nov. (1973).

Table 1. Parameters for Analytic Models of Spectral Irradiance and Actinic Flux

γ_1	0.5777 (0.370)	A_{a1}	0.7879 (1.726)	A_{b1}	0.540	g_o	1.433 (---)	p_a	1.523 (2.094)	p_b	0.785	t_1	1.8×10^{-3}
γ_2	0.427 (0.505)	A_{a2}	2.955 (4.23)	a_{b2}	0.0230	q_o	1.104 (1.166)	A_{03}	3.285 (12.02)	q_b	0.587	t_2	3.0×10^{-4}
γ_3	0.977 (0.983)	A_{a3}	0.198 (1.575)	A_{b3}	0.671	t	0.0199 (.00928)	q_a	1.079 (1.124)			t_3	7.4×10^{-3}

Figure Captions

Fig. 1. $S(\lambda,\theta)$ and $\mathcal{D}(\lambda,\theta)$ for λ = 297.5, 307.5, and 330.0nm. The points represent the "data" for $S(\lambda,0)$; the solid curves are the GCS fit. The broken curves illustrate $\mathcal{D}(\lambda,\theta)$ at the corresponding wavelengths.

Fig. 2. $M(\lambda)$ and $\tilde{M}(\lambda)$. The points represent the "data" for $\tilde{M}(\lambda)$.

Fig. 3. $\tilde{S}(\lambda,\theta)$ and $\tilde{\mathcal{D}}(\lambda,\theta)$ for λ = 297.5, 307.5, and 330.0nm. The points represent the "data" for $\tilde{S}(\lambda,\theta)$; the solid curves are the fit arrived at in the present work. The broken curves illustrate $\tilde{\mathcal{D}}(\lambda,\theta)$ at the corresponding wavelengths.

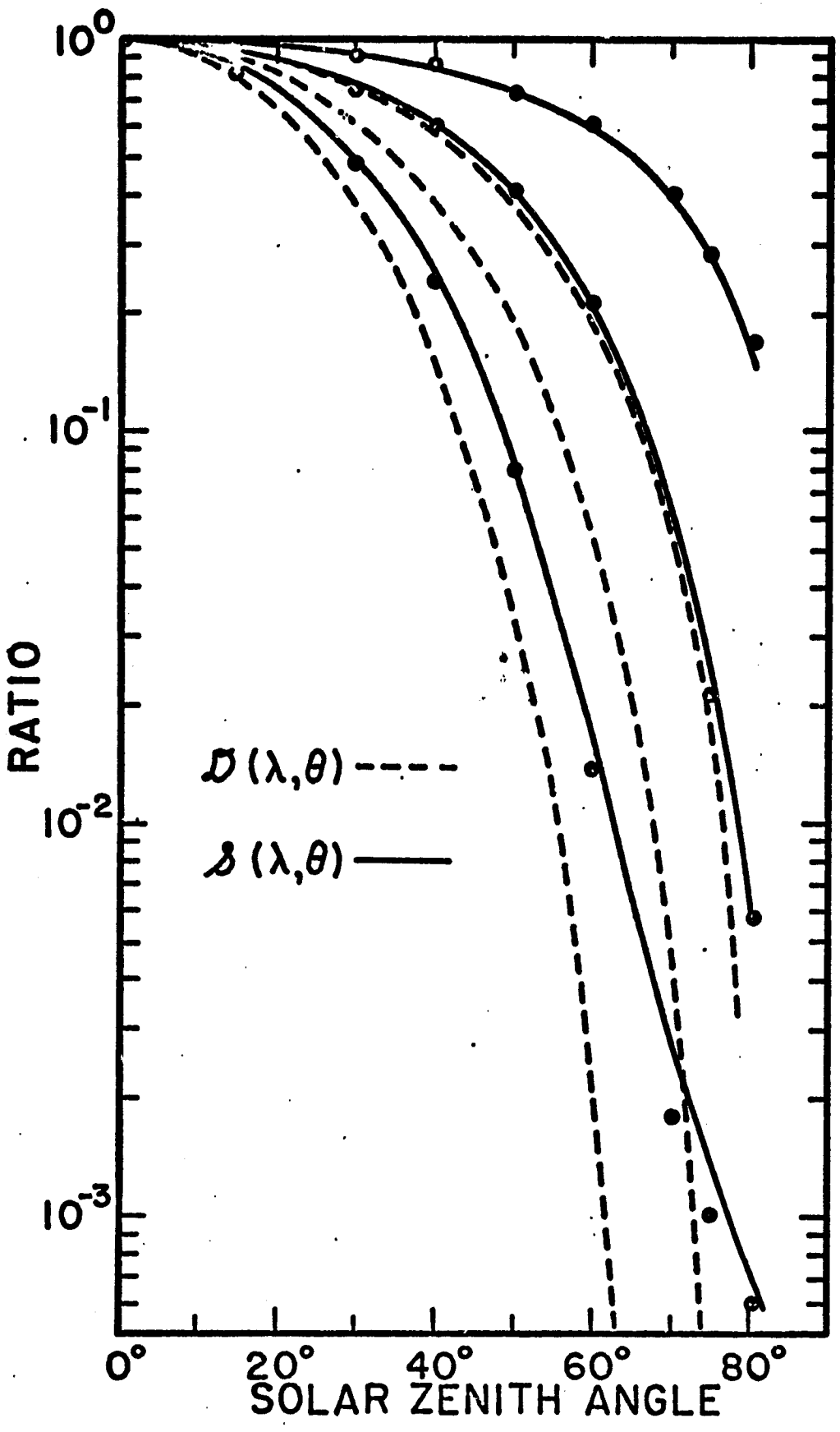

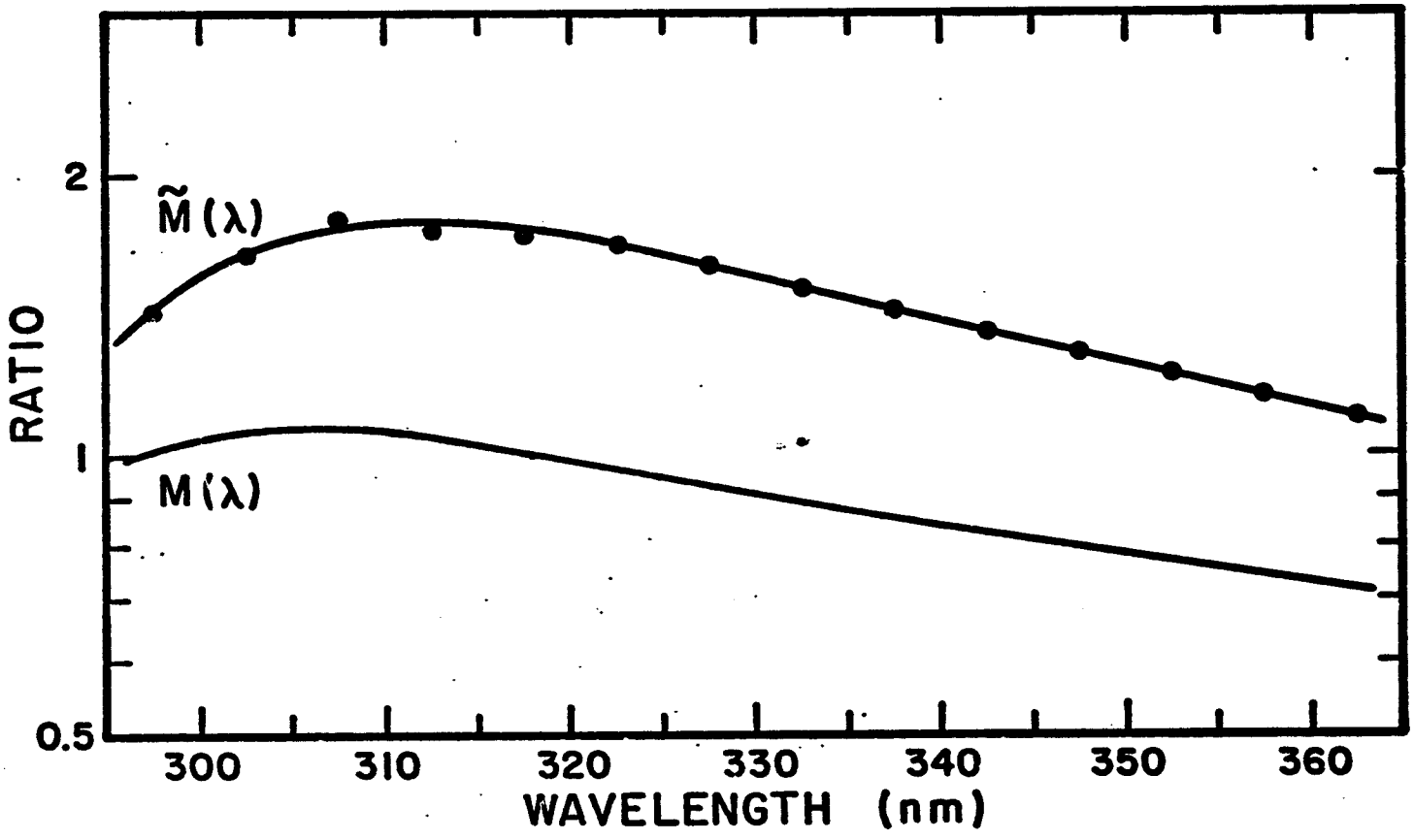
RATIO
2
1
0.5
$\tilde{M}(\lambda)$
M(λ)
300
310
320
330
340
350
360
WAVELENGTH (nm)

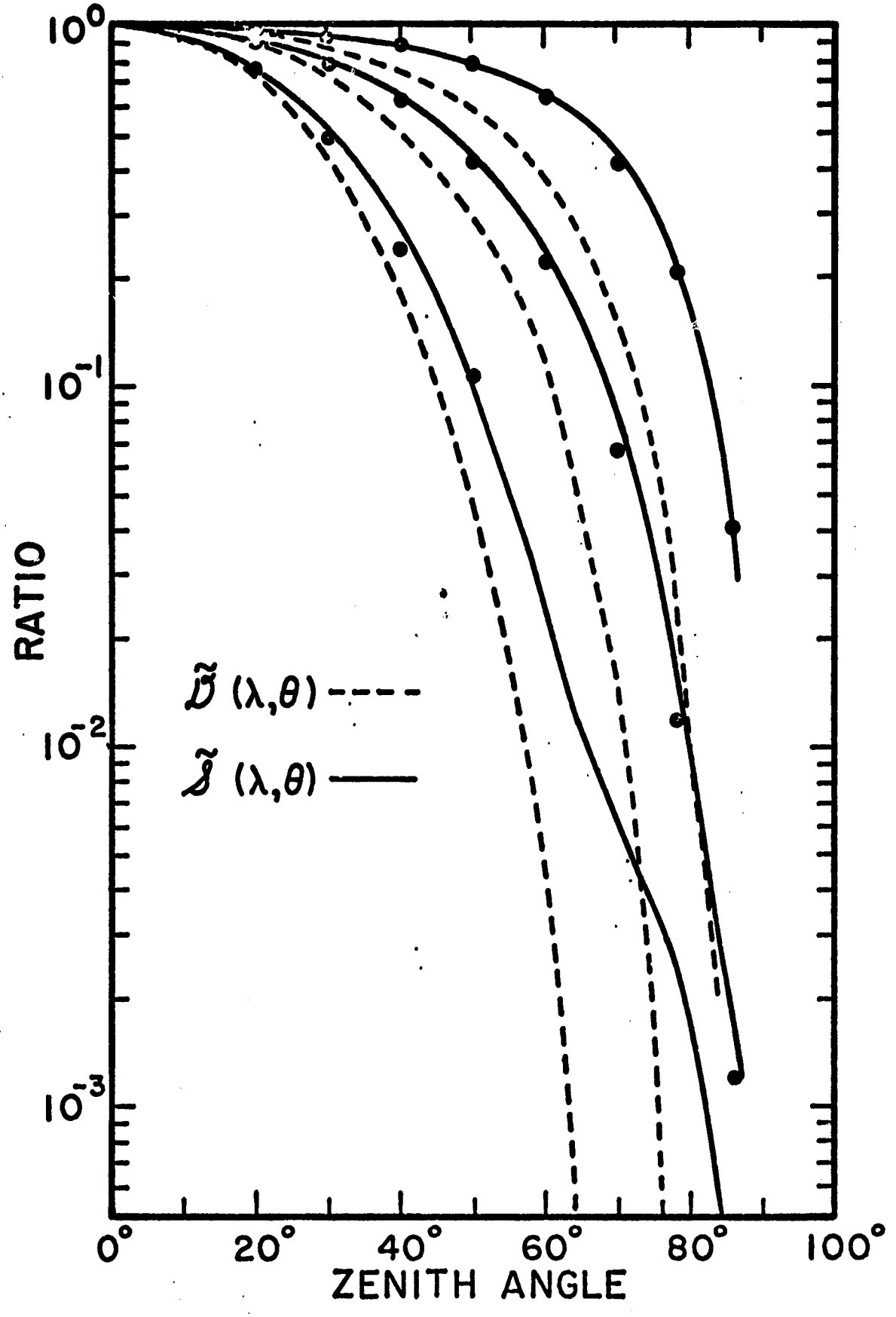
10^0
10^{-1}
10^{-2}
10^{-3}
RATIO
$\tilde{\mathcal{D}}(\lambda,\theta)$ ----
$\tilde{\mathcal{J}}(\lambda,\theta)$ ——
0°
20°
40°
60°
80°
100°
ZENITH ANGLE

ICAAS

UNIVERSITY OF FLORIDA
SPACE SCIENCES RESEARCH BLDG.
GAINESVILLE, FLORIDA 32611
AREA CODE 904 PHONE 392 2027

COAL BURNING ISSUES

A monograph reporting the results of the scoping phase of an interdisciplinary assessment of the impact of the increased use of coal

A. E. S. Green, Editor

Contributions by:

Faculty and Postdoctoral Staff

J. F. Alexander, Jr.
W. E. Bolch, Jr.
E. F. Brigham
E. L. Capehart
L. C. Capehart
W. L. Chameides
R. W. Fahien
F. Fardshisheh
A. E. S. Green
H. P. Hanson
M. J. Jaeger
H. H. Lee
J. W. Little
J. G. Melville
M. J. Ohanian
W. A. Rosenbaum
E. H. Schlenker
R. T. Schneider
J. M. Schwartz
J. J. Street
K. E. Taylor
P. Urone
S. S. Woltz

Research Staff

W. M. Denty, Jr.
L. C. Gapenski
R. K. Hutchinson
M. A. Kenney
D. J. Miller
J. D. O'Connor
D. E. Rio
R. J. Rognstad, Jr.
M. J. Rowe
D P. Swaney

To be published by:

University Presses of Florida
Gainesville, Florida

Pre-publication version November 1, 1979

Interdisciplinary Center for Aeronomy and (other) Atmospheric Sciences

Table of Contents

Contributor, Department and College

John F. Alexander, Jr., Associate Professor, Urban and Regional Planning, Architecture, Acting Director, Center for Wetlands.

William E. Bolch, Jr., Professor, Environmental Engineering Sciences, Engineering.

Eugene F. Brigham, Graduate Research Professor, Director, Public Utility Research Center, Business.

Barney L. Capehart, Professor, Industrial and Systems Engineering, Engineering.

Lynne C. Capehart, Legal Research Associate, ICAAS.

William L. Chamberlain, Assistant Professor, Physics, Liberal Arts and Sciences.

William H. Dusty, Jr., Student Assistant, Industrial and Systems Engineering, Engineering.

Raymond W. Fahien, Professor, Chemical Engineering, Engineering.

Parameswar Fardoshisheh, Adjunct Postdoctoral Research Associate, ICAAS.

Louis C. Gapenski, Research Associate, Public Utility Research Center, Business.

Alex E. S. Green, Graduate Research Professor, Physics and Nuclear Engineering Sciences; Liberal Arts and Sciences and Engineering, Director, ICAAS.

Harold P. Hanson, Professor, Physics, Liberal Arts and Sciences.

Robert K. Hutchinson, Graduate Research Assistant, Urban and Regional Planning, Architecture.

Marc J. Jaeger, Professor, Physiology, Medicine.

Michael A. Kenney, Graduate Assistant, Environmental Engineering Sciences, Engineering.

Hung H. Lee, Assistant Professor, Chemical Engineering, Engineering.

Joseph W. Little, Professor, College of Law.

Joel G. Melville, Assistant Professor, Civil Engineering, Engineering.

Dennis J. Miller, Graduate Assistant, Chemical Engineering, Engineering.

Joseph D. O'Connor, Graduate Assistant, Industrial and Systems Engineering, Engineering.

M. J. Ohanian, Associate Dean for Research; and Professor, Nuclear Engineering Sciences, Engineering.

Daniel E. Rio, Graduate Assistant, Nuclear Engineering Sciences, Engineering.

Ralph J. Ragonese, Jr., Graduate Research Assistant, Urban and Regional Planning, Architecture.

Walter A. Rosenbaum, Professor, Political Science, Liberal Arts and Sciences.

Michael J. Rowe, Staff Engineer, Nuclear Engineering Sciences, Engineering.

Evelyn M. Schlenker, Postdoctoral Research Fellow, Physiology, Medicine.

Richard T. Schneider, Professor, Nuclear Engineering Sciences, Engineering.

Jerome M. Schwartz, Associate in Atmospheric Sciences, ICAAS.

Jimmy J. Street, Assistant Professor, Soil Sciences, IFAS.

Dennis P. Sunney, Adjunct Assistant In Wetland Ecological Research, Center for Wetlands.

Karl E. Taylor, Assistant Professor, Physics, Liberal Arts and Sciences.

Paul Urone, Professor, Environmental Engineering Sciences, Engineering.

Shreve S. Woltz, Professor, Agricultural Research and Education Center, Institute of Food and Agricultural Sciences.

FOREWORD

This book is a product of the collective work of a group of faculty members of the University of Florida. Although each writer is a full-time teaching or researching member of a disciplinary department of the University, all participate regularly in interdisciplinary research conducted under the auspices of the Interdisciplinary Center for Aeronomy and (other) Atmospheric Sciences, known as ICAAS. Since 1970 ICAAS has conducted research projects pertaining to atmospheric pollution and related phenomena. These studies are exemplified by a multidisciplinary assessment of an anticipated large increase in the utilization of coal in Florida, which is now underway with Board of Regents support.

Although many ICAAS members are physical scientists, its research has not been limited to hard science issues. Rather, ICAAS employs a broad gauge public policy approach, bringing together the hard sciences, life and agricultural sciences, social sciences, economics, medicine, law and other disciplines with the goal of seeking technical solutions to complex problems that are also socially and politically acceptable.

ICAAS members foresee a period of severe social stress ahead as this nation is forced to switch to coal from oil and natural gas as its primary energy source. The forces are multiple, posing specific technical, environmental, political, legal, and other kinds of issues that are individually intractable and that in sum pose an extremely formidable barrier to the nation's well-being. ICAAS members believe that a concentrated multidisciplinary effort by academic scholars and researchers can help the nation get over that barrier.

Such efforts have many precedents. After the outbreak of World War II the American academic community rallied quickly to the nation's defense. In addition to specialized training programs, important contributions were made to technological developments, such as radar, missiles, rocket-assisted take-off aircraft, the proximity fuse, weather forecasting techniques, operations analysis methods, and many others which helped win World War II. Beyond doubt, the atomic bomb is the best known World War II product of academic scientists. Although almost all of Japan's war potential was destroyed before it was used, the bomb

still is generally credited with avoiding the invasion of Japan which would have taken many lives.

Today, academicians, like all citizens, are grateful that the nation is not engaged in a shooting war. Nevertheless, the independence of the nation is threatened so severely by the impending energy shortfall that President Carter has called it the moral equivalent of war. The relatively slow development of this "moral war," which truly is an economic struggle for survival, affords the academic community with yet another opportunity to serve the nation. The nature of this war and the general direction that the United States must now take have been outlined in Project Independence (1974), The National Energy Plan (1977), and the Camp David plans (1979). Although wide areas of disagreement about what should be done still remain, both Republican and Democratic administrations have agreed that the essential aims set forth in these plans must be achieved: (1) import less foreign oil; (2) conserve energy; (3) to live within the nation's resources, make coal the major alternative to foreign oil.

How can the academic community help achieve these goals? In general, it is not as well-equipped as large industrial and governmental laboratories to handle major engineering developments, but it can originate new ideas, evaluate and extend innovative technology, and carry out early phases of development work. Perhaps most important, a University faculty, being a repository of experts and scholars of many disciplines, is unusually well-qualified to perform multidisciplinary assessments.

This book singles out one topic, namely Coal Burning Issues, as the focus of its attention. The writers have examined the technical, medical, environmental, legal, economic and public policy issues that must be addressed as the nation increases its dependence on coal. The book does not purport to supply answers; too much work remains to be done such as a more in-depth examination of the apparently most feasible solutions. Instead, it is written with the hope of accelerating examination of a series of critical, long-term strategic and short-term tactical options. This must be done without undue delay because passing time irrevocably closes options.

This book employs no single style. In part it employs quantitative analyses and in part it examines social, political and legal choices influencing the nation's energy future. No attempt has been made as yet to eliminate all disagreements. For example, the reader may note divergencies among some of the chapters in estimates of coal and other resources. These estimates have traditionally varied by large factors depending upon the perspectives of the estimators and divergencies are characteristic of the technical publications examined in the course of this study. Accordingly, they do not detract from but indeed enhance this work, which aims to highlight both settled and disputed facts and viewpoints that will influence imminent public policy choices.

In the past, America's academic community has played a vital role in protecting the nation in shooting wars. It seems certain that no less a role is to be played in winning the economic war of survival that now entangles the nation's future. The writers of this book hope that the presentation made here points the way to solutions to some of the coal burning issues. The next goal of the group is to help supply some of the detailed solutions to the energy, environment and economy problems related to the increased utilization of coal.

ACKNOWLEDGMENTS

In such a broad interdisciplinary effort many persons besides those listed as authors have made important direct or indirect contributions. First, it is a pleasure to thank some of the key University of Florida administrators who ten years ago encouraged the establishment of ICAAS to undertake broad comprehensive analyses of public policy issues. These include H. P. Hanson, S. C. O'Connell, R. B. Mautz, E. T. York, G. K. Davis, H. E. Spivey, R. E. Uhrig, and Pat Rabo. We also want to thank R. Q. Marston, J. A. Mattress, R. A. Bryan and F. M. Wahl who recently encouraged us to continue our quest and made available funds which made this project possible.

Next we wish to thank the contributors to this report, the faculty, research staff and graduate students whose names appear on the title

page, almost all of whom not only met very demanding deadlines, but also worked far beyond the call of duty. Particularly our "tiger team," Dennis J. Miller, Michael J. Rowe, Michael A. Kenney and Daniel E. Rio made extra efforts needed to cover important issues overlooked in our first draft. In addition, Dr. J. R. Jones, Jr., of our University of Florida Libraries deserves special thanks for his invaluable assistance in literature searches. Miss Lisa K. Gregory was of assistance in our research on trace elements.

Philip L. Martin and Daniel J. Ross of University Presses of Florida gave valuable guidance in the formulation of the book from a publishing standpoint. In this same vein, we thank our Scientific Advisory Board members; Dr. Woodrow W. McPherson, Graduate Research Professor in IFAS and Dr. Marvin E. Shaw, Professor of Psychology who were especially helpful in providing advice and assistance.

The copy editing of this monograph was done by Rita H. Barlow who came to us in our hour of need and made it possible to meet our publication schedule. The typing of this manuscript was largely accomplished under considerable pressure by Rosie Mays and Olivia S. Berger. Additionally, the efforts of University department secretaries in Physiology, Environmental Engineering Sciences, Nuclear Engineering and the College of Law should be acknowledged for providing final copy. The drafting services by Wesley E. Bolch and Woodrow W. Richardson and the photographic services by Hans W. Schrader also merit our thanks. We also acknowledge the fiscal services of Grethel Greene and the secretarial services of D. D. Ogle.

The focus of this coal study was indirectly suggested by a request for a proposal formulated by the State Energy Office and issued under the Florida Board of Regents Star Grant Program. We would like to thank the state officials who established this program and Dr. J. S. Dailey and others involved in its administration for their valuable contributions. In addition to the support from the Star Grant Program this work was supported by the Gatorade trust fund, the Francis B. Parker Foundation, the U.S. Department of Energy, and the Colleges and Departments of the listed authors.

CHAPTER 1

INTRODUCTION AND SUMMARY

Interdisciplinary Center for Aeronomy and (other) Atmospheric Sciences

I. INTRODUCTION

The exhaustion of the oil and natural gas of the world, and particularly the United States, has been predicted for some time. While the day when the wells run dry may move into the future as new discoveries are made and old wells are rejuvenated with new recovery methods, no knowledgeable person can deny that ultimate exhaustion of stored fossil fuels is inevitable if consumption continues at present rates. The urgency of the problem was underscored in 1979 by three events that have had a major impact in bringing the energy supply situation to the crisis stage. First, the revolution in Iran supplanted a government friendly to the United States and that has recently made extensive purchases in return for oil with one that is antagonistic to this nation. Second, the Three-Mile Island nuclear reactor accident has had a damping effect on the growth in number of nuclear reactor electric power facilities, thus undercutting a main alternative to the use of oil and gas that the nation had been counting on. Public concerns over storage of radioactive wastes and the proliferation of nuclear technology have now been augmented by concern as to the safety of current reactors and the adequacy of training provided reactor operators. Third, OPEC oil price increases have forced the United States into virtual economic warfare with many of the oil producing countries; a war that the nation appears to be losing, if the rising price of gold, the rising interest

rate, and other signs of inflation may be taken as indicators. The urgency of the need to reduce purchases of foreign oil and, thereby, help stem the net outflow of dollars to pay for imported energy is now so acute that almost everybody acknowledges it.

What can the citizens of the United States do? The most obvious thing, albeit a little old-fashioned, is to take stock of our natural resources, particularly our renewable resources, and use American common sense to find a way to live within the nation's means and re-establish national self-respect. Highest priority must be given to conservation and the use of renewable resources since these actions do not involve any drain upon "energy savings." Nevertheless, phasing in a renewable resource mode of life will take time and could be rather painful. Fortunately, the United States has a goodly supply of coal that is estimated to amount to 30% of the world supply, enough to sustain the nation for a hundred years or so before a new energy resource is discovered. Accordingly, coal is a resource whose use must now be promoted. On the other hand, coal poses dangers of polluted air, dirty water, mangled earth, crushed bodies and blackened lungs. Images of these hazards were created a generation or two ago before oil and gas became so abundant and cheap that they ousted coal as the fuel of choice in America. The nation is now compelled to return to coal and find out how to utilize it without resurrecting those bad images. Modern technology is the key.

This book examines the potential role of coal in the United States in the coming decades. It looks at coal utilization broadly to include burning and other direct uses, liquefaction and gasification. To assure comprehension, the perspectives of scientists, engineers, systems analysts, medical scientists, lawyers, economists and other experts have been employed. Particular attention is given the interim role that coal must assume to meet America's energy needs in the next generation or two. This will give a breathing space for science to ascertain whether or not unlimited energy resources such as fusion machines or breeder fission reactors are feasible, and for society to decide whether or not they are acceptable. If affirmative answers to

both questions are not forthcoming after a few decades, society must then use its remaining coal and other fossil fuels to learn to live entirely on solar energy in direct or indirect forms.

This book has been written with the assumption that society does not know what the future holds with respect to these long-range alternatives. This will be discomforting to some readers who have firmer visions about the future than do the scientists and other experts who wrote this book. This underlines the importance of the collective point of view about the use of coal expressed by these writers--coal buys time for this country and the world until the shape of the long-range future becomes clearer. Thus, this book concerns itself with the best way to utilize coal from the viewpoint of our energy needs, our environmental safety and the health of our economy.

II. QUANTITATIVE FACTS ABOUT ENERGY SUPPLIES AND CONSUMPTION RATES

The old saw about history's continually repeating itself has obvious validity so far as the use of coal is concerned. The curves of Figure 1 depict how during this past century or so the U.S. has shifted from a renewable resource, that is, fuel wood, to coal, and then to petroleum and natural gas. Each shift has been spurred by factors such as availability, convenience, and economic advantage. Since coal is still abundantly available it obviously must have some relative disadvantages that must be coped with. Almost everyone has heard about Pittsburgh's reputation as "the smoky city," a nickname that no longer applies, and the descriptions about the coal smoke pollution of London are even more fearsome. Perhaps fear, both legitimate and apocryphal, about the bad side effects of burning coal even delayed the onset of the industrial revolution in England. History recounts that in the year 1306 King Edward I of England feared it so much that he decreed punishment of death to people who burned coal. Ultimately, however, the power of coal was not to be denied even in England, because history has recorded that about four centuries later that nation used coal to fuel the industrial revolution that made it a great world power. Similarly, coal has been a major source of energy used in the United

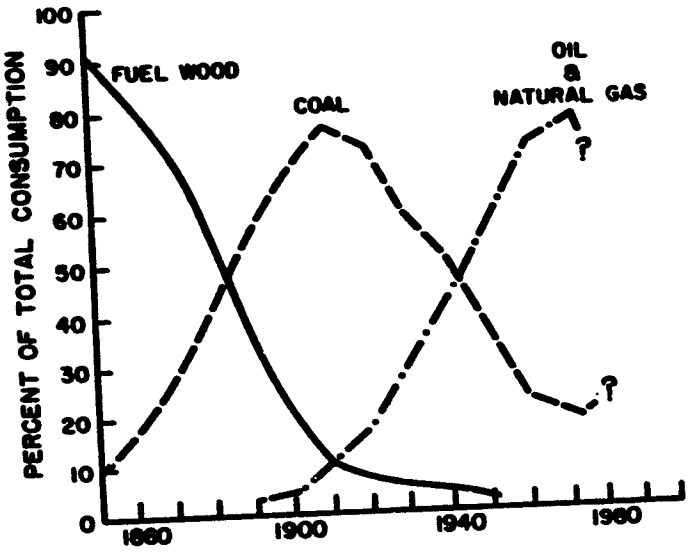

Fig. 1. Percent of Total Energy Consumption

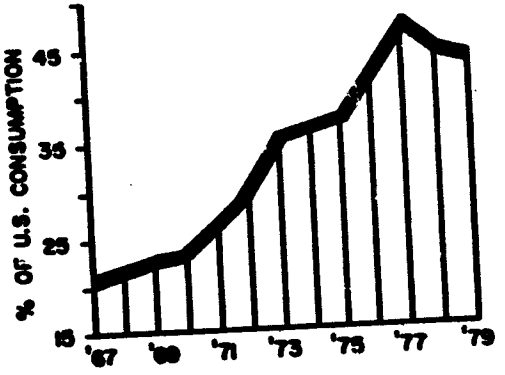

Fig. 2. Imported Oil Use

States during the period illustrated in Figure 1 to build this nation into an industrial power. These and other historical coal landmarks are charted in Table 1.

The world is now on the threshold of shifting back to coal as its major source of energy. Convenience and environmental advantage no longer are the driving forces; this time it is one of necessity. As is well known to everyone, petroleum and natural gas are running out and will by all accounts be depleted as a major source of energy sometime in the first half of the 21st century. Also well known is the fact that escalating American dependence on foreign oil sources has drastically driven up the price of energy in the United States and played havoc with not only the nation's but also the world's economy. The rapidity and the extent of the growth of the nation's oil dependency are depicted in Figure 2. However, the pattern emerging in Figure 1 from 1970 onward suggests that a new age of coal use is at hand during which our dependency on petroleum, prrticularly foreign petroleum, could be driven downward.

Although this book is about coal use, the writers do not want to leave the erroneous impression that energy conservation is unimportant. It takes no more than a slight digression to demonstrate that conservation can offer substantial relief that, when coupled with increased coal use, can help return the United States to a status of energy independence and sustain it there. Per capita energy consumption in the United States is so high by any standard that the very fact suggests that conservation may be of major quantitative importance. For example, as shown in Figure 3 (McPherson, 1965), Americans far exceeded any other of the world's people in both per capita energy consumption and income in 1965. Comparative data for 1974, pictured in Figure 4, show that although the per capita consumption of energy in the United States again exceeded that of any other nation, the equivalent per capita income in many industrialized nations had overtaken or even exceeded that enjoyed here. Taken together, these factors suggest that conservation in America might produce substantial energy savings without curtailing the standard of living.

Table 1: *Some Historical Coal Burning Landmarks*

Time	Country	Person/People	Use or Context
1500 BC	Wales		coal used in funeral pyres
1100 BC	China		heat for homes
950 BC	Israel	King Solomon	mentioned in Bible
300 BC	Greece	Aristotle	noted disagreeable smell
121 AD	England	Hadrian	used in dwellings near wall
852 AD	England	Anglo-Saxon	coal used in rental payment
1306	England	King Edward	decrees use of coal punishable by death
1200	North America	Pueblo	coal used in pottery production
1679	North America	Fra Hennepin	observed black mineral along Illinois river
1694	England	Clayton	first production of coal gas
1750	England		coal fuels industrial revolution and rise of England
1770	United Colonies	Washington	noted coal mine on Ohio river
1771	Pennsylvania		anthracite discovered in eastern Pennsylvania
1840	U.S.A.		coal industry grows 1,000,000 tons mined
1850	U.S.A.	Gesner	coal liquefaction
1890	U.S.A.		electric steam generators expand use of coal
1940	Germany		large-scale liquefaction of coal by Bergins process
1950	U.S.A.		Middle East, Venezuela oil flood world markets
1973	U.S.A.		oil crisis begins
1974	U.S.A.	Nixon*	Project Independence
1977	U.S.A.	Carter*	National Energy Plan
1979	U.S.A.	Carter*	oil crises worsen - Camp David proposals

*proposes major switch to coal utilization

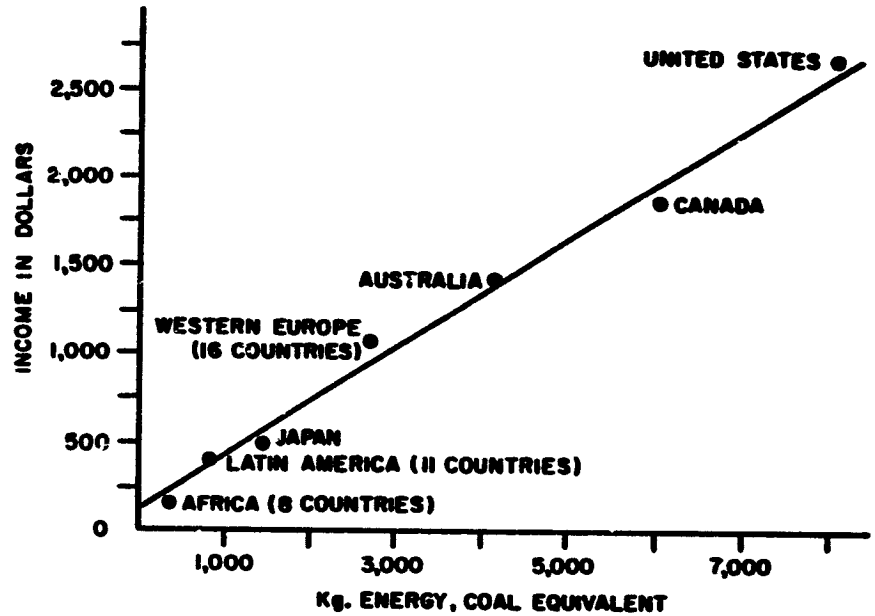

Fig. 3. Consumption of Energy Per Capita, Inanimate Sources, and Gross Domestic Product Per Capita, Selected Areas, 1962 from McPherson (1965)

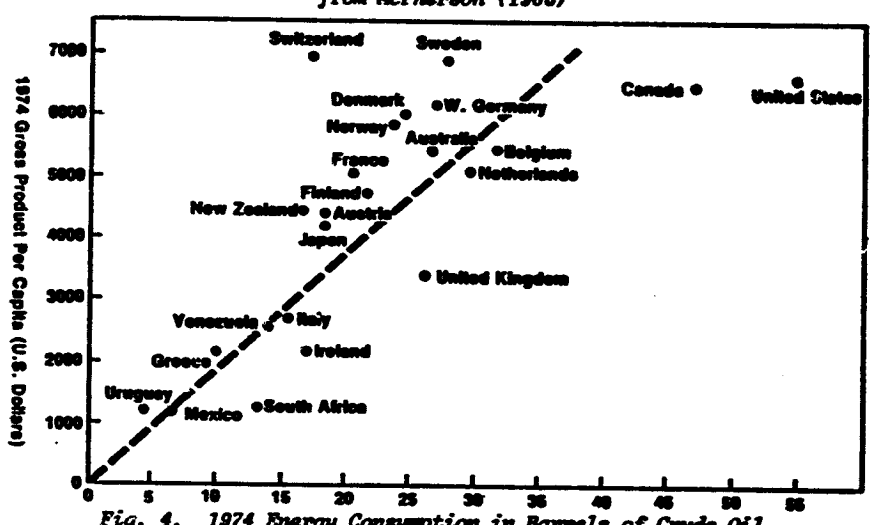

Fig. 4. 1974 Energy Consumption in Barrels of Crude Oil Equivalents Per Capita
Source of Data: U.N. Statistical Yearbook, 1975

This may be illustrated by comparing the fuel efficiency of American cars to that of imported cars. In 1975 the average domestic car used about five gallons of gas to travel the same distance as the average imported car would go on three gallons. Hence, much petroleum could be saved by merely converting to fuel-saving cars. This will occur if present federal programs successfully bring the average rate of fuel use of the domestic fleet down to that of imported cars. The waste in American transportation apparently has its industrial counterpart if comparisons between American and West German industrial fuel consumption data are a reliable guide. For example, the West Germans use about 20% less energy per unit of primary metals produced than does American industry (SRI, 1975). Other major energy intensive industries of West Germany have even greater relative efficiencies. Clearly, a role for better industrial technology in energy conservation is evident. What happens in industry and transportation seems to represent quite faithfully the relative energy voracity of the American way of life. The huge demand for energy imposed by the average American compared to that for people from other countries has been noted by Smil (1979) who compares the per capita amounts of energy consumed measured in kilocalories per day (kcal per day) of the developing world with that of the USA. This work shows that American per capita energy consumption is exorbitantly large, about 215,000 kcal per day whereas many of the world's developing countries get along on about 10,000 kcal per day per capita with little fossil fuel augmentation to solar energy input. In China, for example, the energy use per capita is approximately 13,500 kcal per day. Thus, Americans could help alleviate the energy crisis by moving the per capita energy use downward, possibly to 100,000 kcal per day, the approximate energy use of other western industrialized nations. If, for example, we could just lower the rate of growth of energy use from 3.5% to 2.3% per annum we would save 20 millions barrels of oil per day by the year 2000.

The objective of this book, however, is not to dwell upon the energy conservation measures that the writers unanimously subscribe to, but rather is to examine phenomena associated with a transition to coal

use, particularly in the United States. The use of coal in this country may be what will make it possible for Americans to maintain a high standard of living, leaving the foreign oil to alleviate the plight of poorer people in the world.

Fortunately, the world and especially the United States have large supplies of coal to consume. In gross dimensions, the world's coal reserves are illustrated by the data in Table 2, extracted from Peters and Schilling's (1978) appraisal of world coal resources. The data are presented in metric tons with the energy equivalence of hard coal (HC) rather than in gross weight. Hard coal here encompasses anthracite and bituminous and brown coal (BC) includes sub-bituminous and lignite. Gross supply data also have been adjusted to reflect only supplies that are economically and technically recoverable. Hence, other estimates of coal resources could vary substantially from those shown. Be that as it may, this table indicates that the United States has more recoverable coal resources than any other nation. The last two rows give the U.S. production and export rates in 1975 in million tons.

Table 2. *Economically and Technically Recoverable Coal Resources of Leading Coal Countries in Gigatons (10^9 metric tons)*

		HC	BC	Total	Prod	Exp
	World	492	144	636	2593	199
1	USA	113	64	177	581	60
2	USSR	83	27	110	614	26
3	China	99	—	—	349	3
4	Great Britain	45	—	45	129	2
5	West Germany	24	10	34	126	23
6	India	33	—	33	73	—
7	Australia	18	9	27	69	29
8	South Africa	27	0	27	69	3
9	Poland	20	1	21	181	39
10	Canada	9	1	10	23	12

Peters and Schilling also have predicted how rapidly coal will be put into production in the coming years. As shown in Figure 5, the United States is expected to lead the world in this process. Whether or not it does will depend upon whether or not and how the issues examined in this book are resolved. In any event, it seems certain that a substantial shift-over to coal is coming. Already this is manifested by the fact that virtually all new electric power plants purchased in the U.S. are being designed for coal rather than oil or gas.

The fact that shifting to coal opens up the world's last known major resource of non-renewable energy to consumption with an appetite that will inexorably lead to ultimate exhaustion poses a moral and resource issue for humankind that has yet to be squarely faced. What will be the plight of those unborn generations that come along when the resource is depleted? What should we do about the underdeveloped nations who are demanding the right to develop? This necessarily implies moving away from their current equilibrium with renewable energy (Smil, 1979)

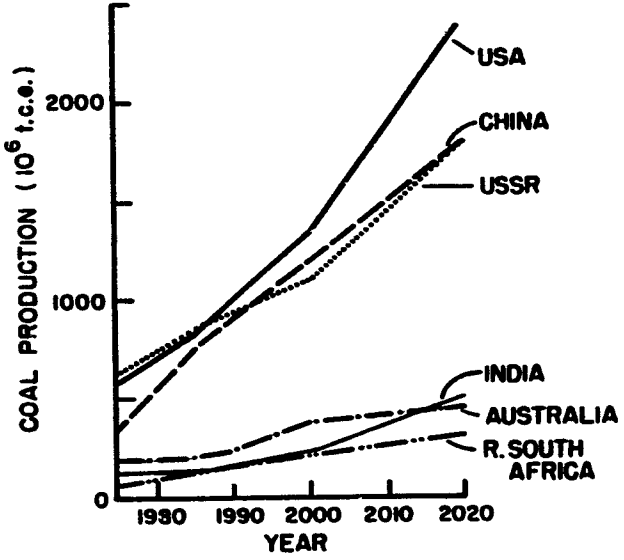

Fig. 5. Survey of the Future Trend in Production

toward a dependence upon stored energy. Certainly if China's billion people were to move up to America's per capita energy consumption rate the world's stored energy resources would be wiped out in short order. This world-wide social dilemma has yet to surface in full force. Unless a new, inexhaustible energy resource is discovered, consideration of equity suggests that some sort of balance must be struck in which those with more, use less and those with less, use more. However, the allocations to each nation of energy resources, property, population limits and emission limits to control adverse climate changes raises complex international issues considerably beyond the scope of this work.

Another issue whose complexity makes it beyond the scope of the present study is the question of monopolistic practices in the energy field. Such practices by the OPEC oil cartel obviously have contributed to our energy crisis. Voices are now being raised that major American companies have established an energy monopoly paralleling the OPEC cartel. However, it is an open question as to whether this cry identifies a real problem or simply diverts the nation's attention from fundamental problems: the inevitable exhaustion of the U.S. oil and gas reserves and the need to use coal to save our economy.

The existing coal supplies of the USA are large enough, even if used up at a voracious rate, to provide time for the development of even more plenteous energy resources that may exist, such as nuclear fusion or breeder fission, or to learn how to live on renewable energy resources better than the developing countries. Referring again to Figure 5, the reader can see that the actual 1979 coal production is 700 million tons per year in the United States. At that rate, the estimated American reserve of 177 Gigatons of economically and technically recoverable coal would last 250 years, and even if the consumption rate were to triple, the supply would last nearly 100 years. This underscores again the central purpose of this book; namely, to examine the issues and problems that must be resolved to make coal a sage and environmentally acceptable energy workhorse for the USA during the coming 50 year or so.

III. ENERGY UNITS AND THE DIMENSIONS OF THE PROBLEM

The units used to describe energy quantities vary greatly, even among professional people. Human energy commonly is measured in consumption of kilocalories (kcal) per capita per day. For example, under moderate exertion the average American male uses 3,220 kcal per day and the average American female 2,320 kcal per day. By contrast, heat engineers describe energy in terms of British Thermal Units (BTU), physicists use the kilojoules (kilowatt-sec), electrical engineers use kilowatt-hours, petroleum engineers use barrels of oil, gas engineers use millions of cubic feet, and mining engineers use tons of coal, either in short-tons (2,000 pounds) or metric tons (1,000 kilograms). All describe the same basic quantity, but in terms that have no readily apparent conversion equivalences, such as the trivial conversion of, say, feet to inches. This communication hitch has been made even worse by the growth in use of a number of new words to describe energy resources in global terms. Thus, the quad = 10^{15} BTU, the Gigaton = 10^{9} tons of coal equivalent (GTC), have come into use and now compete with older terms such as millions of barrels of oil (MBO) and trillions of cubic feet of natural gas (TCF) to describe energy resources.

To supply a common base for communicating about energy quantities, the information in Tables 3 through 5 is provided. Table 3 merely defines the units; Table 4 displays some of them in a fashion that makes conversion among micro-units relatively easy; and Table 5 displays others in a fashion that does the same for macro-units. The BTU is used to tie Tables 4 and 5 together.

As a quantitative overview of the dimensions of the United States problem in terms of these units, Table 6 gives a detailed picture of the U.S. energy supply and demand from 1960 to 1978. Readers may find it helpful to mark these tables for future reference. Right now this nation's coal production capability far exceeds the current demand and production could go to as high as 2 Gigatons by the year 2000. Thus, coal could replace oil and natural gas as our main energy source. Whether or not it should or would is the main concern of this book.

Table 3: *Definition of Energy Units*

Common Abbreviation	Meaning
kcal	Kilocalorie (also denoted Cal)
kwatt-hr	Kilowatt-hour
kjoule	Kilojoule (a kilowatt-sec)
BTU	British Thermal Unit
BOE	Barrel of Oil Equivalent
CFG	Cubic Feet of Natural Gas equivalent
TCE	Metric Ton of Coal equivalent (TCE = 1.032 short ton equivalent)
GTC	Gigaton of Coal equivalent (metric)
quad	10^{15} BTU C = 10^{16} BTU Q = 10^{18} BTU
MBO	million barrels of oil
TCF	trillion cubic feet gas

Table 4: *Energy Unit Conversion Factors (Micro Units)*

One of these energy units	=	Equivalent Number of these units: Kcal	Kwatt-hr	K-joule	BTU
Kcal	=	1	11.627×10^{-4}	4.185	3.968
Kwatt-hr		860	1	3600	3413
K-joule		0.238	27.76×10^{-5}	1	0.948
BTU		0.252	29.29×10^{-5}	1.055	1

Table 5: *Energy Unit Conversion Factors (Macro Units and BTU's)*

Energy Units:		Equivalent number of these units: BTU	BOE	CFG	TCE	quad
BTU	=	1	1.72×10^{-7}	9.79×10^{-4}	3.59×10^{-8}	10^{-15}
BOE	=	5.8×10^{6}	1	5.68×10^{3}	.208	5.8×10^{-9}
CFG	=	1.02×10^{3}	1.76×10^{-4}	1	3.67×10^{-5}	1.02×10^{-12}
TCE	=	27.8×10^{6}	4.79	27.2×10^{3}	1	27.8×10^{-9}
quad	=	10^{15}	1.72×10^{8}	9.79×10^{11}	3.59×10^{11}	1

1 quad = 35.9 MTC = 173 MBO = 0.970 TCF = 41.5 M Short Tons Coal

Table 6. *U.S. Energy Supply and Demand**

	1960	1970	1972	1974	1976	1978
Energy Supply (quads)[a]	46.01	70.91	74.28	75.64	76.93	79.89
Oil[b]	20.39	30.38	32.96	34.17	35.26	38.04
Natural gas	12.82	22.52	23.26	22.20	20.47	20.24
Coal	11.12	15.05	14.49	14.47	15.85	15.11
Nuclear	0.01	0.24	0.58	1.27	2.11	2.98
Hydro, other	1.67	2.72	3.01	3.53	3.24	3.47
Energy consumption (quads)[c]	44.08	66.82	71.63	72.35	74.16	78.01
Transportation	11.23	16.76	18.34	18.40	19.39	20.59
Residential, commercial	14.37	23.77	25.84	25.57	27.18	29.30
Industrial, other	18.48	26.29	27.45	28.39	27.59	28.13
Oil consumption (MBD)	9.80	14.70	16.37	16.65	17.46	18.73
Oil imports	1.62	3.16	4.52	5.89	7.09	7.86
U.S. reserves[d]	31.6	39.0	36.3	34.2	30.9	27.8
Gasoline consumption (MBD)	4.13	5.78	6.38	6.54	6.98	7.41
Natural gas consumption (TCF/yr)	11.97	21.14	22.70	21.22	19.95	19.41
Residential	3.10	4.84	5.13	4.79	5.05	4.97
Industrial	5.77	9.25	9.63	9.77	8.60	8.14
Electric Utilities	1.73	3.93	3.98	3.44	3.08	3.22
U.S. reserves[d]	262.3	290.7	266.1	237.1	216.0	200.3
Coal production (MST)	415.5	602.9	595.4	603.4	678.7	653.8
Underground mines	284.9	338.8	304.1	277.3	294.9	243.5
Surface mines	130.6	264.1	291.3	326.1	383.8	410.3
Coal Use Electric Utilities	173.8	318.3	350.2	390.3	447.0	480.1
Coke	81.0	96.0	87.3	89.7	84.3	71.1
Exports	36.5	70.9	56.0	59.9	55.4	39.8
Electricity production (quads)	8.40	16.51	18.74	19.94	21.51	23.76
From coal (per cent)	53.5	47.3	44.1	44.5	46.4	44.3
From oil	6.1	12.2	15.6	16.0	15.7	16.5
From natural gas	21.0	25.0	21.5	17.1	14.5	13.8
From hydro	19.4	16.7	15.6	16.1	13.9	12.7
From nuclear	0.0	1.5	3.1	6.1	9.4	12.5
Population (millions)	180.0	203.8	208.2	211.4	214.7	218.1
Automobiles (millions)	61.7	89.2	97.1	104.9	110.4	117.1
Gross national product (billions of 72 dollars)	736.8	1,075.3	1,171.1	1,217.8	1,271.0	1,385.7
Energy consumption/GNP	59.8	62.1	61.2	59.4	58.3	56.3

(a) includes U.S. imports, U.S. exports and changes in inventories
(b) includes natural gas liquids
(c) includes distribution loss from electrical generation
(d) proved reserves in billion barrels of oil
(e) proved reserves in trillion cubic feet
(f) in 1000 of BTU/per 72 dollars

* Adapted from National Journal, July 21, 1979, page 1200.

The following section of this chapter consists of summaries of Chapters 2 to 18 of this book. Chapters 2 to 8 largely consist of descriptions of our resources, present and future coal technologies and current coal issues. Chapters 9 to 14 describe known or possible environmental problems. Finally, Chapters 15 to 18 discuss and describe possible assessment techniques which might be used in public policy decisions related to coal burning issues.

In addition to the references cited in this chapter we list below a brief bibliography representing very recent works on energy in general and on coal utilization in particular.

References

Executive Office of the President, 1977, The National Energy Plan, Energy Policy and Planning, U. S. Government Printing Office, Washington, D. C.

McPherson, W. W., 1965, Economic Development of Agriculture, "Input Markets and Economic Development", Chapter 6, pp. 99-117; Iowa State University Press, Ames, Iowa.

Peters, W., and Schilling, H.-D, 1978, "An Appraisal of World Coal Resources and Their Future Availability", World Energy Resources, pp. 1985-2020.

Smil, Vaclav, 1979, Energy Flows in the Developing World; American Scientist, 67, p. 522.

Recent Bibliography

Berkowitz, N., 1979, An Introduction to Coal Technology, Academic Press, New York.

Crane, A. T. et al., 1979, The Direct Use of Coal, Prospects and Problems of Production and Combustion, Congress of The United States, Office of Technology Assessment, Washington, D. C.

Davis, R. M. et al., 1979, National Coal Utilization Assessment, A Preliminary Assessment of Coal Utilization in the South, Oak Ridge National Laboratories Report No. ORNL 1 TM-6122.

Department of Energy, U. S, 1979, Fuel Use Act, Final Environment Impact Statement, Washington, D. C.

Hottel, H. C. and Howard, J. B., 1971, New Energy Technology, Some Facts and Assessments, MIT Press, Cambridge, Mass.

Lamberg, H. H. et al., 1979, Energy: The Next Twenty Years, A Report Sponsored by The Ford Foundation, Ballinger Publishing Company, Cambridge, Mass., pp. 273-408.

Leonard, J. W., 1979, Coal, The World Book Year Book, World Book-Childcraft International, Inc., Chicago, Ill., pp. 566-582.

Loftness, R. L., 1978, Energy Handbook, Van Nostrand Reinhold C. New York.

McNeal, W. H. and Nielson, C. F. et al., 1977, Keystone Coal Industry Manual, McGraw-Hill Mining Publications, New York

Stobaugh, R. and Yergin, et al., 1979, Energy Future, Report of the Energy Project at The Harvard Business School, Random House Publishing, New York.

Surles, T. and Gasper, J. and Hoover, J. J. et al., 1979, An Assessment of National Consequences of Increased Coal Utilization, U. S. Department of Energy, Washington, D. C.

Chapter 2, Coal Availability and Coal Mining, by Ohanian and Fardshisheh, summarizes the U.S. coal resource base by geographic location, access (i.e., deep or shallow mines), and classification. A general assessment of demand projections is based on the assumption that electrical power generation be the primary user of coal over the next two to three decades.

Coal is the most abundant non-renewable energy resource in the United States which has approximately 28% of the world's total coal supply. U.S. coal, which represents 70% of the non-renewable energy resource in the country is located in three distinct regions: Eastern, Central and Western. Bituminous coal comprises 43% of the resource base, sub-bituminous 27%, lignite 28% and anthracite 1%. The sulfur content of Western coal is lowest (generally 1% or less) with Central coal highest at 2-4% and Eastern coal at most 2% or less. However, the heat value of coal per unit weight is, in general, lower for the Western coal reserves.

A summary discussion of modern mining techniques and the factors that give rise to the use of a particular mining methodology are also presented. The role played by technological development through the evolution of machinery and equipment used in the mining system is discussed. The environmental issues arising from coal mining are examined. Since coal crushing, washing, drying, etc. is often required, it is considered an integral part of the mining, and coal preparation is also covered briefly. Since safety plays a significant role, the problems related to safety are discussed. A related topic which is of paramount importance, namely the occupational hazards associated with coal mining, is reviewed. It is seen that since the enactment of the 1969 Federal Coal Mine Health and Safety Act, mine fatalities have been reduced appreciably. However, no greatly measurable reduction in the rate of disabling injuries has occurred. Figures are tabulated which show miners are likely to suffer from occupational health and safety hazards at a rate higher than other occupations.

Chapter 3, An Energetics Analysis of Coal Quality, by Alexander, Swaney, Rognstad and Hutchinson uses energy circuit language, a method of systems analysis, to determine the quality of energy embodied in coal. Three distinctly different approaches are employed to calculate coal's energy quality.

The first method employed to determine the energy embodied in coal uses a theoretical model of the coal formation process. As a starting point a detailed description of the formation of the various ranks of coal is given. From photosynthesis, atmospheric CO_2 is transformed to plant biomass and then to peat via microbial decomposition in water. Then through catagenesis (autoclaving geological processes), peat is transformed to lignites to bituminous and anthricite forms. The geological and ecological energies involved in these tranformations are evaluated.

The second method used to determine coal quality compares the energetics of coal burned as an electrical generating fuel to the use of wood and oil in electrical power production. These two fuels were chosen as a basis for comparison because the energy value of wood is easily traced to the energy flows of natural systems and the energy in oil is the largest component of the contemporary fossil fuel energy base.

The third approach to estimating the energy quality of coal is based on the energetics of converting coal to higher quality synthetic gas. It is postulated that this will give an upper range to the energy quality of coal, while conversion to electricity will approximate the lower limit.

It appears that 1.36 - 2.2 thermal calories of coal are required to do the same amount of work that one calorie of oil or gas can accomplish. In effect, this means that the magnitude of the world's coal reserves when expressed in thermal units, should be reduced by 26 - 55%.

Chapter 4, Coal Transportation, by B. Capehart, O'Connor and Denty discusses the important links in the overall processes of supplying coal to ultimate users. Coal is shipped by a variety of modes and may even require multiple modes, were 65% by rail, 11% by water, 12% by truck and 1% by other modes (slurry pipelines, conveyors, etc.) Eleven percent was used at mine mouth plants. Future expansion of the coal transportation network is clouded by present federal policy which appears to emphasize short-term expansion of natural gas use, rather than coal. If the coal transportation system is to be expanded, the rail system which can most easily be expanded must carry the major burden of growth since it is the most easily expanded transport system. Expansion of the coal transportation network will result in major environmental and social problems attendant on both construction and operation. Air, water and noise pollution accompany the different modes in varying degree. Social impacts such as community disruption and safety also occur.

Operation and future construction of transportation modes are greatly affected by federal regulations and regulatory boards. The extent of regulations concerning the different modes varies from almost no control to, in some cases, a complete roadblock to expansion. Expansion of coal transportation will require the examination of major public policy decisions. Environmental, social and economic problems are all interrelated, and must be considered in a systems approach. Complex cost/benefit studies will be necessary to help determine these public policies. Finally, economic comparisons of the various modes of transportation are needed in order to make optimum economic decisions and expansion plans. This is also a complex area since economic decisions are not independent of environmental, social and regulatory requirements.

The future of the coal transportation system is still very uncertain. Until questions of future demand are answered more completely, few major investments in expansion are likely to be made.

Chapter 5, Coal Burning Technology, by Schneider and Rowe is devoted to combustion aspects of the direct use of coal. The discussion centers primarily on concentrated use such as by electric utilities, or large industries and dilute use, as in residential coal burning which probably will be an environmental problem in populated regions. Concentrated techniques provide for economy of scale for the removal of harmful pollutants. The important parameters in coal combustion are the heat of combustion, the burning temperature, the oxidant control, burning times and the coal quality. These parameters control the energy output as well as waste removal state and gaseous by-product production.

Historically, the first type of coal burner was the "fixed bed" burner where fixed bed refers to the location of the coal burning zone. Here heat rises to an overhead boiler to produce steam. In these installations the stoker for feeding and coal and ash removal involves the majority technology.

Suspension burners in which coal dust is injected into a fire box surrounded by boiler tubes represented the next improvement in coal burning techniques. Improvements of injection technology led to the present day "cyclone" furnace. Suspension burners have a very high temperature which offers good heat transfer and high efficiency. Unfortunately, they produce large amounts of gaseous NO_x.

"Fluidized bed" burners derive their name from the liquid-like properties of the combusting material. With improved heat transfer techniques, fluidized bed burners can be operated at lower temperatures thus producing much less NO_x, yet producing the same amount of steam as a high temperature suspension burner. Furthermore, chemical techniques in the fluidized bed can be used to remove SO_x. Other techniques for the direct use of coal which are still in the development stage include magnetohydrodynamic (MHD) reactors and gas turbine-steam turbine hybrid systems. In the latter the gas turbine could be supplied by an MHD nozzle or water-gas combustor. The gas turbine exhaust would then feed a conventional boiler to produce steam. The established techniques and experimental techniques are all described and assessed in the chapter on coal burning technology.

Chapter 6, Synthetic Fuels from Coal, by Miller and Lee, is devoted to coal conversion, the processes of making clean burning liquid and gaseous fuels from coal. The basic concept of coal conversion chemistry is to enrich raw coal with hydrogen in some form to produce hydrocarbon products with relatively large hydrogen content. This can be accomplished by the reaction of coal with hydrogen or steam, or by removing excess carbon from coal to give a hydrogen-rich product and a carbonaceous by-product. The liquid fuels produced in the liquefaction process range from light gasoline to heavy tars. Liquefaction and gasification reactors involve many overlapping processes and many reactors produce both gases and liquid products.

Several commercially operating gasification processes are now in use and many more are in the pilot plant stage. These gasification processes can be categorized in terms of reactor type and products formed. The raw synthesis gas produced in most gasifiers can be used either as a fuel or as a feed stock to make synthetic natural gas, methanol, hydrogen, ammonia or liquid hydrocarbon fuels, via the Fischer Tropsch synthesis.

Coal conversion to synthetic fuel has the great potential to accommodate cleaning up processes and could provide an important part of the clean gaseous and liquid energies of fuels needed for the next generation or two. The technology is available for producing both gaseous and liquid fuels from coal and only economic considerations, the capital intensive nature of coal conversion plants and the uncertainty as to the OPEC cartel controlled price of foreign oil has inhibited our large-scale development of coal conversion in America.

The possibilities of converting oil shales, tar sands and heavy petroleum residuals into liquid or gaseous synthetic fuels also constitutes an important issue. The relative economics of these synfuels vs. coal-derived synfuels will determine the synthetic fuels which have the greatest short-range and long-range promise in the United States. The environmental impact of the expanded coal mining and disposal of large amounts of sulfur and ash produced in coal conversion is another important issue related to coal conversion.

Chapter 7, Technological Innovations, by Hanson et al. summarizes some technological advances which might ameliorate, postpone, or even eliminate the energy shortage.

Integrated Utility Systems (IUS) as a concept originally involved the tactical use, as dictated by economic circumstance, of gas, oil, coal and solid waste. However, because of the cost and unavailability of petro-fuels, the IUS concept has evolved into one in which coal is augmented by processed solid waste. Nevertheless, such units have certain advantages, including financial, which can make them the unit of choice.

Electrically Propelled Automobiles, an old technology, permits the energy burden of travel to be shifted from gasoline to coal. Batteries, which have been greatly improved, are charged by coal-produced electricity thus freeing the car owner from the dependence on petro-chemicals. Further, by charging at night, the load on the power plant becomes better distributed.

Air Pollution Control Technology could make extensive burning of coal acceptable to society by proper control of effluents and residues. There is continuing research in all phases of the technology of pollution control. Particulates and SO_2 have been given greatest attention, but NO_x control is also under development.

Coal Cleaning makes it possible to eliminate noxious or undesirable by-products before the coal is actually burned. Techniques have been developed for removing incombustible ash, pyritic sulfur, and water from unprocessed coal.

Off-Shore Power Plants originally proposed for nuclear power plants might be applied to coal-fired units to isolate and buffer the power facility. Since almost half of today's power demand exists within a 200 mile strip along our various coasts, the concept might find extensive applications.

Coal Plant Siting Techniques in general provide the opportunities of coal plants to maximize operational efficiency, minimize electric transmission losses and environmental impacts.

Chapter 8, Water Resources, by Melville and Bolch, suggests that two of the primary constraints on the utilization of coal energy will be water availability and the potential for pollution of water that would otherwise be available for other uses. An analysis of the available freshwater reveals a breakdown of 95% groundwater, 3.5% lakes, swamps, reservoirs, and river channels, and 1.5% solid moisture. The groundwater stresses are emphasized and are shown to be the most threatening.

Surface water pollution is easily detectable. The most menacing characteristic of groundwater pollution is that damage is probably irreversible or at least corrective time scales could be measured in terms of years or even generations.

Suggested actions for reduction of water resource constraints are listed.

One of the key issues in the increased use of coal will be the allocation of water resources to competitive users. The competing water demands are enumerated and discussed. The differences between point-source and non-point source pollution are discussed as they apply to coal burning facilities.

The possibility of utilizing to good advantage the water content of lignite, which is usually a problem, to facilitate coal conversion is briefly discussed.

C-2

Chapter 9, Atmospheric Pollution, by Urone and Kenney, considers the increased emissions and possible degradation of ambient air quality arising from the increased use of coal. The combustion of coal leads to major emissions of sulfur and nitrogen oxides, particulate matter, and volatile trace hazardous and toxic substances. Ambient air quality standards prescribe health and welfare endangering levels when surpassed. The amount of emissions with the attendant allowable calculated environmental impact for expanded coal use will depend upon the base line quality or expected quality of the air basin involved.

To estimate the air quality impact of increased coal use is not a simple matter of taking ratios of smoke stack emissions or air measurements to the amount of increased use. Among the factors that must be considered are the type and properties of the coal to be used. Heating value, sulfur, nitrogen, ash, and trace element content must be considered. The local micrometeorology and plume dispersion patterns are important in determining how much of the pollutants will be found at ground level under normal as well as worst-case conditions. Finally, the location and the degree of emissions control required will be determined by both the quality of the area's ambient air and by the potential impact on any environmentally protected areas in the vicinity. Proper proportioning of all the above factors requires an indepth knowledge of each of the mechanisms involved as well as detailed knowledge of the substances emitted when coal is burned. In addition, the enriching emission process for trace toxic substances forms a subtle, long-term and long-range threat to man and the environment.

Many key issues must be addressed including (1) quantification of increases in emissions, (2) possible insult to air quality standards, (3) long-term impacts of trace toxic substances, (4) reactions of sulfur dioxide, (5) synergistic effects to acid rain, visibility degradation, climate change and other environmental questions.

Chapter 10, Air Pollutant Dispersion Modeling, by Fahien, summarizes the status of three major approaches which may be used for the quantitative prediction of the impact of increased coal burning on air quality. Such calculations require not only a knowledge of the emissions to be expected from coals of a certain chemical composition but also a quantitative method to relate emission rates to air quality. To do the latter requires the use of a dispersion model, an important link between emission rates and dose-response or other health effect studies.

Dispersion models are classified as follows: (a) Gaussian models, which assume that the concentration of a pollutant from a point source follows the normal error curve; (b) transport models, which are based on the law of conservation of mass; and (c) stochastic models, which are based on the laws of probability.

The Gaussian model has very limited validity and its use requires knowledge of parameters ("dispersion coefficients") which cannot be predicted accurately. As a result, errors of several hundred percent are not uncommon. Nevertheless, it is widely used and forms the basis for the EPA-recommended "off-the-shelf" models.

The transport models are more rigorous--especially when chemical reactions are involved--but usually require knowledge of eddy diffusivities or "K" values which also cannot be accurately predicted. Since they are less limited than the Gaussian models, they are mathematically more complex and usually require more computer time. Stochastic models are the most rigorous and most adaptable, but these are in a developmental stage and require meteorological data that are not always available. The actual selection of a model for use in a "preconstruction review" is for practical purposes limited by law to EPA-recommended models. Examples of previous modeling studies are discussed.

Most compelling is the great need to develop reliable yet practical methods for the quantitative prediction of the dispersion of the air pollutants emitted in coal burning.

Chapter 11, Atmospheric Modifications, by Taylor, Chameides and Green, is concerned with the atmospheric impact of the release of pollutants from combustion of fossil fuels, particularly coal. Such releases can cause global perturbations by changing the average composition of the earth's lower atmosphere. Whether such perturbations are significant depends upon the magnitudes of the combustion sources as compared to other natural sources and the rapidity with which these pollutants are scavenged before they are dispersed throughout the atmosphere.

In this chapter we focus on the potential impacts of the continued or accelerated release of CO_2, NO_x, SO_2 and aerosols upon global climate and other important environmental parameters. Our present understanding of the atmospheric budgets of these pollutants indicates that anthropogenic emissions of CO_2 have already led to an increase in global CO_2 levels, while NO_x and SO_2 levels may be affected in the coming decades. While the climatic perturbation implied by a global CO_2 increase appears to be the most significant global pollution problem we presently face, the consequences of increases in NO_x and SO_2 upon the environment (i.e., acid rain) are also of concern. In the case of atmospheric particulates, the oxidation of S compounds to produce $SO_4^=$ aerosols in both the troposphere and stratosphere may ultimately lead to a significant degradation in visibility. Some simple techniques for monitoring visibility are described. One important method of monitoring aerosols and the deterioration of visibility on a global scale is the application of remote sensing with space technology. This technology is also applicable to the global monitoring of CO_2, SO_2, NO_x and the earth's radiation budget. The concluding section of the chapter illustrates this rapidly advancing technology.

Chapter 12, Solid Waste and Trace Element Impacts, by Bolch, considers the potential environmental impacts of the solid wastes and trace element releases due to coal utilization for electric power. Coal may contain a wide spectrum of trace elements including As, Cd, Ce, Cr, Cu, Hg, Mn, Pb, Se, Sr, V, Zn, and naturally occurring radioactivity, especially the uranium and thorium series. A recent monograph by Torrey reviews the potential impacts from trace elements, and a companion monograph focuses on the recovery of these waste products as beneficial resources. Both monographs were published before the impact of the Resource Conservation and Recovery Act was reflected in the proposed hazardous waste regulations. Some of the topics not emphasized by Torrey are more adequately covered in the recent impact statement on the Fuel Use Act (DOE, 79).

During the development of the environmental regulations of the last half of this decade, there has been an increasing emphasis on the less obvious pollutants from fossil fuel power plants. The return to coal, a defined national policy, results in the consideration of the ultimate fate of trace elements in coal as a significant coal burning issue.

This chapter summarizes the trace elements in coal and fly ash, including the radioactive components of uranium and thorium. The fractionation of coal ash within a typical power plant is presented and the association of element with various fractions is discussed. A brief review of potential health effects is presented. It is suggested that environmental transport and dose-to-risk models be developed and presented in order to place coal burning on an environmental cost scale with other energy sources. A brief discussion of the impact of mining, coal cleaning, storage and coal conversion are discussed. Lastly, the importance of new laws, namely, The Toxic Substance Control Act (TOSCA) and its companion, The Resource Recovery and Conservation Act, is discussed.

Chapter 13, Agriculture, by Woltz and Street, describes the environmental impact of increased coal usage on agriculture and natural ecosystems. The impact of coal residues on agricultural and forestry environments depends on the partitioning of these materials between bulk solid waste (90%) and released emission products (10%). Main environmental concerns are sulfur oxides released as atmospheric SO_2 and acid rain from sulfuric acid aerosols. These subjects have been well documented qualitatively but not so well quantitatively. The magnitude of the effects is assayed indirectly through appraisal of visible acute damage to plants. Settlement of specific damage claims for SO_2 effects requires a consideration of the pertinent features of etiology, environment and degree of susceptibility of the plant populations at risk.

Ecological effects of SO_2 are recognized in terms of genetic adaptation which takes place in individual plant species in response to airborne SO_2. Also, the makeup of populations by species in exposed areas represents a biological adaptation that occurs. Changes in genetic and species makeup of plant populations may or may not be desirable. Acid rain and acid mist from airborne sulfates and nitrates have been shown to have adverse effects on native and cultivated vegetation, soils, and aquatic ecosystems. These effects have increased in recent years. Trace elements from coal burning may impact adversely on agriculture and ecosystems but the effects will most probably be of a much lower order of magnitude than those of sulfur oxides.

There is a potential benefit from disposing of coal solid waste residue on agricultural and forestry soils insofar as the chemical and physical alterations of the soil are not detrimental to the production of quality food and fiber. Due to the high variability of the chemical and physical nature of coal ash and soil a compatibility must be ascertained before indiscriminatory use of coal ash on soils can be permitted. Preliminary studies indicate that certain plant essential elements contained in coal ash are readily available to plants grown on ash-amended soils. However, there are possible unfavorable changes in the soil upon addition of coal ash which must be investiaged.

Chapter 14, Air Pollution Health Effects, by Schlenker and Jaeger, deals with the possible health effects of air pollution resulting from large-scale coal utilization. The pollutants (primary ones such as SO_2, particulates, NO_2, CO, trace elements, and secondary ones such as O_3 and aerosols) are evaluated according to their physical, chemical and biological properties. To understand the health impacts of these pollutants pertinent epidemiological studies and controlled laboratory studies are presented in which animals and humans were exposed to various pollutants. Each technique has inherent advantages and disadvantages. Animal studies show primarily species-specific responses to exposures, but such studies are invaluable mirrors of biomedical and morphological changes which may occur as a result of exposures. For ethical and legal reasons, studies using human subjects are restricted in length of exposure and concentration of pollutant. However, the most important information obtained from such studies is the acute response by normal and sensitive (such as asthmatic) human beings to well-defined levels of single pollutants or combinations of pollutants. Epidemiological studies allow one to evaluate the effects of air pollution on large numbers of people over a lifetime. Such studies, unfortunately, are the most difficult to conduct.

Epidemiological studies can be subdivided according to the health effect considered. These subdivisions are mortality rates, morbidity rates, and cancer rates. Confounding factors such as location and number of monitoring sites, smoking habits of the population (another form of self-induced pollution, elaborated upon in this chapter), geographical seasonal variations, socio-economic factors, occupational exposures, and migration of individuals make interpretation of epidemiological studies difficult. Taking all these factors into consideration, in many cases the measurable relationship of air pollution to health is decreased. There is evidence, however, that sulfur-dioxide, sulfates and particulates, major products of coal combustion, have some detrimental effects on the health of children and adults; particularly sensitive subjects react to a larger extent.

Chapter 15, Quantitative Public Policy Assessments, by Green and Rio, reports the overall approach and principal results of a study (ICAAS, 1978) which attempted to carry out an integrated interdisciplinary assessment of air pollution abatement alternatives in the Tampa area of Florida, a region where coal is a major source of electric power. ICAAS's initial concept of public policy decision methodologies (PPDM) for regulating air pollution began in connection with a proposed Air Quality Index (AQI) Project (ICAAS, 1970). This AQI project was designed to be a broad socio-technical research program leading to the establishment of a quantitative scale for air quality. From this AQI program plan, we developed our first practical cost/benefit analysis approach (ICAAS, 1971). These two overall systems approaches were implemented in the ICAAS-FSOS study (ICAAS-FSOS, 1978) which involved a chain of component studies within the framework of two types of public policy decision methodologies on sulfur oxide pollution. One methodology, the Disaggregated Benefit/Cost Analysis (DB/CA), was essentially an advanced form of economic analysis in which the distributional aspects of B/C are considered (i.e. the question of who gets the benefits and who pays the costs). The second methodology, the Quantitative Assessment of the Level of Risk (QALR), is a non-economic analysis that by-passes many of the difficult problems of translating all important decision factors into monetary terms.

This chapter concentrates on a few specific but vital facets of these system approaches. In particular we discuss quantitative characterizations of ambient air quality from air pollution health effects viewpoint. We also describe a "factor of safety" approach to quantitative dose response relations based on the use of an air quality index (AQI). These are followed by the application of the QALR-PPDM used in the ICAAS-FSOS study which also uses an AQI. We also describe the essence of the DB/CA-PPDM used in the ICAAS-FSOS study. Finally, we describe some recent dose response results for plants and materials which can be used in PPDM's.

Chapter 16, Financing Capacity Growth and Coal Conversions in the Electric Utility Industry, by Brigham and Gapenski, considers first the demand for electric power which is expected to increase greatly from 1980 to 1995. To meet this demand, and also to finance the conversion of existing oil and gas fired plants to coal, the utility industry must raise and invest unprecedented large sums of money.

At the start of the 1960s, the electric power industry was the epitome of financial strength, with a virtually unlimited ability to raise funds. Today, however, the average company is so weak financially that it simply cannot meet its capital requirements. This deterioration was caused by a combination of economic and political factors—infaltion, both general and in fuel prices, is the root cause of the industry's problem. Cost increases have outstripped productivity gains, which has squeezed profits, necessitating rate increases. However, since utility prices are set by regulatory commissions, time lags are inherent in obtaining rate relief. If costs rise but prices can be increased only after a regulatory delay, then obviously profit margins are squeezed, rates of return on invested capital decline, and the company's financial position suffers.

The situation is masked by the fact that the companies now have excess capacity that arose from the sudden, sharp reduction in growth after 1973. Since this excess capacity has permitted the companies to survive and meet current power demands, the public has not yet suffered to any significant extent. However, excess reserves will soon be used up, so that if construction programs have not been started up well in advance, power shortages will follow, accompanied by severe economic problems. It is possible, however, to avoid capacity shortfalls. What is needed is for utility commissions across the country to realistically analyze the situation and then to allow the utility companies to charge prices that cover the cost of providing service, including the cost of the capital invested in the plant that provides the service.

Chapter 17, Coal and the States: A Public Choice Perspective, by Rosenbaum, discusses the Coal Burning Issues problem from the perspective of a political scientist. The development of a national coal policy will depend heavily upon the states for implementation. The generous discretionary authority exercised by the states in implementing federal coal policy, together with traditional state powers affecting coal use, means the states will be major actors in any national coal-management program. In general, state activities will affect coal utilization through the siting of mines, the siting and design of power generating plants, the location of coal logistical facilities, the enforcement of air and water pollution standards, and much else.

Formulating state coal policy confronts the state governments with competing, and sometimes conflicting, policy objectives and policy priorities. Among the major policy choices that must be resolved by the states are: (a) the relative importance of environmental protection among other policy objectives in coal use; (b) the priority to be accorded economic growth in coal development; (c) the distribution of social costs and benefits from coal development—the "distributive equities"; and, (d) the relative priority to be given state or regional interests compared to national ones in choosing coal policy goals.

While the federal government cannot, and should not, attempt to resolve all these matters at the state level, federal coal policy can constructively assist the states in resolving these issues. In particular, the federal government should restrain massive new coal utilization to a few decades at most, should create a target growth rate figure for the U.S., should emphasize conservation of energy in the coal sector by dampening demand for new electric generating facilities and should encourage great public involvement in coal policy formulation among the Western states where the environmental risks of coal development are especially acute.

Chapter 18, Federal Regulatory and Legal Aspects, by Little and L. Capehart, examines federal laws which simultaneously promote and constrain the increase in coal use as an alternative fuel to natural gas and petroleum. Congressional desire to encourage or require coal use is evident as early as 1974 with passage of the Energy Supply and Environmental Coordination Act which set mandatory coal conversion requirements for power plants with conversion capability. More recent laws have expanded federal authority to require the use of coal by major fuel burning installations.

Congress has recognized that an increase in coal use will be possible only if federal assistance is available to weak links in the coal production-transportation-combustion chain. To date, some limited financial help has been authorized for developing new underground mines, for rehabilitating the rail system, and for buying air pollution control equipment. At the same time, Congress has been standing firm on environmental laws, trying to protect the health of the public by preserving air and water quality standards. Clean air legislation has come in for the biggest attack because the control of emissions from coal combustion places large costs on any coal burning facility. The waste disposal laws may also create additional financial burdens if coal wastes are termed hazardous.

Reform of other federal legislation may be appropriate if the goal of increased coal use is to be met. Regulation of the transportation industry should be examined to determine inequities in the laws which favor one mode over competing modes. Examples are unequal federal subsidies to various modes, and varied formulae for determining rate structures.

Changes in mining laws have been advocated. The mineral leasing program of the federal government has been criticized by almost everyone. The mine safety legislation has been accused of decreasing productivity without a proportionate increase in worker safety. Changes in federal law may be necessary to achieve the goal of increased coal use, but such changes should be carefully examined to determine the side effects as well as the expected result. Furthermore, proposed changes should be considered in light of interrelating laws and problems.

CHAPTER 2

COAL AVAILABILITY AND COAL MINING

M. J. Ohanian and Faramarz Fardshisheh

I. THE CHARACTERISTICS OF COAL

Coal deposits have quite variable characteristics, depending upon the original topography and water movement during its formation. The various types of coal are traditionally classified by a number of parameters, including heating value, ash content, moisture content, sulfur content, and the division of the organic portion of the coal into fixed carbon and volatile matter. The four main ranks of coal are anthracite, bituminous, sub-bituminous, and lignite. Table 1 lists some characteristics of coal in the United States.

The American Society for Testing and Materials (ASTM) rank is based on the degree of lithification and metamorphism of plant material (DOE 1979). According to this system, rank is determined primarily by the percentage of fixed carbon and the heat value (BTU content) of the coal, calculated on a mineral-matter-free basis. A more detailed discussion of the energy quality and other properties of coal based upon the evolutionary history of coal formation as interpreted from an energetic analysis perspective is given in Chapter 3.

As described in Chapter 1, coal is the most abundant non-renewable energy resource in the world, and it comprises the major fraction of the estimated energy reserves of coal, petroleum and natural gas. The United States' share of these recoverable coal reserves is estimated to be about 28% or 4,900 quads (Peters and Schilling, 1978). (The present rate of U.S. energy consumption is ~78 quads, of which 18% is supplied by